A complete cosmic history from Asymptotic Safety

Robin Ooijer

Supervised by Frank Saueressig

Collaborated with Chris Ripken

Radboud University, Institute for Mathematics, Astrophysics and Particle Physics

July 15, 2018

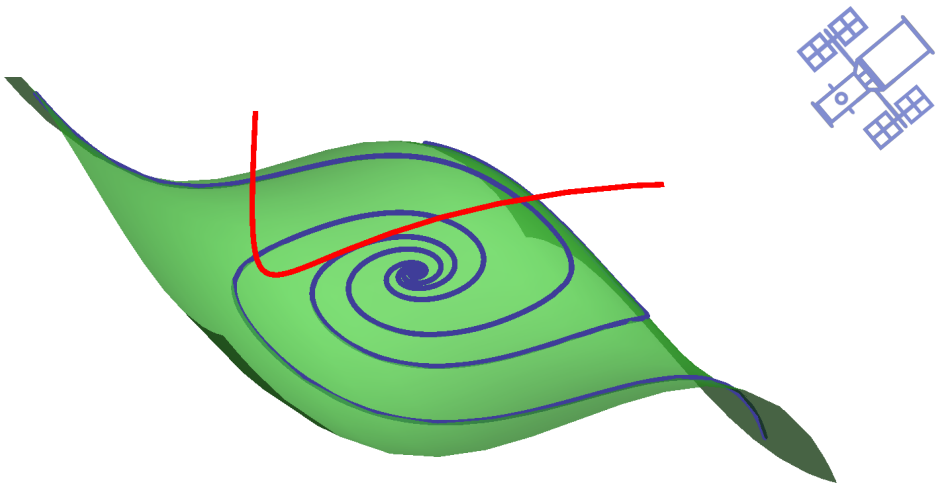

Abstract

The framework of Asymptotic Safety provides a promising approach towards a quantum formalism for gravity. Moreover, it is an attractive mechanism to study cosmological phenomology. In this thesis, we employ the framework of the Functional Renormalization Group to investigate the compatibility of cosmological constraints with the asymptotic safety scenario of quantum gravity. In particular, we show that Asymptotic Safety allows to connect the trans-Planckian regime to a phenomenologically viable phase of inflation at early times, which in turn is linked to a phase of accelerated expansion driven by the cosmological constant at late times. By doing so, we pioneer a new path for cosmological analyses within Asymptotic Safety, opening up a wide range of possibilities for future research.

Contents

Chapter 1

Introduction

The desire to obtain a consistent, fundamental theory of Nature is a driving force for many physicists, at least for those in High Energy Physics. To a large extent, this aspiration has been satisfied by the Standard Model of particle physics. This theory consistently describes three of the four currently known fundamental interactions of Nature: the electromagnetic, weak and strong forces. It has passed experimental tests with incredible success, yet it has some shortcomings. Examples of these flaws are the lacking explanation of dark matter and the issue of UV-completion once neutrino masses are included. Many other shortcomings are rather modest "why?"-problems, which do not harm the consistency of the theory. Hence, one may think that the Standard Model has quite a humble name, and should perhaps be named "the theory of almost everything" [1].

However, there is one major gap in the construction, namely the exclusion of gravity. The importance of this will differ depending on whom you ask. One can couple the Standard Model to classical general relativity and obtain, for all practical purposes, a theory for everything in our solar system.[1] However, this is not very satisfactory since this is not a fundamental theory; it does not describe physics at all scales as quantum fluctuations of gravity are not taken into account. The reason for this is that we do not yet know how to quantize gravity. If one attempts to quantize general relativity along the same lines as the Standard Model, the theory is rendered internally inconsistent. This is because gravity is perturbatively non-renormalizable [2, 3]. The reason for this is the following. As one attempts to quantize gravity in a perturbative setting, one is confronted with divergent expressions originating from loop integrals. In the Standard Model, these terms are dealt with by introducing counterterms which cancel the divergent expressions. However, in the case of gravity, one requires the addition of an infinite number of such terms. This eventually leads to a theory with an infinite number of free parameters to be measured by experiment. Thus, the theory loses predictive power. For this reason, one cannot simply incorporate gravity into the Standard Model. This provides the motivation to search for a fundamental quantum theory of gravity.

Over the past decades, many approaches to quantum gravity have been developed. We can largely categorize these into two classes, those that use a discrete formulation and those that rely on a continuum language. An example of the former type is Causal Dynamical Triangulations

[1] Neglecting dark matter, of course.

(CDT) [4].[2] In this approach, one constructs spacetime itself using simplices[3] of fixed edge length as discrete building blocks. In order to study the quantum fluctuations of spacetime, one allows these triangulations to vary dynamically. Essentially, this amounts to changing the way the simplices are "glued" together to form a triangulation, while keeping the edge lengths constant. Due to the nature of this approach, it takes into account quantum fluctuations at the smallest length scales. However, one of the difficulties in such a discrete program is the reconstruction of a classical spacetime. It is not known whether the spacetime of Nature is fundamentally discrete or continuous, but it is evident that it is continuous on a classical level. As a result, in order to make contact with classical physics, it is required to move towards a continuum limit in such discrete approaches. In essence, this amounts to taking the edge length to zero and the number of simplices to infinity. In doing so, one can attempt to extract physical properties of the constructed spacetime. However, taking the strict continuum limit is not necessary in practice; many properties can be extracted by increasing the number of simplices and simultaneously decreasing the edge length until a certain degree of continuity has been reached. Nonetheless, this is a challenging task since the system becomes increasingly more difficult to handle as one increases the number of building blocks.

In the continuum approaches to quantum gravity, there is no issue of taking a continuum limit as there is in many discrete approaches. In contrast, the ultraviolet (UV) limit can be more troublesome in these methods. The continuum-based program that we will be using throughout this thesis is the asymptotic safety program. This approach adheres to the desire to quantize gravity as a quantum field theory. Since there is no proof that a quantum field theory of gravity is doomed to fail, the asymptotic safety framework entertains the idea that the usual problem of quantizing gravity may be because of the use of perturbation theory. In 1979, Weinberg [5] proposed the idea that gravity may be renormalizable as a non-perturbative quantum field theory. This non-perturbative renormalizability is now known as "Asymptotic Safety". It relies on the notion of renormalization as formulated by Kadanoff and Wilson [6–8]. The very basic idea behind this notion is that the description of a system changes as one adjusts the resolution of the measurement apparatus. The way in which the dynamics changes is described by the Renormalization Group (RG) flow. A detailed description of this approach is given in chapter 2.

Whatever one's inclinations may be about the correct path towards a quantum formalism for gravitational phenomena, one could argue that the ultimate test for a theory is the experiment. To paraphrase Feynman: "It doesn't matter how beautiful your theory is. If it disagrees with experiment, it's wrong." However, doing experiments is not so easy in the case of quantum gravity, for the following reason. The energy scale at which quantum fluctuations are expected to have an effect is the Planck scale, which is of the order of 10^{19} GeV. For comparison, experimental tests of the Standard Model occurring at the Large Hadron Collider are perfomed at center-of-mass energies of 10^4 GeV. This immediately explains why for practical purposes, one does not need to have a quantum theory of gravity to explain the Standard Model physics; the relevant energy scales are separated by at least 15 orders of magnitude. Nonetheless, this also means

[2] The use of a discrete formulation does not imply the assertion that spacetime is fundamentally discrete. Instead, in this approach discreteness is merely a regulator to be removed in the continuum limit.

[3] A simplex is a generalization of the two-dimensional triangle to an arbitrary number of dimensions. Hence the name *triangulation*.

that we are currently unable to directly measure quantum fluctuations of gravity, due to the resolution of our measurement instruments.

In search of a solution, we can look up at the sky. Even though man-induced particle collisions do not reach the necessary energies, it might be that cosmological phenomena come much closer. An example is the phase of primordial cosmology known as inflation [9–11]. This process is believed to have occured in the very early universe, about 10^{-34} seconds after the Big Bang. It consists of a phase of exponential expansion of the universe and solves a number of cosmological problems, such as the horizon and the flatness problems. For an extensive review of inflationary cosmology, see [12]. The relevant energy scale corresponding to this period, as discussed in more detail in chapter 4, is only a few orders of magnitude below the Planck scale. Hence, we can argue that inflation, and more generally cosmology, is a fruitful place to look for imprints of quantum gravity.

In this thesis, we apply the framework of the Renormalization Group to investigate the compatibility of cosmological constraints with the asymptotic safety scenario of quantum gravity. One of the reasons to use the RG is that it provides the possibility to take the relevant energy scales of observations into account, enabling us to track the evolution of the universe. A detailed overview of this framework and how it applies to the concept of Asymptotic Safety is given in chapter 2. This knowledge is then applied in chapter 3 to study the model for a scalar field minimally coupled to gravity, with a scalar field potential. Depending on the shape of this potential, this could serve as a model to study inflation. Sadly, it is found that this system exhibits the triviality problem. These conclusions then encourage the investigation of a different model in chapter 4. Here, we do not only explore the possibility of Starobinsky inflation, but also the evolution of the universe into its current state. Chapter 5 provides concluding remarks, and we end the main body of this thesis with an overview of prospects for future investigations. Finally, the appendices provide detailed calculations that are omitted from the main text.

Chapter 2

Functional renormalization group

In this chapter, we introduce the Functional Renormalization Group (FRG) and the concept of Asymptotic Safety in quantum gravity. We mainly follow the exposition of [13]. The FRG merges the modern view of renormalization as introduced by Wilson [7,8] with functional methods from quantum field theory, connecting the realms of micro- and macrophyiscs through a process known as coarse-graining. The implementation of the FRG uses the effective average action (EAA), which is introduced below. For didactic reasons, it is introduced in the context of a scalar field on a fixed flat, Euclidean space in section 2.1. This allows us to focus on the central properties in a simpler setting, before introducing gravity in section 2.4. Moreover, some technical and conceptual difficulties irrelevant to this thesis will be omitted. For more information on such details, see [13] and references therein.

2.1 The Effective Average Action

Here we introduce the concept of the EAA for a real, scalar quantum field $\widehat{\phi}$ on a d-dimensional Euclidean spacetime.[1] As $\widehat{\phi}$ is a random field, one is usually interested in its moments, or n-point functions

$$\langle\widehat{\phi}(x_1)\widehat{\phi}(x_2)\cdots\widehat{\phi}(x_n)\rangle = \int \mathcal{D}\widehat{\phi}\big(\widehat{\phi}(x_1)\widehat{\phi}(x_2)\cdots\widehat{\phi}(x_n)\big)\exp\left(-S[\widehat{\phi}]\right), \tag{2.1}$$

where the functional $S[\widehat{\phi}]$ is the bare action of the theory. A convenient way of discussing these Green's functions is through their generating functional

$$Z[J] \equiv \int \mathcal{D}\widehat{\phi}\exp\left(-S[\widehat{\phi}] + \int \mathrm{d}^d x\widehat{\phi}(x)J(x)\right), \tag{2.2}$$

where the field $\widehat{\phi}(x)$ is coupled to a source $J(x)$. Using this formulation, the Green's functions are calculated as functional derivatives of $Z[J]$ with respect to the source as

$$\langle\widehat{\phi}(x_1)\widehat{\phi}(x_2)\cdots\widehat{\phi}(x_n)\rangle = \frac{\delta^n Z[J]}{\delta J(x_1)\delta J(x_2)\cdots\delta J(x_n)}\bigg|_{J=0}. \tag{2.3}$$

[1] The circumflex is used to discriminate $\widehat{\phi}$ from its expectation value denoted by ϕ.

The generating functional for the *connected* Green's functions is introduced as the logarithm of $Z[J]$:

$$W[J] \equiv \ln Z[J] \,. \tag{2.4}$$

Finally, a third generating functional is introduced, the *effective action* $\Gamma[\phi]$.[2] The effective action is defined as the Legendre transform of $W[J]$ and hence depends on the expectation value of the field, $\phi \equiv \langle \widehat{\phi} \rangle$. One can show that $\Gamma[\phi]$ generates the 1-particle irreducible Green's functions. From this point on, expectation values are calculated in the presence of the source, i.e. J is not put to zero after calculating functional derivatives as in eq. (2.3).

Before we proceed, note that the functional integral (2.2) is a rather formal expression and is only well-defined in the presence of an UV-cutoff. Here, we assume that such a cutoff is present without considering its explicit form. Justification for this will be given once we discuss the properties of the EAA.

Now that we have given some details regarding the regular effective action, let us move onto the EAA. Its construction [15] is based on the introduction of an IR-cutoff scale k. Using this scale, one classifies the Fourier modes of $\widehat{\phi}$ as "short wavelength" (fine) if $|p| > k$, or "long wavelength" (coarse) if $|p| < k$. One implements this cutoff by suppressing the coarse modes while the fine modes are integrated out in the usual way. By lowering the scale k from the UV to the IR, one integrates out more finer modes and hereby connects the micro-scale to the macro-world. This process is schematically depicted in figure 2.1.

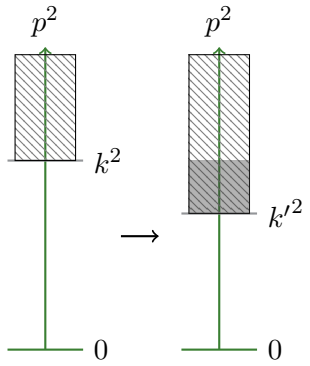

Figure 2.1: Schematic overview of the process of integrating out modes by lowering the RG scale k. In the left figure, the modes with $p^2 \gtrsim k^2$ are integrated out whereas those below are suppressed. Moving to the right figure, the scale k is lowered to k', which results in the integration of the modes in the shaded area. This figure is inspired by [14].

This mode suppression is achieved by adding an extra, scale-dependent term to the bare action. This modifies the generating functional $W[J]$ into a new $W_k[J]$, whose scale-dependence is denoted by the subscript k. In particular, one defines

$$Z_k[J] \equiv \exp\left(W_k[J]\right) \equiv \int \mathcal{D}\widehat{\phi} \exp\left(-S[\widehat{\phi}] - \Delta S_k[\widehat{\phi}] + \int \mathrm{d}^d x \widehat{\phi}(x) J(x)\right) \tag{2.5}$$

where the cutoff action is denoted by $\Delta S_k[\widehat{\phi}]$. It takes the form

$$\Delta S_k[\widehat{\phi}] \equiv \frac{1}{2} \int \frac{\mathrm{d}^d p}{(2\pi)^d} \mathcal{R}_k(p^2) |\widehat{\phi}_p|^2 \tag{2.6}$$

in momentum space, where $\widehat{\phi}_p$ is the Fourier transform of $\widehat{\phi}$. The regulator $\mathcal{R}_k(p^2)$ suppresses low-momentum modes. The precise form of this regulator is not important, as long as it leaves

[2] Note that this is the *standard* effective action, not the effective *average* action that is introduced at a later stage.

the high-momentum modes unaffected. The usual requirement is that

$$\mathcal{R}_k(p^2) \approx \begin{cases} k^2 & \text{for } p^2 \ll k^2\,, \\ 0 & \text{for } p^2 \gg k^2\,. \end{cases} \tag{2.7}$$

This ensures that the regulator vanishes for high-momentum modes while providing a mass term for the low-momentum modes. The exact form one takes for $\mathcal{R}_k$ depends on a number of factors, one of which is calculational convenience. We will indicate the particlar choice of regulator whenever it is required to perform explicit calculations.

Having introduced the cutoff action, the derivation of the effective average action proceeds along familiar lines. One defines

$$\tilde{\Gamma}_k[\phi] = \sup_{J(x)} \left(\int \mathrm{d}^d x J(x)\phi(x) - W_k[J] \right) \tag{2.8}$$

as a Legendre-Fenchel transform [16]. Then, the effective average action is defined as the subtraction of $\Delta S_k[\phi]$ from $\tilde{\Gamma}_k[\phi]$:

$$\boxed{\Gamma_k[\phi] \equiv \tilde{\Gamma}_k[\phi] - \frac{1}{2}\int \mathrm{d}^d x \phi(x)\mathcal{R}_k(-\partial^2)\phi(x)} \tag{2.9}$$

where we used the position space representation of $\Delta S_k[\phi]$. Next, we list a number of important properties of the EAA introduced in (2.9).

(1) As $k \to 0$, the EAA approaches the ordinary effective action $\Gamma[\phi]$. This is obvious since in this limit, the cutoff action $\Delta S_k[\phi]$ vanishes. Moreover, as $k \to \infty$, the EAA approaches the bare action $S[\phi]$. Since the proof of this property is rather technical and unimportant for this thesis, we refer the reader to the discussions in [15, 17].

(2) The EAA satisfies the *functional renormalization group equation* (FRGE)

$$\boxed{\partial_t \Gamma_k[\phi] = \frac{1}{2}\mathrm{Tr}\left[\left(\Gamma_k^{(2)}[\phi] + \mathcal{R}_k \right)^{-1} \partial_t \mathcal{R}_k \right]}\,. \tag{2.10}$$

Here we introduce *logarithmic RG time* $t := \ln(k/k_0)$ where k_0 is some arbitrary reference scale. Furthermore, the operator $\Gamma_k^{(2)}[\phi]$ is the Hessian of the EAA, meaning that its matrix elements are given by $\Gamma_k^{(2)}(x,y) = \delta^2\Gamma_k/\delta\phi(x)\delta\phi(y)$. The derivation of eq. (2.10) is rather straightforward to perform using the definitions (2.5), (2.6), (2.8) and (2.9).

An important property of the FRGE is that it is not plagued by any UV- or IR-divergences. This is evident from the form of the operator that is traced over. In momentum space representation one has, schematically,

$$\left(\Gamma_k^{(2)} + \mathcal{R}_k \right)^{-1} \sim \left(p^2 + \mathcal{R}_k(p^2) + \ldots \right)^{-1} \tag{2.11}$$

where the dots denote terms obtained when calculating the Hessian, which are irrelevant to the

current discussion. Furthermore, from eq. (2.7) we have

$$\partial_t \mathcal{R}_k(p^2) \sim \begin{cases} k^2 & \text{for } p^2 \ll k^2\,, \\ 0 & \text{for } p^2 \gg k^2\,. \end{cases} \tag{2.12}$$

Hence, when inspecting the interesting limits, we find

$$\left(\Gamma_k^{(2)} + \mathcal{R}_k\right)^{-1} \partial_t \mathcal{R}_k(p^2) \sim \begin{cases} \frac{0}{p^2+0+\ldots} \to 0 & \text{for } p \to \infty\,, \\ \frac{k^2}{p^2+k^2+\ldots} \to \frac{k^2}{k^2+\ldots} & \text{for } p \to 0\,. \end{cases} \tag{2.13}$$

Thus, we see that both limits are regular and the FRGE has no need for an additional cutoff. This, amongst other things, makes it very attractive to work with. In fact, the FRGE is the primary tool for investigating the RG flow of gravity and we shall see more of it in chapters 3 and 4. However, coming back to the question raised earlier in this section regarding an implicit UV cutoff of the functional integral, one may wonder how this is resolved. In fact, the problem of dealing with the UV limit has translated itself into a different problem that will be adressed in section 2.3.

2.2 Theory space

In the previous section we derived the functional differential equation (2.10) that describes the change of the effective average action as the scale k is altered. To solve such an equation, one requires an inital condition, that is, a particular form of the EAA at a certain scale. However, before discussing such an initial condition, we need to define the space of action functionals over which the FRGE is defined. This space, commonly referred to as *theory space*, consists of all possible action functionals that can be forged from the quantum fields in play and are compatible with symmetry requirements. Thus, each point in theory space represents one such action functional. One can think of theory space as being spanned by all (allowed) field monomials, in which case the coupling constants play the role of coefficients in such an expansion. More explicitly, one may write for a generic action A in theory space $\mathcal{T}$,

$$A[\phi] = \sum_\alpha \bar{u}^\alpha I_\alpha[\phi] \tag{2.14}$$

where the $I_\alpha[\phi]$ are the field monomials making up a basis of functionals $\{I_\alpha\}$ and the $\bar{u}^\alpha$ are the couplings, fulfilling the role of coefficients in this expansion, or *coordinates* on $\mathcal{T}$. In order to make this notion more tangible, assume the symmetries of our system allow us to use all terms that can occur in a derivative expansion and only those that are $\mathbb{Z}_2$-symmetric, i.e.

$A[\phi] = A[-\phi]$. In that case, the allowed actions would have the following form:

$$\begin{aligned} A[\phi] = \int \mathrm{d}^d x \Big(& \bar{u}_{0,0} + \bar{u}_{0,2}\phi(x)^2 + \bar{u}_{0,4}\phi(x)^4 + \dots \\ & + \bar{u}_{2,0}\partial_\mu\phi(x)\partial^\mu\phi(x) + \bar{u}_{2,2}\phi(x)^2\partial_\mu\phi(x)\partial^\mu\phi(x) + \dots \\ & \vdots \\ & + \dots \Big) . \end{aligned} \tag{2.15}$$

Of course, this is merely schematic and meant as an illustration of the (infinite) multitude of terms allowed in an action.

Moving back to the FRGE, we can expand its solutions $\Gamma_k[\phi]$ in the same way as eq. (2.14):

$$\Gamma_k[\phi] = \sum_\alpha \bar{u}^\alpha(k) I_\alpha[\phi] . \tag{2.16}$$

We see that the k-dependence of the EAA presents itself in the form of scale-dependent couplings $\bar{u}^\alpha(k)$. Such a solution $\Gamma_k[\phi]$ represents a *RG trajectory* in theory space, parametrized by the RG scale k.

Inserting the expansion (2.16) into the FRGE, one can derive the flow equations for the couplings, rather than the entire functional $\Gamma_k[\phi]$:

$$\sum_\alpha \partial_t \bar{u}^\alpha(k) I_\alpha[\phi] = \frac{1}{2}\mathrm{Tr}\left[\left(\sum_\alpha \bar{u}^\alpha(k) I^{(2)}_\alpha[\phi] + \mathcal{R}_k \right)^{-1} \partial_t \mathcal{R}_k \right] . \tag{2.17}$$

The RHS of this equation is rather complicated. However, since we argued that theory space consists of terms that can occur in a derivative expansion, one can expand this equation to yield

$$\sum_\alpha \partial_t \bar{u}^\alpha(k) I_\alpha[\phi] = \sum_\alpha \bar{\beta}^\alpha(\bar{u}(k); k) I_\alpha[\phi] \tag{2.18}$$

where the set $\{\bar{\beta}^\alpha\}$ conists of the coefficients in the expansion in basis functionals $\{I_\alpha\}$.[3] These in principle depend on the scale k both explicitly as well as implicitly through the dependence on $\bar{u}(k) \equiv \{\bar{u}^\alpha(k)\}$. Now that the FRGE has taken the form (2.18), one can use that the $I_\alpha[\phi]$ are linearly independent to obtain

$$\partial_t \bar{u}^\alpha(k) = \bar{\beta}^\alpha(\bar{u}(k); k) . \tag{2.19}$$

This equation defines the β-functions of the couplings involved in the theory. It consists of an infinite set of coupled first order differential equations. This system is incredibly complex, for a number of reasons. First of all, since the system of equations is coupled, couplings that are zero at one scale k_1 may be driven to non-zero values at another scale k_2. This means that, if we provide a simple initial condition for $\Gamma_{k_1}[\phi]$ comprising only a finite number of terms, a

[3] The notation used in this section for the couplings and β-functions involving the bar is for future convenience. At this point, the canonical mass dimensions of the couplings are not all zero, whereas in future sections we switch to dimensionless variables, upon which we drop the overhead bar on u and β.

plethora of new terms will be generated at other scales. Secondly, a more practical complexity of the system is that there exist infinitely many differential equations, making it very difficult to perform explicit calculations. An approach to overcome this issue is described in the following.

2.2.1 Truncations of theory space

So far, our entire exposition has been exact. However, as we just observed, for practical computations one is often required to make approximations. A compelling approximation to solve the aforementioned problem is to *truncate theory space*. This means that we discard all contributions from an (infinite) set of basis elements, and only work with a (usually finite) number of terms. In order to define which terms are included, one specifies a *truncation ansatz* of the form

$$\Gamma_k[\phi] = \sum_{i=1}^{N} \bar{u}^i(k) I_i[\phi] \,. \tag{2.20}$$

Hence, in such a case one only works with a finite subset of N terms in the effective average action. Up to this point, this may just seem like a (possibly valid) initial condition. However, the important step in the approximation is the following. Consider now equations (2.17) and (2.18). In the case of such a truncation, the step between these two equations poses a problem: performing a derivative expansion of the RHS of eq. (2.17) will generate terms that are not part of the subset of terms allowed by the truncation. Hence, in order to stay within the truncated theory space, one has to set all coefficients of the undesired terms in the derivative expansion to zero. Obviously, this is a severe approximation and one is bound to lose information through this process. In general, it is extremely difficult to quantify the accuracy of such a truncation. In this thesis, we will not go into details regarding this technical issue. Instead, we comment on qualitative resolutions where relevant, and we refer the reader to [13] for further details.

2.3 Asymptotic Safety

Now that we have given a brief overview of the FRG, it is possible to see how it is used in the asymptotic safety mechanism. Recall that the FRGE (2.10) describes the k-evolution of the effective average action. Physically, this means that it describes the change of the system as one integrates out details of the microscopic world when going to a lower resolution. Geometrically, it describes a trajectory in theory space. In this section, we will mainly consider this geometric aspect as we introduce the concepts important to the notion of Asymptotic Safety.

(1) First of all, it is convenient to work with dimensionless variables. Hence, we introduce

$$u^\alpha = k^{-d_\alpha} \bar{u}^\alpha \tag{2.21}$$

where d_α is the canonical mass dimension of the running coupling $\bar{u}^\alpha$, i.e. $[\bar{u}^\alpha] \equiv d_\alpha$. Using this notation, one obtains the dimensionless counterpart of eq. (2.19),

$$\partial_t u^\alpha(t) = \beta^\alpha(u(t)) \,. \tag{2.22}$$

An important advantage of working with these couplings is evident from this equation; the β-functions become autonomous, i.e. they no longer exhibit an *explicit* t- (or k)-dependence.

(2) Important points in theory space are so-called *fixed points*. These are defined as the points where the RG flow stops, that is, the points $\{u_*\}$ where the β-functions vanish:

$$\beta^\alpha(u_*) = 0 \quad \forall\, \alpha\,. \tag{2.23}$$

At such a point, the dimensionless couplings become scale-independent by definition. As a consequence, the dimensionful couplings exhibit a simple scaling law:

$$\bar{u}^\alpha(k) = u_*^\alpha k^{d_\alpha}\,. \tag{2.24}$$

As we will see later, fixed points are extremely important to the asymptotic safety scenario.

(3) In the vicinity of a fixed point, one can study the flow in a simple way. Taylor expanding the flow equation to first order in $(u(k) - u_*)$, one finds

$$k\partial_k u^\alpha(k) = \sum_\gamma B^\alpha{}_\gamma (u^\gamma(k) - u_*^\gamma)\,. \tag{2.25}$$

Here, one defines the stability matrix B as

$$B^\alpha{}_\gamma = \frac{\partial \beta^\alpha(u)}{\partial u^\gamma}\Big|_{u=u_*}\,. \tag{2.26}$$

By definition, the stability matrix is specific to a fixed point. One then defines the critical exponents θ_J of a fixed point as

$$\sum_\gamma B^\alpha{}_\gamma V_J^\gamma = -\theta_J V_J^\alpha \quad \forall\, J\,. \tag{2.27}$$

Here, J labels the eigenvectors V_J. Thus, the critical exponents of a fixed point are defined as *minus* the eigenvalues of the stability matrix. In fact, the values and in particular the signs of these critical exponents provide a great deal of information about the flow near the fixed point. This becomes clear once we write down the solution to the linearized equation (2.25),

$$u^\alpha(k) = u_*^\alpha + \sum_J C_J V_J^\alpha \left(\frac{k_0}{k}\right)^{\theta_J}\,. \tag{2.28}$$

Here, the C_J denote integration constants that are fixed by the initial conditions. It is now instructive to investigate the factor $(k_0/k)^{\theta_J}$. If the exponent θ_J has a non-zero imaginary part, one writes this as

$$\left(\frac{k_0}{k}\right)^{\theta_J} = \exp\left(-\theta_J t\right) = \Big(\cos\left(\mathrm{Im}\ \theta_J t\right) - i\sin\left(\mathrm{Im}\ \theta_j t\right)\Big)\left(\frac{k_0}{k}\right)^{\mathrm{Re}\ \theta_J}\,. \tag{2.29}$$

In such a case, the flow shows oscillatory behaviour close to the fixed point. In fact, this is quite

common and we will encounter examples of this behaviour in chapters 3 and 4.

Next, let us investigate the behaviour of $(u(k)-u_*)$ as k is lowered. Equation (2.28) dictates that the component of $(u(k)-u_*)$ in the direction of the eigenvector V_J is increased if Re $\theta_J > 0$, decreased if Re $\theta_J < 0$ and is purely oscillatory in the case of Re $\theta_J = 0$. Eigenvectors in these three cases are referred to as *relevant*, *irrelevant* and *marginal*, respectively. The reasoning behind these names will become clear later in this section.

Now considering increasing k, one observes that eigendirections whose critical exponents come with a positive real part attract the flow for increasing k, whereas critical exponents with a negative real part are UV repulsive. This will be important when discussing the suitability of particular fixed points for an asymptotic safety scenario.

(3) The values of the critical exponents provide us with a simple classification scheme for the types of fixed points. For a Gaussian fixed point (GFP), the critical exponents are equal to the canonical mass dimensions of the couplings $\bar{u}^\alpha$. Such a fixed point is trivial in the sense that $u_*^\alpha = 0 \,\forall\, \alpha$. Conversely, for a non-Gaussian fixed point (NGFP) at least one of the θ_J differs from the canonical dimensions.

(4) Critical exponents are *universal* [18]. By this statement, one implies that the values are invariant under a change of coordinates $\{u^\alpha\}$, or a change of regulator $\mathcal{R}_k$. However, this independence only holds in the exact case. If one truncates theory space, this property is possibly lost. Hence, a possible qualitative test of the quality of a truncation consists of checking this property.

(5) Before we move to the concept of Asymptotic Safety, it is instructive to define one more notion. The *UV critical hypersurface* associated with a certain fixed point is made up of all points in theory space that are attracted towards the fixed point in the UV, that is, as the scale k is increased. It should be clear that if a RG trajectory is on this surface at one scale, it will remain so on all other scales.

The dimension of this surface plays an important role in the asymptotic safety scenario. To determine this dimension, it is useful to consider eq. (2.28) and examine the limit $k \to \infty$. One can split up the sum into three parts, depending on the corresponding critical exponent. For Re $\theta_J > 0$, the terms in the sum vanish, no matter the values of the C_J's. However, for Re $\theta_J < 0$, the terms diverge unless one sets the corresponding C_J's to zero. Finally, for Re $\theta_J = 0$, the terms only vanish if one chooses the C_J's to be zero. Furthermore, a trajectory lies on the UV critical hypersurface if and only if the terms in the sum all vanish as $k \to \infty$. This means that only the C_J's corresponding to relevant eigenvectors are free, whereas all other integration constants must be fixed to zero to ensure that the UV limit is controlled by the fixed point. Hence, the dimension of the UV critical hypersurface, denoted by Δ_{UV}, is given by the number of relevant eigendirections,

$$\Delta_{\mathrm{UV}} = \#\{\theta_J |\ \mathrm{Re}\ (\theta_J) > 0\}\,. \tag{2.30}$$

As it turns out, in most studied systems, including those appearing in this thesis, Δ_{UV} is a

finite and small number. This is of great importance for the theory's predictive power, as will be demonstrated soon.

At this point, we have introduced all necessary ingredients to start our pursuit of a non-perturbatively renormalizable theory. One commences by choosing the stage of the game; the type of fields present must be specified, as well as the symmetry requirements. This defines the theory space of allowed action functionals. In order to exploit the FRGE, one must also specify a regulator $\mathcal{R}_k$. This allows us to investigate the flow generated by the FRGE. We already mentioned that the FRGE is not afflicted with any divergences. In particular, one can safely take the UV limit at the level of the equation, which was not an option at the level of the functional integral. We can now discuss where this problem has moved to. As discussed previously, not every trajectory in theory space stays finite in the UV; depending on the critical exponents of the fixed points, this required specific inital conditions to set the undesired integration constants to zero. Hence, the problem of finding a non-perturbatively renormalizable theory has been translated to the quest for trajectories that are finite as $k \to \infty$. At the level of the effective average action Γ_k, this means that we must find a Γ_k that is well-defined in the entire range $k \in [0, \infty)$.

In the pioneering work [5], Weinberg proposed a conjecture regarding the concept of non-perturbative renormalizability known as Asymptotic Safety. It boils down to the following two statements about the gravitational theory space:

(A) Theory space contains a non-trivial fixed point with a low-dimensional UV critical hypersurface.

(B) Any trajectory that does not hit the fixed point eventually develops unacceptable singularities and leaves theory space.

Assuming that both (A) and (B) are true, a theory is non-perturbatively renormalizable if and only if its RG trajectory flows into the fixed point in the UV.

At this point it is instructive to explain how such a complete trajectory signals the property of renormalizability. Recall that the absence of this property resulted in a theory without predictive power. Hence, we must figure out how an asymptotically safe theory retains its predictive power in the high-energy limit. In essense, this comes down to the requirement that for such a desirable theory, the corresponding RG trajectory must lie on the critical hypersurface, according to (B). This requirement is very strong, as it fixes the number of free parameters to a small number, according to (A). Recall that Δ_{UV} is equal to the number of free constants of integration C_J, since many are set to zero by the requirement of asymptotic safety. One can absorb one of these into the arbitrary scale k_0 to be left with $(\Delta_{\mathrm{UV}} - 1)$ free parameters, to be determined by experiment. The remaining, possibly infinite, number of parameters is completely fixed by the embedding of the critical surface into theory space, i.e. by the requirement that the trajectory lies within this surface. This is an amazing property since it gives the theory immense predictive power; one can predict an infinite number of parameters by making a small

number of measurements.

2.4 The EAA for gravity

In this section, we introduce the effective average action for gravity and discuss its relevant properties. Having introduced the basic concepts of the FRG and Asymptotic Safety previously, we are able to include gravity. The introduction of gravity to the system brings along several difficulties, both technical and conceptual. For a detailed overview, see [13]. Here, we omit most technical difficulties and sketch the origin of the conceptual issues to motivate the choice for the EAA. In fact, it is important to note at this point that the functional renormalization group for gravity is not unique. The version presented here is a choice motivated by the issues involved when considering gravity.

Following the outline of section 2.3, we start by discussing the fields present in the theory, as well as the symmetry requirements. Since we ideally want to recover classical gravity in some semi-classical limit, we use the structure of general relativity to inspire us. Hence, the gravitational degrees of freedom are represented by a symmetric tensor field $\widehat{g}_{\mu\nu}$. Furthermore, we require the theory to be invariant under spacetime diffeomorphisms. Finally, the theory must be background independent. These last two requirements are at the core of many technical and conceptual issues related to defining a theory of quantum gravity, in this Asymptotic Safety framework or otherwise [19]. Below, we sketch the basics of these requirements.

2.4.1 Gauge invariance

The classical theory of general relativity is a gauge theory; it is invariant under spacetime diffeomorphisms, which are basically coordinate transformations. However, in the framework of the FRG, working with such a diffeomorphism invariant functional provides difficulties that one has to deal with. The problem boils down to the fact that such a Γ_k contributes a divergent piece to the FRGE, spoiling its convergent properties. This can be solved by the method of gauge fixing. In the functional integral formulation, the gauge fixing is achieved by the method of Faddeev and Popov [20]. This method adds two new action terms to the functional integral and introduces *ghost fields*. We will cover the important features when we write down the EAA for gravity.

2.4.2 Background independence

The requirement of background independence is the cause of most technical and conceptual difficulties involved in setting up a satisfactory quantum theory of gravity. It demands that no spacetime plays a distinguished role; one should recover, rather than presuppose, the spacetime of our Universe. Since many standard methods of quantum field theory depend on a given background spacetime, this poses many new complications.

In this thesis, we will not go into the details of the complications that arise due to these requirements. Let it suffice to say that it proves to be problematic to define a proper notion of coarse-graining in this context. However, it turns out that this is solved by the so-called

background field method [21, 22]. Even though using a method that uses a background field sounds like it does not satisfy background independence, it in fact does. Moreover, it provides a clear notion of coarse-graining. We outline how this works in the following.

In this method, one splits the dynamical field $\widehat{g}_{\mu\nu}$ into a classical background $\bar{g}_{\mu\nu}$ and a dynamical field $\widehat{h}_{\mu\nu}$. The functional integral then integrates over the dynamical field $\widehat{h}_{\mu\nu}$ on a given classical spacetime described by $\bar{g}_{\mu\nu}$. In principle, to ensure background independence, one then has to repeat this for all possible background metrics $\bar{g}_{\mu\nu}$.

This particular method provides a canonical notion of coarse graining. In the scalar case studied earlier, modes of the dynamical field were classified based on the eigenvalue of the Laplacian operator $-\partial^2$. Now, one promotes this to the covariant Laplacian of the background field, $-D^2(\bar{g}) \equiv -\bar{D}^2 = -\bar{g}^{\mu\nu}\bar{D}_\mu\bar{D}_\nu$.

One has a choice regarding the parametrization of the field $\widehat{g}_{\mu\nu}$, depending on whether the field is allowed to degenerate. If one allows the tensor to degenerate, the functional integration extends over *all symmetric tensor fields of this rank*, and one can simply parametrize the field as

$$\widehat{g}_{\mu\nu} = \bar{g}_{\mu\nu} + \widehat{h}_{\mu\nu}\,. \tag{2.31}$$

This provides a lot of calculational ease, at the cost of dealing with tensors that are not genuine metrics. Alternatively, if one insists on integration over metrics, i.e. tensors that do not degenerate, then the space one integrates over is not a linear space and one cannot use a simple linear parametrization as (2.31). This provides calculational challenges absent in the other case, but is perhaps more *physical*. Throughout this thesis, we opt for the linear split and integrate over all symmetric tensor fields.

We are now in position to introduce the EAA for gravity.[4] We start with a functional integral of the form

$$\int \mathcal{D}\widehat{g}_{\mu\nu} \exp\big(-S[\widehat{g}_{\mu\nu}] + \text{source terms}\big)\,. \tag{2.32}$$

The tensor $\widehat{g}_{\mu\nu}$ is split up linearly as in eq. (2.31), changing the integration variable to $\widehat{h}_{\mu\nu}$. Furthermore, the bare action $S[\bar{g}+\widehat{h}]$ is taken to be invariant under diffeomorphisms. To deal with this, we employ the Faddeev-Popov trick which modifies the funtional integral to

$$Z[\bar{g},\ \text{sources}] = \int \mathcal{D}\widehat{h}_{\mu\nu}\mathcal{D}C^\mu\mathcal{D}\bar{C}_\mu \exp\big(-S[\bar{g}+\widehat{h}] - S_{\text{gf}}[\widehat{h};\bar{g}] - S_{\text{gh}}[\widehat{h},C,\bar{C};\bar{g}] + \text{source terms}\big)\,. \tag{2.33}$$

Here we introduced a number of new fields and actions. First of all, the Faddeev-Popov ghost and anti-ghost fields are denoted by C^μ and $\bar{C}_\mu$, respectively. Furthermore, we introduce the gauge-fixing action as

$$S_{\text{gf}}[\widehat{h};\bar{g}] = \frac{1}{2\alpha}\int \mathrm{d}^d x\sqrt{\bar{g}}\bar{g}^{\mu\nu}F_\mu(\widehat{h};\bar{g})F_\nu(\widehat{h};g) \tag{2.34}$$

where α is a gauge parameter which is left arbitrary at the moment. Additionally, $F_\mu(\widehat{h};g)$ is

[4] This presentation contains a number of equations that are mainly listed for completeness and will not be dealt with once we obtain a flow equation for gravity.

the gauge fixing function usually taken to be of the form

$$F_\mu(\widehat{h};\bar{g}) \equiv \sqrt{2}\kappa \mathcal{F}_\mu{}^{\alpha\beta}[\bar{g}]\widehat{h}_{\alpha\beta} \quad \text{with} \quad \mathcal{F}_\mu{}^{\alpha\beta} = \delta_\mu^\beta \bar{g}^{\alpha\gamma}\bar{D}_\gamma - \varpi \bar{g}^{\alpha\beta}\bar{D}_\mu\,, \tag{2.35}$$

with $\kappa \equiv (32\pi\bar{G})^{-\frac{1}{2}}$ and $\bar{G}$ some reference value of Newton's constant, and ϖ a free parameter for now. The *ghost action* present in eq. (2.33) then becomes

$$S_{\rm gh}[\widehat{h}, C, \bar{C}; \bar{g}] = -\sqrt{2}\int \mathrm{d}^d x \sqrt{\bar{g}} \bar{C}_\mu \mathcal{M}[\widehat{g},\bar{g}]^\mu{}_\nu C^\nu \tag{2.36}$$

with the Faddeev-Popov operator

$$\mathcal{M}[\widehat{g},\bar{g}]^\mu{}_\nu = \bar{g}^{\mu\rho}\bar{g}^{\sigma\lambda}\bar{D}_\lambda\big(\widehat{g}_{\rho\nu}D_\sigma + \widehat{g}_{\sigma\nu}D_\rho\big) - 2\varpi\bar{g}^{\rho\sigma}\bar{g}^{\mu\lambda}\bar{D}_\lambda\widehat{g}_{\sigma\nu}D_\rho\,. \tag{2.37}$$

Note that coavriant derivatives constructed from $\widehat{g}_{\mu\nu}$ and $\bar{g}_{\mu\nu}$ are denoted by D_μ and $\bar{D}_\mu$, respectively.

As in the simple scalar case, the functional renormalization group for gravity is implemented using a mode suppression term in the functional integral. Inspired by the form of eq. (2.6) one defines

$$\Delta S_k = \frac{\kappa^2}{2}\int \mathrm{d}^d x \sqrt{\bar{g}}\, \widehat{h}_{\mu\nu}\mathcal{R}_k^{\rm grav}[\bar{g}]^{\mu\nu\rho\sigma}\,\widehat{h}_{\rho\sigma} + \sqrt{2}\int \mathrm{d}^d x\sqrt{\bar{g}}\,\bar{C}_\mu \mathcal{R}_k^{\rm gh}[\bar{g}]C^\mu\,. \tag{2.38}$$

The second term provides a scale-dependent mass term for the ghost fields. The regulators for gravitational and ghost sectors, $\mathcal{R}_k^{\rm grav}$ and $\mathcal{R}_k^{\rm gh}$, may differ though. Both have the general structure

$$\mathcal{R}_k[\bar{g}] = \mathcal{Z}_k k^2 R^{(0)}\left(-\frac{\bar{D}^2}{k^2}\right) \tag{2.39}$$

where the shape function $R^{(0)}$ must interpolate between $R^{(0)}(0) = 1$ and $R^{(0)}(\infty) = 0$, but its specific shape is specified later. Furthermore, the factor $\mathcal{Z}_k$ takes into account the different field sectors. For the ghosts, it is a number, whereas it is a tensor in gravitational sector. We will see how this works when we work through our first calculation in chapter 3.

Having defined the ingredients of the functional integral, we can define the generating functional using

$$\begin{aligned}\exp\big(W_k[t^{\mu\nu},\sigma^\mu,\bar{\sigma_\mu};\bar{g}_{\mu\nu}]\big) = \int \mathcal{D}\widehat{h}_{\mu\nu}\mathcal{D}C^\mu\mathcal{D}\bar{C}_\mu \exp\Big(&-S[\bar{g}+\widehat{h}] - S_{\rm gf}[\widehat{h};\bar{g}] \\ &-S_{\rm gh}[\widehat{h},C,\bar{C};\bar{g}] - \Delta S_k[\widehat{h},C,\bar{C};\bar{g}] - S_{\rm source}\Big)\end{aligned} \tag{2.40}$$

with the source functional

$$S_{\rm source} = -\int \mathrm{d}^d x\sqrt{\bar{g}}\Big(t^{\mu\nu}h_{\mu\nu} + \bar{\sigma}_\mu C^\mu + \sigma^\mu\bar{C}_\mu\Big)\,. \tag{2.41}$$

From the form of $S_{\rm source}$, one observes that the sources coupling to $\widehat{h}_{\mu\nu}$, C^μ and $\bar{C}_\mu$ are denoted by $t^{\mu\nu}$, $\bar{\sigma}_\mu$ and σ^μ, respectively.

Before we formally introduce the EAA, it is first required to introduce some notation. The

expectation values of the fluctuating fields are denoted by

$$h_{\mu\nu} = \langle \widehat{h}_{\mu\nu} \rangle = \frac{1}{\sqrt{\bar{g}}} \frac{\delta W_k}{\delta t^{\mu\nu}} \,, \quad \xi^\mu = \langle C^\mu \rangle = \frac{1}{\sqrt{\bar{g}}} \frac{\delta W_k}{\delta \bar{\sigma}_\mu} \,, \quad \bar{\xi}_\mu = \langle \bar{C}_\mu \rangle = \frac{1}{\sqrt{\bar{g}}} \frac{\delta W_k}{\delta \sigma^\mu} \,. \tag{2.42}$$

With these in place, one uses the Legendre-Fenchel transform to define

$$\tilde{\Gamma}_k[h, \xi, \bar{\xi}; \bar{g}] = \int \mathrm{d}^d x \sqrt{\bar{g}} \big(t^{\mu\nu} h_{\mu\nu} + \bar{\sigma}_\mu \xi^\mu + \sigma^\mu \bar{\xi}_\mu \big) - W_k[t, \sigma, \bar{\sigma}; \bar{g}] \tag{2.43}$$

where it is understood that there is no source-dependence on the RHS of this equation, since this can be expressed in terms of the expectation values using equations (2.42). Finally, one then obtains the effective average action for gravity as

$$\Gamma_k[h, \xi, \bar{\xi}; \bar{g}] = \tilde{\Gamma}_k[h, \xi, \bar{\xi}; \bar{g}] - \Delta S_k[h, \xi, \bar{\xi}; \bar{g}] \,. \tag{2.44}$$

With this formal definition in place, we discuss its relevant properties below.

The EAA for gravity as derived above shares many properties with the one derived in the scalar case. In particular, it satisfies a flow equation, the FRGE for gravity:

$$\begin{aligned} \partial_t \Gamma_k[h, \xi, \bar{\xi}; \bar{g}] = {} & \frac{1}{2} \mathrm{Tr} \left[\left(\Gamma_k^{(2)} + \widehat{\mathcal{R}}_k \right)^{-1}_{hh} \left(\partial_t \widehat{\mathcal{R}}_k \right)_{hh} \right] \\ & - \frac{1}{2} \mathrm{Tr} \left[\left\{ \left(\Gamma_k^{(2)} + \widehat{\mathcal{R}}_k \right)^{-1}_{\bar{\xi}\xi} - \left(\Gamma_k^{(2)} + \widehat{\mathcal{R}}_k \right)^{-1}_{\xi\bar{\xi}} \right\} \left(\partial_t \widehat{\mathcal{R}}_k \right)_{\bar{\xi}\xi} \right] . \end{aligned} \tag{2.45}$$

At first sight, this equation may seem more involved than the one for the scalar case. However, we shall see that it can be written in a concise way, resembling the FRGE (2.10). Nevertheless, let us first explain the ingredients of this version (2.45).

The regulator $\widehat{\mathcal{R}}_k$ is a matrix in field space, whose components are given by

$$\left(\widehat{\mathcal{R}}_k \right)^{\mu\nu\rho\sigma}_{hh} = \kappa^2 \left(\mathcal{R}_k^{\mathrm{grav}}[\bar{g}] \right)^{\mu\nu\rho\sigma} \,, \tag{2.46a}$$

$$\left(\widehat{\mathcal{R}}_k \right)_{\bar{\xi}\xi} = \sqrt{2}\, \mathcal{R}_k^{\mathrm{gh}}[\bar{g}] \,. \tag{2.46b}$$

Just as eq. (2.10), the FRGE for gravity is convergent both in the IR and the UV, and the implicit UV cutoff can be removed. However, this equation does exhibit a new feature absent in the simpler scalar case; it has a bi-metric character since it depends on both g and $\bar{g}$. Hence, the actions that make up theory space exhibit a dependence on both g and $\bar{g}$ as well as the (anti-)ghost fields, signifying that the space on which the flow equation is defined is extremely complicated. Nonetheless, one can formulate the FRGE in a simpler form:

$$\boxed{\partial_t \Gamma_k = \frac{1}{2} \mathrm{STr} \left[\left(\Gamma_k^{(2)} + \widehat{\mathcal{R}}_k \right)^{-1} \partial_t \widehat{\mathcal{R}}_k \right]} \,, \tag{2.47}$$

where the supertrace denoted by "STr" implicitly provides a sum over the fields $\{h, \xi, \bar{\xi}\}$ as well as providing necessary minus signs for the (anti-)ghost fields.

Chapter 3

A first example: scalar-tensor theory

In order to perform explicit calculations, one generally resorts to truncating theory space. The main focus of many of these calculations is the search for a non-Gaussian fixed point suitable for the asymptotic safety scenario. In essence, these investiations aim to provide evidence for part (A) of Weinberg's conjecture, see section 2.3. The natural starting point for such investigations is to truncate the effective average action to the form of the standard Einstein-Hilbert action,

$$S[g] = \frac{1}{16\pi G}\int \mathrm{d}^d x\sqrt{g}\big(-R+2\Lambda\big)\,. \tag{3.1}$$

It was found in [23] that such a suitable fixed point exists for spacetime dimensions $d > 2$. Beyond $d = 4$, it was found that the critical exponents acquired a more severe dependence on the shape function $R^{(0)}$.

This evidence in favour of the asymptotic safety conjecture was further substantiated by extending the truncation. For example, the inclusion of an R^2-term was performed in [24] and this was extended even further to higher-order polynomials of the Ricci curvature in [25]. By now, many more investigations have occured, and there is substantial evidence that such a fixed point for gravity exists [26–32]. However, most investigations rely on a particular type of truncation, known as the "single-metric type", in which one disregards the bi-metric character of the FRGE. We will see shortly how this works in more detail.

Nevertheless, a number of investigations have included the proper bi-metric dependence of the FRG. Examples include [33–37]. Summarizing the conclusions from this research, one finds that after a certain degree of complexity has been reached in single-metric investigations, it is advised to include the dependence of the fluctuating field $\widehat{h}$. In particular, this seems to improve quantitative results. Note also that the bi-metric investigations too provide evidence in favour of the asymptotic safety conjecture.

In this chapter, we perform the analysis of a single metric truncation. In particular, we consider a scalar field with a potential, minimally coupled to gravity. There are a number of motivations for this choice. First of all, such a scalar-tensor model provides a fruitful starting example since it builds on known results from the Einstein-Hilbert truncation. Investigating this system will illustrate the calculations involved in the FRG analysis outlined in chapter 2. Secondly, there exist known solutions for this model if one disregards gravity altogether. It has been

established that in this case, there exists a non-Gaussian fixed point in $d = 3$ that disappears as one increases the dimension to $d = 4$ [38]. It will be interesting to see if this property persists in the presence of gravity. For a similar investigation, see [39]. Finally, if the fixed point analysis yields satisfactory results, this system can provide a model to compare with cosmological observations, in particular those regarding inflation.

The rest of this chapter is outlined as follows. In section 3.1 we introduce the system to be investigated. We then derive its flow equations in section 3.2, before analyzing the fixed point solutions in section 3.3. We end this chapter with concluding remarks in section 3.4.

3.1 Ansatz

In order to study this scalar-tensor system, we are required to make an ansatz for the effective average action. It takes the form

$$\Gamma_k[g,\phi,\xi,\bar{\xi},\bar{g}] = \Gamma_k^{\text{grav}}[g] + \Gamma_k^{\text{matter}}[g,\phi] + \Gamma_k^{\text{gf}}[g,\bar{g}] + S^{\text{gh}}[g,\xi,\bar{\xi},\bar{g}]\,, \tag{3.2}$$

with the gravitational term taken to be of Einstein-Hilbert form,

$$\Gamma_k^{\text{grav}}[g] = -\frac{1}{16\pi G_k}\int \mathrm{d}^d x\sqrt{g}R\,, \tag{3.3}$$

where G_k denotes the scale-dependent Newton's coupling. The cosmological constant has been moved to the potential in the matter sector, which is given by

$$\Gamma_k^{\text{matter}}[g,\phi] = \int \mathrm{d}^d x\sqrt{g}\left(\frac{1}{2}\phi\Delta\phi + V_k(\phi)\right) \quad \text{with} \quad V_k(\phi) = \sum_{n=0}^{N} u_{k,2n}\phi^{2n}\,. \tag{3.4}$$

The scalar field ϕ has a canonical kinetic term with the Laplacian defined as $\Delta \equiv -D^2$. Moreover, the polynomial potential $V_k(\phi)$ contains scale-dependent couplings $u_{k,2n}$ and its order N is left unspecified for the moment. Note the relation between the constant (ϕ-independent) term in the potential, $u_{k,0}$ and the cosmological constant Λ_k:

$$u_{k,0} = \frac{\Lambda_k}{8\pi G_k}\,. \tag{3.5}$$

This relation will prove convenient to compare our results to the literature.

The gravitational and matter sectors are supplemented by a gauge-fixing term. Adopting harmonic gauge, this takes the form

$$\Gamma_k^{\text{gf}}[g,\bar{g}] = \frac{1}{32\pi G_k}\int \mathrm{d}^d x\sqrt{\bar{g}}F_\mu\bar{g}^{\mu\nu}F_\nu \quad \text{with} \quad F_\mu = \bar{D}^\nu g_{\nu\mu} - \frac{1}{2}\bar{g}^{\alpha\beta}\bar{D}_\mu g_{\alpha\beta}\,. \tag{3.6}$$

Finally, these three sectors are accompanied by a scale-independent ghost action

$$S^{\text{gh}}[g,\xi,\bar{\xi},\bar{g}] = -\sqrt{2}\int \mathrm{d}^d x\sqrt{\bar{g}}\,\bar{\xi}_\mu\big(\bar{g}^{\mu\rho}\bar{D}^\sigma(g_{\rho\nu}D_\sigma + g_{\sigma\nu}D_\rho) - g^{\rho\sigma}\bar{D}^\mu\bar{g}_{\sigma\nu}D_\rho\big)\xi^\nu\,. \tag{3.7}$$

Here we assume that the ghost action S^{gh} is independent of the scale k. In other words, we

expect that this behaves classically and its quantum contributions are negligible [40,41]. Upon making this ansatz, the FRGE (2.45) takes a slightly different form,

$$\partial_t \Gamma_k[g,\phi,\bar{g}] = \frac{1}{2}\mathrm{Tr}\left[\left(\Gamma_k^{(2)}[g,\phi,\bar{g}] + \mathcal{R}_k^{\mathrm{g,m}}[\bar{g}]\right)^{-1}\partial_t \mathcal{R}_k^{\mathrm{g,m}}[\bar{g}]\right] - \mathrm{Tr}\left[\left(-\mathcal{M}[g,\bar{g}] + \mathcal{R}_k^{\mathrm{gh}}[\bar{g}]\right)^{-1}\partial_t \mathcal{R}_k^{\mathrm{gh}}[\bar{g}]\right]. \tag{3.8}$$

Here, the superscript "g,m" denotes the combined gravitational-matter sector. Furthermore, the Faddeev-Popov operator $\mathcal{M}[g,\bar{g}]$ is given by eq. (2.37) with $\varpi = 1/2$.

3.2 Derivation of the flow equations

The aim of this section is to evaluate the flow equation (3.8) to obtain the β-functions of the couplings involved. The first step in this calculation involves computing the Hessian $\Gamma_k^{(2)}$. After this step has been completed, we employ the actual single metric approximation, that is, we set the fluctuation field $h_{\mu\nu}$ to zero, or $g_{\mu\nu} = \bar{g}_{\mu\nu}$.

3.2.1 Hessian

The calculation of the Hessian operator $\Gamma_k^{(2)}$ is technically quite involved. Therefore, in the main body of this thesis we focus on the results and refer the reader to appendix A.2 for the details of the calculation.[1]

Since the system under investigation involves both symmetric $(0,2)$-tensors and scalars, there are four components of the Hessian: a tensor-tensor component, a scalar-scalar component and two off-diagonal components.[2]

For the tensor-tensor component, one obtains

$$\begin{aligned}\left[\Gamma_{k,hh}^{(2)}\right]_{\mu\nu}^{\ \ \rho\sigma} =& \frac{1}{32\pi G_k}\Big(\delta^\rho{}_\mu\delta^\sigma{}_\nu R + \frac{1}{2-d}g_{\mu\nu}g^{\rho\sigma}R - \frac{2}{2-d}g_{\mu\nu}R^{\rho\sigma} + g^{\rho\sigma}R_{\mu\nu} - 2\delta^\rho{}_\mu R^\sigma{}_\nu \\ &+ 2R^\rho{}_{\mu\nu}{}^\sigma + \delta^\rho{}_\mu\delta^\sigma{}_\nu\Delta\Big) - \frac{1}{2}\delta^\rho{}_\mu\delta^\sigma{}_\nu V_k(\phi) - \frac{1}{4}g^{\rho\sigma}(D_\mu\phi)(D_\nu\phi) \\ &+ \frac{1}{2}\frac{1}{2-d}g_{\mu\nu}(D^\rho\phi)(D^\sigma\phi) + \delta^\sigma{}_\mu(D^\rho\phi)(D_\nu\phi) - \frac{1}{4}\frac{1}{2-d}g_{\mu\nu}g^{\rho\sigma}(D^\lambda\phi)(D_\lambda\phi) \\ &- \frac{1}{4}\delta^\sigma{}_\mu\delta^\rho{}_\nu(D^\lambda\phi)(D_\lambda\phi)\,.\end{aligned} \tag{3.9}$$

The scalar-scalar component is found to be

$$\Gamma_{k,\phi\phi}^{(2)} = \Delta + V_k''(\phi) \tag{3.10}$$

[1] The resulting expressions for the components of the Hessian (3.9) - (3.12) may differ from those found in the literature due to different calculational methods. Generally, one expands Γ_k to second order in the fluctuation fields to read off the matrix elements of the Hessian. Instead, our calculation relies on the definitions in appendix A.2, in particular equations (A.37), (A.48), (A.51) and (A.54). Nonetheless, the resulting flow equations do agree with the literature.

[2] All components of the Hessian are symmetric in their appropriate indices. However, we suppress this symmetrization for presentational ease. Hence, it is understood that there is an implicit symmetrization present in equations (3.9), (3.11) and (3.12).

where the primes on $V_k''(\phi)$ denote derivatives w.r.t. the argument ϕ. Furthermore, the tensor-scalar component is

$$\left[\Gamma^{(2)}_{k,h\phi}\right]_{\mu\nu} = \frac{1}{2-d} g_{\mu\nu} V_k'(\phi) - (D_\mu \phi) D_\nu \,. \tag{3.11}$$

Finally, the scalar-tensor component is

$$\left[\Gamma^{(2)}_{k,\phi h}\right]^{\mu\nu} = \frac{1}{2} g^{\mu\nu}(\Delta\phi) + \frac{1}{2} g^{\mu\nu} V_k'(\phi) - \frac{1}{2} g^{\mu\nu}(D^\lambda \phi) D_\lambda + (D^\mu D^\nu \phi) + (D^\mu \phi) D^\nu \,. \tag{3.12}$$

These different components can be combined into the full Hessian in matrix notation,

$$\Gamma^{(2)}_k = \begin{bmatrix} \Gamma^{(2)}_{k,hh} & \Gamma^{(2)}_{k,h\phi} \\ \Gamma^{(2)}_{k,\phi h} & \Gamma^{(2)}_{k,\phi\phi} \end{bmatrix} . \tag{3.13}$$

Looking at eq. (3.8), the next step is to add the regulators. We add these to the diagonal components only, obtaining

$$\Gamma^{(2)}_k + \mathcal{R}_k = \begin{bmatrix} \Gamma^{(2)}_{k,hh} + \mathcal{R}_{k,hh} & \Gamma^{(2)}_{k,h\phi} \\ \Gamma^{(2)}_{k,\phi h} & \Gamma^{(2)}_{k,\phi\phi} + \mathcal{R}_{k,\phi\phi} \end{bmatrix} . \tag{3.14}$$

The regulators in the tensor and scalar sector, $\mathcal{R}_{k,hh}$ and $\mathcal{R}_{k,\phi\phi}$, are left unspecified for the moment.

3.2.2 Inversion

In order to calculate the inverse of (3.14), we make use of the following identity for block matrix inversion:

$$\begin{bmatrix} A & B \\ C & D \end{bmatrix}^{-1} = \begin{bmatrix} A^{-1} + A^{-1}B(D - CA^{-1}B)^{-1}CA^{-1} & -A^{-1}B(D - CA^{-1}B)^{-1} \\ -(D - CA^{-1}B)^{-1}CA^{-1} & (D - CA^{-1}B)^{-1} \end{bmatrix} . \tag{3.15}$$

Here, A, B, C and D are block matrices of (mostly) arbitrary size.[3] Applying this identity to eq. (3.14), it is obvious that the expressions are going to be complicated. Since we are going to calculate the trace of this matrix, we only require the expressions on the diagonal. For the top-left component of the inverse, we find

$$\begin{aligned} \left[\left(\Gamma^{(2)}_k + \mathcal{R}_k\right)^{-1}\right]_{hh} &= \left(\Gamma^{(2)}_{k,hh} + \mathcal{R}_{k,hh}\right)^{-1} \\ &+ \left(\Gamma^{(2)}_{k,hh} + \mathcal{R}_{k,hh}\right)^{-1} \Gamma^{(2)}_{k,h\phi} \left(\Gamma^{(2)}_{k,\phi\phi} + \mathcal{R}_{k,\phi\phi} - \Gamma^{(2)}_{k,\phi h} \left(\Gamma^{(2)}_{k,hh} + \mathcal{R}_{k,hh}\right)^{-1} \Gamma^{(2)}_{k,h\phi}\right)^{-1} \times \\ &\times \Gamma^{(2)}_{k,\phi h} \left(\Gamma^{(2)}_{k,hh} + \mathcal{R}_{k,hh}\right)^{-1} . \end{aligned} \tag{3.16}$$

Furthermore, the other diagonal component is found to equal

$$\left[\left(\Gamma^{(2)}_k + \mathcal{R}_k\right)^{-1}\right]_{\phi\phi} = \left(\Gamma^{(2)}_{k,\phi\phi} + \mathcal{R}_{k,\phi\phi} - \Gamma^{(2)}_{k,\phi h} \left(\Gamma^{(2)}_{k,hh} + \mathcal{R}_{k,hh}\right)^{-1} \Gamma^{(2)}_{k,h\phi}\right)^{-1} . \tag{3.17}$$

[3] The only requirement on their size is that A and D are square in order to be invertible.

These expressions, combined with the results for the Hessian components, are quite horrendous. Luckily, we can make some drastic simplifications.

3.2.3 Projection

Without loss of generality, we are allowed to make suitable projections onto basis functionals of theory space. If chosen properly, such projections can greatly reduce the number of terms in the equations. To decide what is suitable in this case, is is instructive to consider the LHS of the FRGE. Upon identifying $\bar{g} = g$, the gauge-fixing action vanishes and one obtains

$$\partial_t \Gamma_k[g, \phi] = -\frac{1}{16\pi} \partial_t \left(\frac{1}{G_k} \right) \int \mathrm{d}^d x \sqrt{g} R + \int \mathrm{d}^d x \sqrt{g} \partial_t V_k(\phi) \,. \tag{3.18}$$

Hence, if we choose to set $\phi = 0$, only Newton's constant and the constant term in the potential remain. In particular, we obtain

$$\partial_t \Gamma_k[g, 0] = -\frac{1}{16\pi} \partial_t \left(\frac{1}{G_k} \right) \int \mathrm{d}^d x \sqrt{g} R + \int \mathrm{d}^d x \sqrt{g} \partial_t u_{k,0} \,. \tag{3.19}$$

In order to obtain the β-functions for the remaining couplings G_k and $u_{k,0}$ it suffices to work on maximally symmetric spaces and expand the RHS of the FRGE in powers of the Ricci curvature R. Matching the powers of R on the left- and right-hand-side then yields these β-functions.

However, when we wish to calculate the flow equations of the other couplings in the potential V_k, we require a different projection. Since in that case we no longer care about the gravitational couplings, projecting on flat space is convenient. This is achieved by setting $g = \delta$, which implies $R = 0$. Moreover, as we are not considering terms with derivatives acting on the scalar field, we can set it to a constant value $\phi(x) = \bar{\phi}$.[4] Expanding the RHS of the FRGE in powers of $\bar{\phi}$ enables us to match the powers of $\bar{\phi}$ on both sides and obtain the β-couplings for the couplings $u_{k,2n}$, $n \neq 0$.

Gravitational sector

We start by investigating the gravitational sector. To this end, we set $\phi = 0$ and project on a maximally symmetric space. In this case, the Riemann and Ricci tensors are given by [42]

$$R_{\mu\nu\rho\sigma} = \frac{1}{d(d-1)} (g_{\mu\rho} g_{\nu\sigma} - g_{\mu\sigma} g_{\nu\rho}) R \,, \tag{3.20a}$$

$$R_{\mu\nu} = \frac{1}{d} g_{\mu\nu} R \,. \tag{3.20b}$$

With these choices, the off-diagonal components of the Hessian vanish and others simplify. The

[4] Only the kinetic term for the scalar field contains derivatives, but we did not associate a coupling constant to this term. This addition of a wavefunction renormalization could be a next extension of this truncation, though.

non-vanishing components are

$$\left[\Gamma^{(2)}_{k,hh}\right]_{\mu\nu}{}^{\rho\sigma}\Big|_{\phi=0} = \frac{1}{32\pi G_k}\left(\delta^\rho{}_\mu\delta^\sigma{}_\nu\left[\Delta + C_T R - 16\pi G_k u_{k,0}\right] + g_{\mu\nu}g^{\rho\sigma}CR\right)\,, \tag{3.21a}$$

$$\Gamma^{(2)}_{k,\phi\phi}\Big|_{\phi=0} = \Delta + 2u_{k,2}\,, \tag{3.21b}$$

where we have defined the dimension-dependent constants

$$C_T \equiv \frac{d(d-3)+4}{d(d-1)}\,, \qquad C \equiv \frac{-2}{d(d-1)}\,. \tag{3.22}$$

The tensor-tensor component (3.21a) is not proportional to the unit operator working on symmetric $(0,2)$-tensors, $\mathbb{1}^{\rho\sigma}{}_{\mu\nu} = \frac{1}{2}(\delta^\rho{}_\mu\delta^\sigma{}_\nu + \delta^\rho{}_\nu\delta^\sigma{}_\mu)$,[5] but instead contains the additional term $g_{\mu\nu}g^{\rho\sigma}CR$. In order to make use of convenient calculational techniques later on, we need (3.21a) to be proportional to the unit operator on a suitable subspace. To this end, we decompose the symmetric $(0,2)$-tensor into a traceless $(0,2)$-tensor and a trace-mode. This is achieved by introducing the projector on trace-modes

$$(P_t)_{\mu\nu}{}^{\rho\sigma} = \frac{1}{d}g_{\mu\nu}g^{\rho\sigma}\,. \tag{3.23}$$

Now, the tensor-tensor component may be rewritten as

$$\left[\Gamma^{(2)}_{k,hh}\right]_{\mu\nu}{}^{\rho\sigma}\Big|_{\phi=0} = \frac{1}{32\pi G_k}\Big(\left(\mathbb{1} - P_t\right)_{\mu\nu}{}^{\rho\sigma}\left[\Delta - 2\Lambda_k + C_T R\right] + \left(P_t\right)_{\mu\nu}{}^{\rho\sigma}\left[\Delta - 2\Lambda_k + C_S R\right]\Big) \tag{3.24}$$

where we introduced the cosmological constant using the relation (3.5) in order to make contact with the literature at a later stage. Furthermore, we have defined

$$C_S \equiv \frac{d-4}{d}\,. \tag{3.25}$$

The next step in the calculations involves choosing the regulators $\mathcal{R}_{k,hh}$ and $\mathcal{R}_{k,\phi\phi}$. Either of these has the structure (2.39). Since the kinetic terms of the traceless and the trace part in (3.24) have the same normalization, we choose the matrix $\mathcal{Z}_{k,hh}$ proportional to the identity:

$$\mathcal{Z}_{k,hh} = \frac{1}{32\pi G_k}\mathbb{1}\,. \tag{3.26}$$

Furthermore, since there is no tensor structure in the scalar sector and there is no wavefunction renormalization for the scalar field, we choose $\mathcal{Z}_{k,\phi\phi} = 1$. As we have split the tensor-tensor

[5] Recall the implicit symmetrization carrying through into eq. (3.21a).

component in a trace and a traceless part, we now obtain three operators

$$\Gamma^{(2)}_{k,hh,tl} + \mathcal{R}_{k,hh} = \frac{1}{32\pi G_k}\left[\Delta + k^2 R^{(0)}\left(\frac{\Delta}{k^2}\right) - 2\Lambda_k + C_T R\right], \tag{3.27a}$$

$$\Gamma^{(2)}_{k,hh,t} + \mathcal{R}_{k,hh} = \frac{1}{32\pi G_k}\left[\Delta + k^2 R^{(0)}\left(\frac{\Delta}{k^2}\right) - 2\Lambda_k + C_S R\right], \tag{3.27b}$$

$$\Gamma^{(2)}_{k,\phi\phi} + \mathcal{R}_{k,\phi\phi} = \Delta + k^2 R^{(0)}\left(\frac{\Delta}{k^2}\right) + 2u_{k,2}\,. \tag{3.27c}$$

Here, the subscripts tl and t represent the traceless and trace-modes, respectively. With these expressions in place, we are almost ready to assemble the traces. However, so far we have not considered the second term in the FRGE (3.8), the trace over ghost fields. At $\bar{g} = g$, the Faddeev-Popov operator evaluates to

$$\mathcal{M}^{\mu}{}_{\nu} = -\delta^{\mu}{}_{\nu}[\Delta + C_V R]\,, \quad \text{with} \quad C_V \equiv -\frac{1}{d}\,. \tag{3.28}$$

Since we have neglected all scale-dependence in the ghost sector, we choose $\mathcal{Z}_k = 1$. The fourth operator to join the list (3.27) then becomes

$$-\mathcal{M} + \mathcal{R}^{\rm gh}_k = \Delta + k^2 R^{(0)}\left(\frac{\Delta}{k^2}\right) + C_V R\,. \tag{3.29}$$

Now, we can write down the components of the inverse, (3.16) and (3.17). Due to the projection, these equations simplify significantly. One finds

$$\left[\left(\Gamma^{(2)}_k + \mathcal{R}_k\right)^{-1}\right]_{hh}\Big|_{\phi=0} = \left(\Gamma^{(2)}_{k,hh} + \mathcal{R}_{k,hh}\right)^{-1}, \tag{3.30a}$$

$$\left[\left(\Gamma^{(2)}_k + \mathcal{R}_k\right)^{-1}\right]_{\phi\phi}\Big|_{\phi=0} = \left(\Gamma^{(2)}_{k,\phi\phi} + \mathcal{R}_{k,\phi\phi}\right)^{-1}. \tag{3.30b}$$

This allows us to write down the RHS of the FRGE as

$$\begin{aligned}
&\frac{1}{2}\mathrm{Tr}\left[\left(\Gamma^{(2)}_k + \mathcal{R}_k\right)^{-1}\partial_t \mathcal{R}_k\right] - \mathrm{Tr}\left[\left(-\mathcal{M} + \mathcal{R}^{\rm gh}_k\right)^{-1}\partial_t \mathcal{R}^{\rm gh}_k\right] = \\
&\frac{1}{2}\mathrm{Tr}_T\left[\left(\Gamma^{(2)}_{k,hh,tl} + \mathcal{R}_{k,hh}\right)^{-1}\partial_t \mathcal{R}_{k,hh}\right] + \frac{1}{2}\mathrm{Tr}_S\left[\left(\Gamma^{(2)}_{k,hh,t} + \mathcal{R}_{k,hh}\right)^{-1}\partial_t \mathcal{R}_{k,hh}\right] \\
&+ \frac{1}{2}\mathrm{Tr}_S\left[\left(\Gamma^{(2)}_{k,\phi\phi} + \mathcal{R}_{k,\phi\phi}\right)^{-1}\partial_t \mathcal{R}_{k,\phi\phi}\right] - \mathrm{Tr}_V\left[\left(-\mathcal{M} + \mathcal{R}^{\rm gh}_k\right)^{-1}\partial_t \mathcal{R}^{\rm gh}_k\right].
\end{aligned} \tag{3.31}$$

Here, the subscript on a trace denotes the space on which the operator acts. T denotes symmetric traceless $(0,2)$-tensors, S represents scalars and V represents vectors.

Above we obtained the expressions for the inverses. The final ingredients of the traces are

the derivatives of the regulators. These are

$$\partial_t \mathcal{R}_{k,hh} = \frac{1}{16\pi G_k}\left[\left(1-\frac{1}{2}\eta_N\right)k^2 R^{(0)}\left(\frac{\Delta}{k^2}\right) - \Delta R^{(0)'}\left(\frac{\Delta}{k^2}\right)\right], \tag{3.32a}$$

$$\partial_t \mathcal{R}_{k,\phi\phi} = 2\left[k^2 R^{(0)}\left(\frac{\Delta}{k^2}\right) - \Delta R^{(0)'}\left(\frac{\Delta}{k^2}\right)\right], \tag{3.32b}$$

$$\partial_t \mathcal{R}^{\mathrm{gh}}_k = 2\left[k^2 R^{(0)}\left(\frac{\Delta}{k^2}\right) - \Delta R^{(0)'}\left(\frac{\Delta}{k^2}\right)\right]. \tag{3.32c}$$

Here, a prime denotes a derivative w.r.t. the argument. Additionally, we introduced the *anomalous dimension* of Newton's constant as

$$\eta_N = -\partial_t \ln\left(\frac{\bar{G}}{G_k}\right) \tag{3.33}$$

where $\bar{G}$ is a fixed reference scale for Newton's coupling.

Finally, we have gathered all ingredients of the traces. The next step involves the introduction of some new notation. Denoting the RHS of the FRGE evaluated at $\bar{g} = g$ by $\mathcal{S}_k(R)$, we write

$$\begin{aligned}\mathcal{S}_k(R) =& \mathrm{Tr}_T[\mathcal{N}\left(\mathcal{A}+C_T R\right)^{-1}] + \mathrm{Tr}_S[\mathcal{N}\left(\mathcal{A}+C_S R\right)^{-1}] + \mathrm{Tr}_S[\mathcal{N}_0\left(\mathcal{A}_0+2u_{k,2}\right)^{-1}] \\ &- 2\mathrm{Tr}_V[\mathcal{N}_0\left(\mathcal{A}_0+C_V R\right)^{-1}]\end{aligned} \tag{3.34}$$

where we have defined

$$\mathcal{A} = \Delta + k^2 R^{(0)}\left(\frac{\Delta}{k^2}\right) - 2\Lambda_k\,, \tag{3.35a}$$

$$\mathcal{N} = \left(1-\frac{1}{2}\eta_N\right)k^2 R^{(0)}\left(\frac{\Delta}{k^2}\right) - \Delta R^{(0)'}\left(\frac{\Delta}{k^2}\right). \tag{3.35b}$$

Moreover, $\mathcal{A}_0$ and $\mathcal{N}_0$ are defined with $\Lambda_k = 0$ and $\eta_N = 0$.

In order to obtain the β-functions, we need to expand the RHS of the FRGE. To this end, we expand eq. (3.34) in powers of R,

$$\begin{aligned}\mathcal{S}_k(R) =& \mathrm{Tr}_T[\mathcal{N}\mathcal{A}^{-1}] + \mathrm{Tr}_S[\mathcal{N}\mathcal{A}^{-1}] + \mathrm{Tr}_S[\mathcal{N}_0\left(\mathcal{A}_0+2u_{k,2}\right)^{-1}] - 2\mathrm{Tr}_V[\mathcal{N}_0\mathcal{A}_0^{-1}] \\ &- R\big(C_T\mathrm{Tr}_T[\mathcal{N}\mathcal{A}^{-2}] + C_S\mathrm{Tr}_S[\mathcal{N}\mathcal{A}^{-2}] - 2C_V\mathrm{Tr}_V[\mathcal{N}_0\mathcal{A}_0^{-2}]\big) + \mathcal{O}(R^2)\,.\end{aligned} \tag{3.36}$$

Since the LHS of the FRGE (3.19) only has terms up to $\mathcal{O}(R)$, we neglect the higher order terms on the RHS.[6]

At this point, we are very close to obtaining the flow equations for G_k and Λ_k. The next step involves the calculation of the traces in eq. (3.36). To do so, we employ the *heat kernel techniques* reviewed in appendix A.3. The results are then conveniently written in terms of

[6] This is precisely one of the aspects of the Renormalization Group that makes it hard to work with. Even if at a certain scale k_1, there are no terms of $\mathcal{O}(R^2)$ and higher present in the EAA, these will be generated on the RHS of the flow equation. Thus, the key of the truncation approximation is setting these terms to zero.

dimensionless threshold functions defined as

$$\Phi_n^p(w) \equiv \frac{1}{\Gamma(n)} \int_0^\infty dz z^{n-1} \frac{R^{(0)}(z) - zR^{(0)\prime}(z)}{[z + R^{(0)}(z) + w]^p}\,, \tag{3.37a}$$

$$\tilde{\Phi}_n^p(w) \equiv \frac{1}{\Gamma(n)} \int_0^\infty dz z^{n-1} \frac{R^{(0)}(z)}{[z + R^{(0)}(z) + w]^p}\,. \tag{3.37b}$$

The results of the individual traces are given in the appendix. Combining those at $\mathcal{O}(R)$ and matching with the LHS of the FRGE gives the flow equation for G_k,

$$\begin{aligned}\partial_t\left(\frac{1}{G_k}\right) = &-\frac{1}{3}(4\pi)^{1-\frac{d}{2}}k^{d-2}\times \\ &\times\Bigg[d(d+1)\left\{\Phi^1_{\frac{d}{2}-1}\left(-2\frac{\Lambda_k}{k^2}\right) - \frac{1}{2}d(d+1)\eta_N(k)\tilde{\Phi}^1_{\frac{d}{2}-1}\left(-2\frac{\Lambda_k}{k^2}\right)\right\} \\ &- 6d(d-1)\left\{\Phi^2_{\frac{d}{2}}\left(-2\frac{\Lambda_k}{k^2}\right) - \frac{1}{2}\eta_N(k)\tilde{\Phi}^2_{\frac{d}{2}}\left(-2\frac{\Lambda_k}{k^2}\right)\right\} \\ &+ 2\Phi^1_{\frac{d}{2}-1}\left(2\frac{u_{k,2}}{k^2}\right) - 4d\Phi^1_{\frac{d}{2}-1}(0) - 24\Phi^2_{\frac{d}{2}}(0)\Bigg]\,.\end{aligned} \tag{3.38}$$

Similarly, combining the terms at $\mathcal{O}(1)$ yields the flow equation for $u_{k,0} = \Lambda_k/(8\pi G_k)$,

$$\begin{aligned}\partial_t\left(\frac{\Lambda_k}{G_k}\right) = \frac{1}{2}(4\pi)^{1-\frac{d}{2}}k^d\Bigg[&2d(d+1)\Phi^1_{\frac{d}{2}}\left(-2\frac{\Lambda_k}{k^2}\right) - d(d+1)\eta_N(k)\tilde{\Phi}^1_{\frac{d}{2}}\left(-2\frac{\Lambda_k}{k^2}\right) \\ &+4\Phi^1_{\frac{d}{2}}\left(2\frac{u_{k,2}}{k^2}\right) - 8d\Phi^1_{\frac{d}{2}}(0)\Bigg]\,.\end{aligned} \tag{3.39}$$

Following eq. (2.21) it is convenient to switch to the dimensionless couplings

$$g_k \equiv k^{d-2}G_k\,, \qquad \lambda_k \equiv k^{-2}\Lambda_k\,, \qquad v_{k,2n} \equiv k^{d(n-1)-2n}u_{k,2n}\,. \tag{3.40}$$

The β-function for the dimensionless Newton's coupling becomes

$$\partial_t g_k = [d - 2 + \eta_N(g_k, \lambda_k, v_{k,2})]g_k\,, \tag{3.41}$$

with the anomalous dimension $\eta_N(g_k, \lambda_k, v_{k,2})$ obtained from the flow equation of G_k, eq. (3.38),

$$\eta_N(g_k, \lambda_k, v_{k,2}) = \frac{g_k B_1(\lambda_k, v_{k,2})}{1 - g_k B_2(\lambda_k)}\,. \tag{3.42}$$

The functions B_1 and B_2 are given by

$$B_1(\lambda_k, v_{k,2}) \equiv \frac{1}{3}(4\pi)^{1-\frac{d}{2}}\Big[d(d+1)\Phi^1_{\frac{d}{2}-1}(-2\lambda_k) - 6d(d-1)\Phi^2_{\frac{d}{2}}(-2\lambda_k) - 4d\Phi^1_{\frac{d}{2}-1}(0) - 24\Phi^2_{\frac{d}{2}}(0) + 2\Phi^1_{\frac{d}{2}-1}(2v_{k,2})\Big]\,, \tag{3.43a}$$

$$B_2(\lambda_k) \equiv -\frac{1}{6}(4\pi)^{1-\frac{d}{2}}\Big[d(d+1)\tilde{\Phi}^1_{\frac{d}{2}-1}(-2\lambda_k) - 6d(d-1)\tilde{\Phi}^2_{\frac{d}{2}}(-2\lambda_k)\Big]\,. \tag{3.43b}$$

Finally, one finds for the cosmological constant

$$\partial_t\lambda_k = -(2-\eta_N)\lambda_k + \frac{1}{2}g_k(4\pi)^{1-\frac{d}{2}}\Big[2d(d+1)\Phi^1_{\frac{d}{2}}(-2\lambda_k) - d(d+1)\eta_N\tilde{\Phi}^1_{\frac{d}{2}}(-2\lambda_k) - 8d\Phi^1_{\frac{d}{2}}(0) + 4\Phi^1_{\frac{d}{2}}(2v_{k,2})\Big]\,. \tag{3.44}$$

This concludes the search for the β-functions of the gravitational sector. The final results are

$$\beta_g(g_k, \lambda_k, v_{k,2}) = \partial_t g_k\,, \tag{3.45a}$$

$$\beta_\lambda(g_k, \lambda_k, v_{k,2}) = \partial_t \lambda_k\,, \tag{3.45b}$$

which are given by equations (3.41) and (3.44). Before moving on to the potential sector, we mention a few of their properties.

(1) Upon comparing these flow equations with those for the pure-gravity Einstein-Hilbert truncation as found in [23], one finds that the sets of equations agree in the corresponding limit. In fact, the only differences arise from the mass of the scalar field, which has been set to zero in [23]. Thus, the addition of a scalar field potential does not alter the gravitational flow equations all that much. One therefore expects that the gravitational non-Gaussian fixed point still exists in this truncation. This will be investigated in section 3.3.

(2) The flow equations exhibit a singular structure, since they depend on the choice of shape function $R^{(0)}(z)$ through the dependence on the threshold functions. Recall that the shape function interpolates between $R^{(0)}(0) = 1$ and $R^{(0)}(\infty) = 0$. Then, owed to the form of the threshold functions (3.37), $\Phi^p_n(w)$ and $\tilde{\Phi}^p_n(w)$ are only well-defined for $w > -1$. For $w \leq -1$, the denominator vanishes for values of z in the region of integration. Inspecting the gravitational β-functions, we see that they are only well-defined for $v_{k,2} > -\frac{1}{2}$ and $\lambda_k < \frac{1}{2}$ only.

Matter sector

Next, we turn to the matter sector. As mentioned earlier, to isolate the couplings in the potential V_k, we work with a flat background spacetime and set $\phi(x) = \bar{\phi}$. The components of

the Hessian, equations (3.9) - (3.12) then reduce to

$$\left[\Gamma^{(2)}_{k,hh}\right]_{\mu\nu}{}^{\rho\sigma} = \delta^{\rho}{}_{\mu}\delta^{\sigma}{}_{\nu}\left[\frac{1}{32\pi G_k}\Delta - \frac{1}{2}V_k(\bar{\phi})\right], \tag{3.46a}$$

$$\Gamma^{(2)}_{k,\phi\phi} = \Delta + V_k''(\bar{\phi}), \tag{3.46b}$$

$$\left[\Gamma^{(2)}_{k,h\phi}\right]_{\rho\sigma} = \frac{1}{2-d}\delta_{\rho\sigma}V_k'(\bar{\phi}), \tag{3.46c}$$

$$\left[\Gamma^{(2)}_{k,\phi h}\right]^{\mu\nu} = \frac{1}{2}\delta^{\mu\nu}V_k'(\bar{\phi}). \tag{3.46d}$$

Unfortunately, in this case the off-diagonal components do not vanish. For this reason, the components of the inverse do not simplify quite as much as was the case previously.

Restricting the regulators in eq. (3.27) to this background gives

$$\mathcal{R}_{k,hh} = \frac{1}{32\pi G_k}k^2R^{(0)}\left(\frac{\Delta}{k^2}\right), \tag{3.47a}$$

$$\mathcal{R}_{k,\phi\phi} = k^2R^{(0)}\left(\frac{\Delta}{k^2}\right). \tag{3.47b}$$

which combines nicely with the diagonal components of the Hessian, (3.46a) and (3.46b).

Moreover, the ghost sector does not contribute as it is independent of $\bar{\phi}$. We can then split the RHS of the FRGE into three traces,

$$\mathrm{Tr}\left[\left(\Gamma^{(2)}_k + \mathcal{R}_k\right)^{-1}\partial_t\mathcal{R}_k\right] = S_1 + S_2 + S_3, \tag{3.48}$$

where we have defined

$$S_1 = \mathrm{Tr}_T\left[\left(\Gamma^{(2)}_{k,hh} + \mathcal{R}_{k,hh}\right)^{-1}\partial_t\mathcal{R}_{k,hh}\right], \tag{3.49a}$$

$$S_2 = \mathrm{Tr}_S\left[\left(\Gamma^{(2)}_{k,hh} + \mathcal{R}_{k,hh}\right)^{-1}\Gamma^{(2)}_{k,h\phi}\left(\Gamma^{(2)}_{k,\phi\phi} + \mathcal{R}_{k,\phi\phi} - \Gamma^{(2)}_{k,\phi h}\left(\Gamma^{(2)}_{k,hh} + \mathcal{R}_{k,hh}\right)^{-1}\Gamma^{(2)}_{k,h\phi}\right)^{-1}\times\right.$$
$$\left.\times\,\Gamma^{(2)}_{k,\phi h}\left(\Gamma^{(2)}_{k,hh} + \mathcal{R}_{k,hh}\right)^{-1}\partial_t\mathcal{R}_{k,hh}\right], \tag{3.49b}$$

$$S_3 = \mathrm{Tr}_S\left[\left(\Gamma^{(2)}_{k,\phi\phi} + \mathcal{R}_{k,\phi\phi} - \Gamma^{(2)}_{k,\phi h}\left(\Gamma^{(2)}_{k,hh} + \mathcal{R}_{k,hh}\right)^{-1}\Gamma^{(2)}_{k,h\phi}\right)^{-1}\partial_t\mathcal{R}_{k,\phi\phi}\right]. \tag{3.49c}$$

Here, the subscript T denotes a trace over the space of symmetric $(0,2)$-tensors, and the subscript S indicates a trace over scalars.[7]

As we did in the calculation of the gravitational β-functions, we introduce some notation to

[7]Note the subscript S of the trace in S_2. Since this trace originates from the top-left component of the inverse, eq. (3.16), one would expect this to be a trace over $(0,2)$-tensors. However, inspecting the operator inside the trace shows that it is proportional to $\delta_{\rho\sigma}\delta^{\mu\nu}$ and hence projects on the trace-modes of the tensors. Thus, S_2 traces over scalars only.

rewrite these traces:

$$\mathcal{B} = \Delta + k^2 R^{(0)}\left(\frac{\Delta}{k^2}\right) - 16\pi G_k V_k(\bar{\phi})\,, \tag{3.50a}$$

$$\mathcal{D} = \Delta + k^2 R^{(0)}\left(\frac{\Delta}{k^2}\right) + V_k''(\bar{\phi})\,, \tag{3.50b}$$

$$\mathcal{E} = \frac{1}{32\pi G_k V_k'(\bar{\phi})^2}\mathcal{D}\,. \tag{3.50c}$$

We then write

$$S_1 = 2\mathrm{Tr}_T[\mathcal{N}\mathcal{B}^{-1}]\,, \tag{3.51a}$$

$$S_2 = \frac{d}{2-d}\mathrm{Tr}_S\left[\mathcal{B}^{-1}\left(\mathcal{E} - \frac{1}{2}\frac{d}{2-d}\mathcal{B}^{-1}\right)^{-1}\mathcal{B}^{-1}\mathcal{N}\right]\,, \tag{3.51b}$$

$$S_3 = \mathrm{Tr}_S\left[\left(\mathcal{D} - 16\pi G_k \frac{d}{2-d}V_k'(\bar{\phi})^2\mathcal{B}^{-1}\right)^{-1} 2\mathcal{N}_0\right] \tag{3.51c}$$

where the operators $\mathcal{N}$ and $\mathcal{N}_0$ are the same as in the gravitational sector.

To evaluate these expressions, we again employ the heat kernel expansion. Since we are working on flat space, we only need the term at $\mathcal{O}(1)$. This time, the results can be cast in terms of *generalized threshold functionals* defined as

$$\Phi_n^{(a,b)}[w,r] \equiv \frac{1}{\Gamma(n)}\int dz z^{n-1}\frac{R^{(0)}(z) - zR^{(0)\prime}(z)}{\big(P(z)+w\big)^a\big(P(z)+r\left(P(z)\right)\big)^b}\,, \tag{3.52a}$$

$$\tilde{\Phi}_n^{(a,b)}[w,r] \equiv \frac{1}{\Gamma(n)}\int dz z^{n-1}\frac{R^{(0)}(z)}{(P(z)+w)^a\big(P(z)+r\left(P(z)\right)\big)^b} \tag{3.52b}$$

where $P(z) = z + R^{(0)}(z)$. Note that these are functionals since they exhibit an additional dependence on a function r, as opposed to the threshold *functions* (3.37) which only depend on the argument w. For the explicit evaluation of the traces (3.51), we refer the reader to appendix A.3. The results are the following:

$$\begin{aligned} S_1 = {} & (4\pi)^{-\frac{d}{2}} d(d+1)k^d\Big\{\Phi^1_{\frac{d}{2}}\left(-16\pi k^{-2}G_k V_k(\bar{\phi})\right) \\ & - \frac{1}{2}\eta_N\tilde{\Phi}^1_{\frac{d}{2}}\left(-16\pi k^{-2}G_k V_k(\bar{\phi})\right)\Big\}\int \mathrm{d}^d x\,, \end{aligned} \tag{3.53a}$$

$$\begin{aligned} S_2 = {} & \frac{8d}{2-d}(4\pi)^{1-\frac{d}{2}}G_k V_k'(\bar{\phi})^2 k^{d-4}\Bigg\{\Phi^{(2,1)}_{\frac{d}{2}}\left[-16\pi G_k k^{-2}V_k(\bar{\phi}),\rho\right] \\ & - \frac{1}{2}\eta_N\tilde{\Phi}^{(2,1)}_{\frac{d}{2}}\left[-16\pi G_k k^{-2}V_k(\bar{\phi}),\rho\right]\Bigg\}\int \mathrm{d}^d x\,, \end{aligned} \tag{3.53b}$$

$$S_3 = 2(4\pi)^{-\frac{d}{2}}k^d\Phi^{(0,1)}_{\frac{d}{2}}[0,\rho]\int \mathrm{d}^d x\,, \tag{3.53c}$$

where the function ρ is defined as

$$\rho(x) \equiv k^{-2} V_k''(\bar{\phi}) + \frac{d}{2(d-2)} \frac{32\pi G_k k^{-4} V_k'(\bar{\phi})^2}{x - 16\pi G_k k^{-2} V_k(\bar{\phi})} \,. \tag{3.54}$$

In the following step, we switch to dimensionless variables. We define the dimensionless potential and scalar field as

$$\tilde{V}_k(\bar{\varphi}) \equiv k^{-d} V_k(\bar{\phi}) \,, \tag{3.55a}$$

$$\bar{\varphi} \equiv k^{\frac{2-d}{2}} \bar{\phi} \,. \tag{3.55b}$$

In terms of these quantities, the traces become

$$S_1 = d(d+1)(4\pi)^{-\frac{d}{2}} k^d \left\{ \Phi^1_{\frac{d}{2}} \left(-16\pi g_k \tilde{V}_k(\bar{\varphi}) \right) - \frac{1}{2} \eta_N \tilde{\Phi}^1_{\frac{d}{2}} \left(-16\pi g_k \tilde{V}_k(\bar{\varphi}) \right) \right\} \int \mathrm{d}^d x \,, \tag{3.56a}$$

$$S_2 = \frac{8d}{2-d} (4\pi)^{1-\frac{d}{2}} k^d g_k \tilde{V}_k'(\bar{\varphi})^2 \left\{ \Phi^{(2,1)}_{\frac{d}{2}} \left[-16\pi g_k \tilde{V}_k(\bar{\varphi}), \rho \right] \right.$$
$$\left. - \frac{1}{2} \eta_N \tilde{\Phi}^{(2,1)}_{\frac{d}{2}} \left[-16\pi g_k \tilde{V}_k(\bar{\varphi}), \rho \right] \right\} \int \mathrm{d}^d x \,, \tag{3.56b}$$

$$S_3 = 2(4\pi)^{-\frac{d}{2}} k^d \Phi^{(0,1)}_{\frac{d}{2}}[0, \rho] \int \mathrm{d}^d x \,. \tag{3.56c}$$

where now ρ can also be expressed in therms of the dimensionless variables,

$$\rho(x) = \tilde{V}_k''(\bar{\varphi}) - \frac{d}{4-2d} \frac{32\pi g_k \tilde{V}_k'(\bar{\varphi})^2}{x - 16\pi g_k \tilde{V}_k(\bar{\varphi})} \,. \tag{3.57}$$

There is now one more step left before we write down the RHS of the FRGE. Since it is convenient to extract the constant term from the potential, we write[8]

$$\tilde{V}_k(\bar{\varphi}) = W_k(\bar{\varphi}) + \lambda_k (8\pi g_k)^{-1} \,. \tag{3.58}$$

Now we are able to write down the RHS of the FRGE, having discarded the ghost sector since it does not contribute to the flow equation of W_k. One finds

$$\left\{ \frac{d(d+1)}{2} (4\pi)^{-\frac{d}{2}} k^d \left[\Phi^1_{\frac{d}{2}} \left(-2\lambda_k - 16\pi g_k W_k(\bar{\varphi}) \right) - \frac{1}{2} \eta_N \tilde{\Phi}^1_{\frac{d}{2}} \left(-2\lambda_k - 16\pi g_k W_k(\bar{\varphi}) \right) \right] \right.$$
$$+ \frac{4d}{2-d} (4\pi)^{1-\frac{d}{2}} k^d g_k W_k'(\bar{\varphi})^2 \left[\Phi^{(2,1)}_{\frac{d}{2}} \left[-2\lambda_k - 16\pi g_k W_k(\bar{\varphi}), \rho \right] \right.$$
$$\left. \left. - \frac{1}{2} \eta_N \tilde{\Phi}^{(2,1)}_{\frac{d}{2}} \left[-2\lambda_k - 16\pi g_k W_k(\bar{\varphi}), \rho \right] \right] + (4\pi)^{-\frac{d}{2}} k^d \Phi^{(0,1)}_{\frac{d}{2}}[0, \rho] \right\} \int \mathrm{d}^d x \,. \tag{3.59}$$

[8] This step is not strictly necessary since we already obtained the β-function for λ previously. However, we wish to find an expression for the flow equation of the full potential W_k that does not contain a constant term.

Next, we turn to the LHS of the FRGE. This becomes

$$\int \mathrm{d}^d x \partial_t V_k(\bar{\phi}) = k^d \left[dW_k(\bar{\varphi}) + \partial_t W_k(\bar{\varphi}) + \frac{1}{8\pi g_k}\big(\partial_t \lambda_k + \lambda_k(2-\eta_N)\big) + \frac{2-d}{2}\bar{\varphi}W_k'(\bar{\varphi})\right] \int \mathrm{d}^d x\,. \tag{3.60}$$

Equating both sides of the FRGE, we find the flow equation for the potential W_k,

$$\partial_t W_k(\bar{\varphi}) = -dW_k(\bar{\varphi}) - \frac{2-d}{2}\bar{\varphi}W_k'(\bar{\varphi}) + \mathcal{W}_1 + \eta_N \mathcal{W}_2 \tag{3.61}$$

with

$$\begin{aligned}\mathcal{W}_1[g_k,\lambda_k,W_k] = (4\pi)^{-\frac{d}{2}}\Bigg(&\frac{1}{2}d(d+1)\left[\Phi^1_{\frac{d}{2}}(-2\lambda_k - 16\pi g_k W_k(\bar{\varphi})) - \Phi^1_{\frac{d}{2}}(-2\lambda_k)\right]\\ &-\Phi^1_{\frac{d}{2}}(2v_{k,2}) + \frac{16\pi d}{2-d}g_k W_k'(\bar{\varphi})^2 \Phi^{(2,1)}_{\frac{d}{2}}[-2\lambda_k - 16\pi g_k W_k(\bar{\varphi}),\rho] + \Phi^{(0,1)}_{\frac{d}{2}}[0,\rho]\Bigg)\,,\end{aligned} \tag{3.62a}$$

$$\begin{aligned}\mathcal{W}_2[g_k,\lambda_k,W_k] = (4\pi)^{-\frac{d}{2}}\Bigg(&\frac{1}{4}d(d+1)\left[\tilde{\Phi}^1_{\frac{d}{2}}(-2\lambda_k) - \tilde{\Phi}^1_{\frac{d}{2}}(-2\lambda_k - 16\pi g_k W_k(\bar{\varphi}))\right]\\ &-\frac{8\pi d}{2-d}g_k W_k'(\bar{\varphi})^2 \tilde{\Phi}^{(2,1)}_{\frac{d}{2}}[-2\lambda_k - 16\pi g_k W_k(\bar{\varphi}),\rho]\Bigg)\,.\end{aligned} \tag{3.62b}$$

This concludes the search for the flow equations of this system. The flow equation (3.61) is the generating functional for the β-functions of the couplings $v_{k,2n}$ in the polynomial expansion of the potential W_k.

3.3 Analysis

Now that we obtained the flow equations for this system, we are able to analyze them. This analysis consists of finding the fixed points of the flow, as well as the critical exponents. If this yields interesting results, the following step is to integrate the flow to obtain a flow diagram consisting of RG-trajectories.

3.3.1 Cutoff choice

Before we are able to analyze the flow equations explicitly, we are required to choose the shape function $R^{(0)}(z)$. We choose the "optimized" cutoff [43],

$$R^{(0)}(z)^{\mathrm{opt}} = (1-z)\theta(1-z) \tag{3.63}$$

where $\theta(x)$ is the Heaviside step function. One of the advantages of this particular choice is that the generalized threshold functionals can be evaluated analytically. In particular, one finds

$$\Phi_n^p(w)^{\text{opt}} = \frac{1}{\Gamma(n+1)}\frac{1}{(1+w)^p}\,, \tag{3.64a}$$

$$\tilde{\Phi}_n^p(w)^{\text{opt}} = \frac{1}{\Gamma(n+2)}\frac{1}{(1+w)^p}\,, \tag{3.64b}$$

$$\Phi_n^{(a,b)}[w,r]^{\text{opt}} = \frac{1}{\Gamma(n+1)}\frac{1}{(1+w)^a(1+r(1))^b}\,, \tag{3.64c}$$

$$\tilde{\Phi}_n^{(a,b)}[w,r]^{\text{opt}} = \frac{1}{\Gamma(n+2)}\frac{1}{(1+w)^a(1+r(1))^b}\,. \tag{3.64d}$$

3.3.2 Fixed point analysis

We are now able to analyze the flow generated by the β-functions of the system. At this moment, the order of the potential, $2N$, is unspecified, as is the dimension of spacetime, d. The starting point of our analysis is $N = 2$, after which we gradually increase N as long as the computation time stays within reasonable bounds.

The β-function for the potential W_k is broken down into N flow equations for the couplings $v_{k,2n}$. These are found by expanding eq. (3.61) in powers of $\bar{\varphi}$. Together with the gravitational β-functions, we obtain a set of $2 + N$ equations. In order to find the fixed points, we look for simultaneous zeroes of the flow equations. These are sought for using Mathematica's function *NSolve*.

Three dimensions

We start our analysis in three-dimensional spacetime. The main reason for this is that in $d = 3$ and for $N = 2$, it is known that in the pure-scalar case, there exist a trivial (Gaussian) and a nontrivial (non-Gaussian) fixed point. The latter is known as the Wilson-Fisher (WF) fixed point [38] and will provide a useful reference to test our results. Its coordinates are[9]

$$v_2 \approx -0.03846 \qquad , \qquad v_4 \approx 0.3234 \tag{3.65}$$

and the corresponding critical exponents are

$$\theta_1 \approx 1.8425 \qquad , \qquad \theta_2 \approx -1.1759\,. \tag{3.66}$$

An interesting question to ask is what happens to this fixed point under the influence of gravity. Our obtained results for $N = 2$ are given in table 3.1.

In the first table, the coordinates $(g^*, \lambda^*, v_2^*, v_4^*)$ of the fixed points are given. The left-most column indicates the type of fixed point in the gravitational and scalar sector. For example, a fixed point of type "GFP × NGFP" indicates that the fixed point has a trivial gravitational part, i.e. $g^* = \lambda^* = 0$, whereas the scalar part is non-trivial.[10] The second table displays the

[9] These values originate from [44]. For a more extensive review, see [45].

[10] Note that, despite what the abbreviations GFP and NGFP suggest, we are actually discussing whether they are trivial or not, i.e. if the coordinates vanish. This does not always match the definition of *Gaussian* as given in section 2.3. An example of this is the NGFP × GFP fixed point, where one would expect the critical exponents θ_3 and θ_4 to match the canonical mass dimensions of $v_{k,2}$ and $v_{k,4}$. However, this is not of importance to our discussion.

grav. × scalar	g^*	λ^*	v_2^*	v_4^*
GFP × GFP	0	0	0	0
GFP × NGFP	0	0	-0.0385	0.323
NGFP × GFP	0.181	0.106	0	0
NGFP × NGFP_1	0.179	0.110	-0.0517	-0.0326
NGFP × NGFP_2	0.182	0.104	0.0228	-0.0435

grav. × scalar	θ_1	θ_2	θ_3	θ_4
GFP × GFP	2	-1	2	1
GFP × NGFP	2	-1	1.84	-1.18
NGFP × GFP	$1.12 \pm 1.11i$	-0.781	0.219	
NGFP × NGFP_1	$1.13 \pm 1.10i$	-2.65	-0.289	
NGFP × NGFP_2	$1.11 \pm 1.10i$	$0.190 \pm 0.425i$		

Table 3.1: Fixed point coordinates in the upper table and corresponding critical exponents in the bottom table, for $d = 3$ and $N = 2$. The fixed points are labeled by their type in the gravitational (grav.) and scalar sector.

critical exponents of the fixed points.

As is evident from the table, there exist five fixed points of the flow. The first is completely trivial; all couplings vanish at this point. The second is trivial in the gravitational sector while being non-trivial in the matter sector. This resembles the Wilson-Fisher fixed point. Comparing to the values (3.65) and (3.66), we see that these match very well. Thirdly, there exists a fixed point that is non-trivial in the gravitational sector and trivial in the matter sector. Finally, there are two fixed points that are completely non-trivial. The gravitational fixed point coordinates and critical exponents of these solutions do not differ much from those of the NGFP × GFP type.

However, this is just a single truncation and it is wise to investigate possible extensions. This means that we wish to see if the fixed points survive as we add higher orders to the potential. To this end, we do the same calculation for $N = 3$, $N = 4$ and $N = 5$. It turns out that adding even higher orders requires too much computation time and, as we will see shortly, we can draw reasonable conclusions from these extensions alone. In table 3.2, the results for $N = 5$ are given. The results for $N = 3$ and $N = 4$ are not given and will only be commented on briefly.

As is evident from the table, in this truncation we obtain six fixed points. Before we compare the results to the case of $N = 2$, recall that critical exponents are universal. Hence, they are suitable to compare different truncations and deduce whether a certain fixed point is merely a truncation artifact, or possibly a fixed point of the full theory. Below, we discuss each type of fixed point separately.

grav. × scalar	g^*	λ^*	v_2^*	v_4^*	v_6^*	v_8^*	v_{10}^*
GFP × GFP	0	0	0	0	0	0	0
GFP × NGFP_1	0	0	0.00376	−0.0376	0.0821	−0.0378	0.0467
GFP × NGFP_2	0	0	−0.0941	0.612	1.42	3.02	4.34
GFP × NGFP_3	0	0	−0.0243	0.213	−0.150	−0.788	−1.20
NGFP × GFP	0.181	0.106	0	0	0	0	0
NGFP × NGFP	0.179	0.111	−0.0555	−0.0415	−0.0201	−0.00973	−0.00524

grav. × scalar	θ_1	θ_2	θ_3	θ_4	θ_5	θ_6	θ_7
GFP × GFP	2	−1	2	1	0	−1	−2
GFP × NGFP_1	2	−1	$0.148 \pm 2.80i$		2	0.938	0.190
GFP × NGFP_2	2	−1	−60.3	−22.0	−6.52	1.54	−0.781
GFP × NGFP_3	2	−1	−17.6	−5.02	2.07	1.51	−0.381
NGFP × GFP	$1.12 \pm 1.11i$		−3.78	−2.78	−1.78	−0.781	0.219
NGFP × NGFP	$1.13 \pm 1.10i$		$-7.88 \pm 1.45i$		−4.55	−2.16	−0.282

Table 3.2: Fixed point coordinates in the upper table and corresponding critical exponents in the bottom table, for $d = 3$ and $N = 5$. The fixed points are labeled by their type in the gravitational (grav.) and scalar sector.

(1) As one would expect, the fully Gaussian fixed point is present in all studied cases. Moreover, the critical exponents match the canonical mass dimensions of the couplings.

(2) There are now three fixed points of the type GFP × NGFP. It is interesting to compare these to the WF fixed point of $N = 2$. Matching the critical exponents of GFP × NGFP_1, it is clear that this does not resemble the WF fixed point. The main reason for this is the absence of a negative, real critical exponent of GFP × NGFP_1. Furthermore, investigating the cases of $N = 3$ and $N = 4$, one finds that this fixed point only comes into existence at $N = 5$. It is therefore less likely that this fixed point is a solution of the full theory.

Looking at the critical exponents of GFP × NGFP_2 and GFP × NGFP_3, it is hard to tell which resembles the WF fixed point. Upon investigating the other studied values of N, one finds that GFP × NGFP_2 seems to be connected to the WF fixed point, whereas GFP × NGFP_3 only comes into existence at $N = 4$.

(3) The fixed point of the type NGFP × GFP has survived the extension to $N = 5$. Its coordinates and critical exponents are stable in all tested values of N, indicating that this fixed point is likely a solution to the full theory. We also expect to find this fixed point in the four-dimensional case.

(4) Finally, there exists only one fully non-Gaussian fixed point for $N = 5$. This means that one of the fully non-Gaussian fixed points of the $N = 2$ case was likely a truncation artifact. Comparing critical exponents, one concludes that NGFP $\times$ NGFP$_1$ is robust, whereas NGFP $\times$ NGFP$_2$ was an artifact of the $N = 2$ truncation.

Four dimensions

Now, we study the physically more interesting case of $d = 4$. It is known that without gravity, the WF fixed point disappears in four spacetime dimensions. Therefore, we expect to find no fixed point of the type GFP $\times$ NGFP, at least for $N = 2$. The question is, however, if this is affected by the introduction of gravity. Thus, the main point of interest is to see if we obtain a fully non-Gaussian fixed point, and if so, to test its stability.

The results for $N = 2$ are given in table 3.3 below. We see that in four dimensions, there

grav. $\times$ scalar	g^*	λ^*	v_2^*	v_4^*
GFP $\times$ GFP	0	0	0	0
NGFP $\times$ GFP	0.661	0.206	0	0

grav. $\times$ scalar	θ_1	θ_2	θ_3	θ_4
GFP $\times$ GFP	2	-2	2	0
NGFP $\times$ GFP	$1.61 \pm 3.24i$		-2.07	-4.07

Table 3.3: Fixed point coordinates in the upper table and corresponding critical exponents in the bottom table, for $d = 4$ and $N = 2$. The fixed points are labeled by their type in the gravitational (grav.) and scalar sector.

are only two fixed points of the flow. The Gaussian fixed point has survived the switch to four dimensions but, as expected, the GFP $\times$ NGFP has not. Furthermore, the NGFP $\times$ GFP has survived as well. This was to be expected; from equations (3.61) and (3.62), one can see that a vanishing potential is a zero of its β-function:

$$\beta_W|_{W=0} = 0\,. \tag{3.67}$$

This holds for any spacetime dimension and for any N, hence we expect to find a NGFP $\times$ GFP at all orders. Finally, we observe that there exists no fully non-Gaussian fixed point, indicating that, at least for $N = 2$, the influence of gravity is not strong enough to create a non-Gaussian fixed point in $d = 4$.

Let us now see what happens at higher orders. Again, we only give the results for $N = 5$ in table 3.4 and briefly comment on the other investigated orders. We observe that there are now more fixed points of the flow than for $N = 2$.

(1) As expected, the fully Gaussian fixed point is stable under the addition of higher orders. This also holds for the fixed point of the type NGFP $\times$ GFP. The physical implications of this

grav. × scalar	g^*	λ^*	v_2^*	v_4^*	v_6^*	v_8^*	v_{10}^*
GFP × GFP	0	0	0	0	0	0	0
GFP × NGFP_1	0	0	0.0109	−0.598	1.68	13.46	52.0
GFP × NGFP_2	0	0	0.0226	−1.30	7.74	33.56	−681
NGFP × GFP	0.661	0.206	0	0	0	0	0
NGFP × NGFP	0.660	0.207	−0.00709	−0.381	−15.6	−467	-8.90×10^3

grav. × scalar	θ_1	θ_2	θ_3	θ_4	θ_5	θ_6	θ_7
GFP × GFP	2	−2	2	0	−2	−4	−6
GFP × NGFP_1	2	−2	−4.16	2.07	−0.674	$0.430 \pm 1.34i$	
GFP × NGFP_2	2	−2	−3.50	2.22	0.313	$3.69 \pm 2.00i$	
NGFP × GFP	$1.61 \pm 3.24i$	−2.07	−4.07	−6.07	−8.07	−10.07	
NGFP × NGFP	$1.61 \pm 3.24i$	−2.00	3.17	−4.98	$-10.9 \pm 1.09i$		

Table 3.4: Fixed point coordinates in the upper table and corresponding critical exponents in the bottom table, for $d = 4$ and $N = 5$. The fixed points are labeled by their type in the gravitational (grav.) and scalar sector.

are disccused in section 3.4.

(2) A striking new feature of the $N = 5$ case is the existence of two fixed points of the type GFP × NGFP that were not present at the level of $N = 2$. The number of these differs per order though. For $N = 3, 6, 7$ there exists one, whereas for $N = 4, 5$ there are two. None of these seem to be stable; the coordinates and critical exponents do not exhibit a convergence behaviour and there seems to be no fixed point that exists at all orders larger than $N = 2$. Hence, it is likely that these are all truncation artifacts.

(3) The other new feature is the existence of a fully non-Gaussian fixed point. A solution of this type exists at all tested orders, $N = 3, \ldots, 7$. However, the critical exponents are not stable and the fixed point coordinates seem to diverge for increasing N. Due to this, we conclude that this finding is likely unphysical.

3.4 Conclusion

In section 2.3, we presented Weinberg's conjecture regarding Asymptotic Safety. From this we learned that in order to have an asymptotically safe theory, one requires an UV-attractive fixed point that is non-trivial in the gravitational sector. Hence, the purpose of the previous investigation was to find such a suitable fixed point that is also of interest for cosmological investigations.

In three spacetime dimensions, we found the existence of two robust fixed points suitable for Asymptotic Safety, namely the NGFP $\times$ GFP and NGFP $\times$ NGFP_1 listed in table 3.1. Investigating the corresponding critical exponents, one finds that both fixed points have two relevant directions and the addition of higher orders only included irrelevant directions, signalled by the negative critical exponents. Hence, these fixed points are UV-attractive and the corresponding UV critical hypersurfaces have dimension 2.

However, the physically interesting case is $d = 4$. Here we found that this change of dimensionality destroyed a number of nice properties. Most prominently, in four dimensions there exists no stable fixed point which is fully non-Gaussian. Nevertheless, the NGFP $\times$ GFP found in this case is also suitable for Asymptotic Safety. We now discuss whether this solution is also interesting for cosmology. As it has a Gaussian matter sector, the scalar interactions are switched off at the fixed point. Moreover, due to eq. (3.67), a non-zero potential is not generated by lowering the scale k. This property, known as the triviality problem, means that this fixed point is unfit for a cosmological investigation. Thus, we conclude that the toy model studied in this chapter is not suitable for our purposes. In order to make this system interesting for cosmology, one likely requires a more realistic ansatz including other couplings.

Finally, we remark that these findings are in accordance with other studies of scalar-tensor models. In particular, in [39] it was also concluded that the fully non-Gaussian fixed points in $d = 4$ are truncation artifacts. Moreover, it was reported that the scalar minimal coupling is self consistent, signifying the triviality problem.

Chapter 4

Consistent cosmology from the RG flow of gravity

The motivation for studying the scalar-tensor model in the previous chapter was twofold. First, it served as an example calculation to demonstrate applications of the FRGE. For this reason, the exposition was technically quite involved. Secondly, the particular system could provide a mechanism for inflation, since many inflationary models contain a scalar field potential of the form as studied by us. See table 1 of [46] for an overview. This property, in principle, could allow for a phenomenological study. However, as it was found that the studied system suffered from the triviality problem, this goal was abandoned.

In the remainder of this thesis, we will take a different approach. Motivated by the goal to investigate cosmology, we let cosmological observations guide us towards a particular choice of truncation. We review the relevant cosmological eras in section 4.1 , before making the connection to the RG in section 4.2. This part of the thesis is based on [47] by Gubitosi, Ooijer, Ripken and Saueressig.

4.1 Cosmology

4.1.1 Late time cosmology

Observations of superovea explosions [48, 49] suggest that the universe is currently undergoing a phase of accelerated expansion. In this section we review the necessary components of the standard model of cosmology to understand how this conclusion comes about. Our exposition is inspired by [50].

This cosmological model, also referred to as the ΛCDM model, is based on two large-scale properties of our universe, spatial isotropy and homogeneity. Upon making these assumptions, one arrives at the following particular form for the metric,

$$\mathrm{d}s^2 = -\mathrm{d}t^2 + a(t)^2\Big(\frac{\mathrm{d}r^2}{1-\kappa r^2} + r^2\mathrm{d}\Omega^2\Big) \tag{4.1}$$

where $a(t)$ is the dimensionless scale factor, κ is a curvature parameter and $\mathrm{d}\Omega^2$ is the usual

metric on the two-sphere,

$$\mathrm{d}\Omega^2 = \mathrm{d}\theta^2 + \sin^2\theta \mathrm{d}\phi^2 \,. \tag{4.2}$$

The metric defined by (4.1) is known as the Friedmann-Lemaître-Robertson-Walker (FLRW) metric. Since the ΛCDM model assumes standard Einstein gravity described by the Einstein-Hilbert action[1]

$$S[g] = \frac{1}{16\pi G} \int \mathrm{d}^4x \sqrt{-g}(2\Lambda - R) \,, \tag{4.3}$$

the behaviour of the scale factor $a(t)$ is obtained by evaluating the Einstein equations[2]

$$R_{\mu\nu} - \frac{1}{2} g_{\mu\nu} R = 8\pi G T_{\mu\nu} \,. \tag{4.4}$$

In order to obtain the dynamics, one models matter and energy by a perfect fluid, which results in a stress-energy tensor of the form

$$T_{\mu\nu} = \mathrm{diag}(-\rho, p, p, p) \,. \tag{4.5}$$

Here, the density ρ and pressure p are related by the equation of state

$$p = w\rho \tag{4.6}$$

with w a constant parameter. Below we give its values for the most relevant cosmological fluids:

$$w = \begin{cases} 0 & \text{for non-relativistic particles,} \\ \frac{1}{3} & \text{for relativistic particles,} \\ -1 & \text{for vacuum energy.} \end{cases} \tag{4.7}$$

Evaluating the Einstein equations (4.4), one arrives at the Friedmann equations,

$$\left(\frac{\dot{a}}{a}\right)^2 = \frac{8\pi G}{3}\rho - \frac{\kappa}{a^2} \,, \tag{4.8a}$$

$$\frac{\ddot{a}}{a} = -\frac{4\pi G}{3}(\rho + 3p) \,. \tag{4.8b}$$

Furthermore, the requirement of energy conservation results in

$$\frac{\dot{\rho}}{\rho} = -3(1+w)\frac{\dot{a}}{a} \tag{4.9}$$

which can be integrated to yield

$$\rho \propto a^{-3(1+w)} \,. \tag{4.10}$$

[1] In this section on cosmology, we work in a Lorentzian setting. We move back to a Euclidean setting when we make the connection to the FRG in section 4.2, where we will also comment on the relation between the two settings.

[2] The cosmological constant appearing in eq. (4.3) does not appear in this form of the Einstein equations as it is absorbed into the stress-energy tensor $T_{\mu\nu}$.

For the different kinds of fluids listed in eq. (4.7), this entails

$$\rho \propto \begin{cases} a^{-3} & \text{for non-relativistic particles,} \\ a^{-4} & \text{for relativistic particles,} \\ a^{0} & \text{for dark energy.} \end{cases} \tag{4.11}$$

Hence, one observes that if the universe expands, the energy densities of matter (non-relativistic particles) and radiation (relativistic particles) decrease, whereas the density of dark energy remains constant. Therefore, if there is dark energy present in the universe, eventually it will dominate the late time dynamics, provided that the universe keeps expanding.

At this point, it is useful to introduce a few parameters that are often quoted in the context of cosmological observations. One defines the Hubble parameter as

$$H = \frac{\dot{a}}{a} \tag{4.12}$$

which characterizes the rate of expansion of the universe. Moreover, the relative density parameter is given by

$$\Omega = \frac{8\pi G}{3H^2}\rho = \frac{\rho}{\rho_c} \tag{4.13}$$

where the second equation defines the critical density ρ_c.

Going back to the Friedmann equations, we see why ρ_c is called the *critical* density. One can write eq. (4.8a) as

$$\Omega - 1 = \frac{\kappa}{H^2 a^2} \equiv -\Omega_k \tag{4.14}$$

where we define the curvature density parameter Ω_k. Hence, if $\rho = \rho_c$, the curvature parameter κ vanishes, signalling a flat universe. At this moment, evidence [51] suggests that this is indeed the case for our universe.

Let us get back to the accelerated expansion mentioned at the start of this section. Such a cosmological evolution requires $\ddot{a} > 0$. From eq. (4.8b), one sees that this is possible if $\rho + 3p < 0$. For a universe occupied by both matter and dark energy, one finds

$$\frac{\ddot{a}}{a} = -\frac{4\pi G}{3}(\rho_M - 2\rho_\Lambda)\,. \tag{4.15}$$

Hence, if the density of dark energy is large enough, the universe expands at an accelarated rate. In order to measure this, one often makes use of the so-called *luminosity distance* d_L. Below, we show how this quantity is related to the density parameters.

First, we introduce some new notation. We define the curvature parameter k as the dimensionless counterpart of the parameter κ introduced earlier by the relation

$$k = \kappa \tilde{R}^2 \tag{4.16}$$

where $\tilde{R}$ is a reference parameter with the dimension of length. Moreover, we introduce a

dimensionless radial coordinate χ and a function $S_k(\chi)$ via

$$S_k(\chi) \equiv \begin{cases} \sin(\chi) & \text{for } k = +1\,, \\ \chi & \text{for } k = 0\,, \\ \sinh(\chi) & \text{for } k = -1\,. \end{cases} \tag{4.17}$$

The line element (4.1) can now be written as

$$\mathrm{d}s^2 = -\mathrm{d}t^2 + a(t)^2\tilde{R}^2\Big(\mathrm{d}\chi^2 + S_k(\chi)^2\mathrm{d}\Omega^2\Big)\,. \tag{4.18}$$

With these definitions in place, we can introduce the luminosity distance d_L. For a source with absolute luminosity L and an observer measuring a flux F, one has

$$d_L^2 = \frac{L}{4\pi F}\,. \tag{4.19}$$

In flat Euclidean space, the flux and luminosity are related to the area of a sphere centered around the source via

$$\frac{F}{L} = \frac{1}{A}\,. \tag{4.20}$$

However, due to the geometry of the FLRW universe, this relation changes due to redshift effects, into

$$\frac{F}{L} = \frac{1}{(1+z)^2 A} \tag{4.21}$$

where we conveniently introduced the redshift factor z, defined via[3]

$$a = \frac{1}{1+z}\,. \tag{4.22}$$

The area of this sphere is given by

$$A = 4\pi\tilde{R}^2 S_k(\chi)^2\,, \tag{4.23}$$

which is the prefactor of the two-sphere line element with $a(t)$ set to unity since the photons are measured today. Hence, one obtains

$$d_L = (1+z)\tilde{R}S_k(\chi)\,. \tag{4.24}$$

Since we desire to make contact with observations, we want to rid ourselves of parameters that are unobservable. Hence, we must remove $\tilde{R}$ and χ from eq. (4.24). To this end, we write

$$\chi(z) = \frac{1}{\tilde{R}}\int_0^z \frac{\mathrm{d}z'}{H(z')} \tag{4.25}$$

which follows from the fact that photons move on null-geodesics.

Next, we wish to relate the Hubble parameter in (4.25) to the density parameters. This will

[3]Here we have adopted the conventional normalization $a(t_0) = 1$ where t_0 is the current time. Moreover, from this point onwards, quantities with a subscript zero are taken at current time.

allow measurements of d_L to provide values for the density parameters Ω_i, where i represents the possible components of the cosmic fluid, e.g. matter, radiation and dark energy. This is achieved by emplyoing the Friedmann equation (4.8a). One finds

$$H(z) = H_0 \left(\sum_{i(k)} \Omega_{i,0} (1+z)^{n_i} \right)^{\frac{1}{2}} \equiv H_0 E(z) \,. \tag{4.26}$$

Here, the $i(k)$ below the sum indicates that we not only sum over the components of the cosmic fluid, but also include the curvature component Ω_k. Moreover, n_i is related to the scaling of $\rho(a)$ as

$$\rho_i \propto a^{-n_i} \,. \tag{4.27}$$

This allows us to write the luminosity distance as

$$d_L(z) = \frac{1+z}{H_0 \sqrt{|\Omega_{k,0}|}} S_k \left(\sqrt{|\Omega_{k,0}|} \int_0^z \frac{\mathrm{d}z'}{E(z')} \right) \,. \tag{4.28}$$

This equation allows one to find the density parameters by measuring the luminosity distance of certain standard candles. Observations of Type Ia supernovae, reported in [48, 49], indicate that Ω_Λ is large enough for eq. (4.15) to be positive, implying that our universe is currently expanding at an accelerated rate. More recent data [51] is compatible with

$$\Omega_\Lambda = 0.692 \pm 0.012 \,, \tag{4.29a}$$

$$\Omega_M = 0.308 \pm 0.012 \,, \tag{4.29b}$$

which also indicates an accelerated expansion of the universe.

4.1.2 Early time cosmology

Although the cosmological model discussed in the previous section provides an adequate description of observed cosmological phenomena at present time, it also provides some puzzles. One of these is known as the *horizon problem*. To formulate this problem, it is useful to introduce the *comoving (particle) horizon* η. It is the maximum distance a light ray can travel in a certain time t,

$$\eta \equiv \int_0^t \frac{\mathrm{d}t'}{a(t')} = \int_0^a \frac{\mathrm{d}a'}{a'} \frac{1}{a'H} \,. \tag{4.30}$$

The final part of the integrand, the term $(aH)^{-1}$, is known as the *Hubble radius*. If there is a dominant fluid component, this radius behaves as

$$(aH)^{-1} = H_0^{-1} a^{\frac{1}{2}(1+3w)} \,. \tag{4.31}$$

This allows us to evaluate the integral (4.30). One obtains

$$\eta \propto \begin{cases} a & \text{for radiation,} \\ \sqrt{a} & \text{for matter.} \end{cases} \tag{4.32}$$

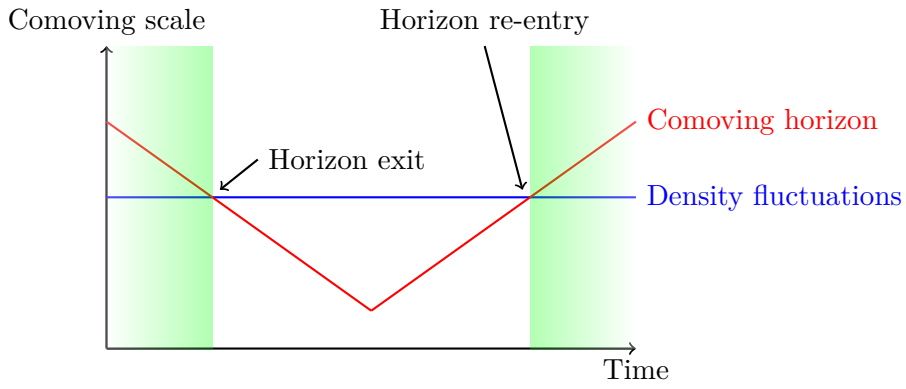

Figure 4.1: Schematic overview of the inflationary mechanism, based on [12]. The first half, signified by the decrease of the comoving Hubble horizon, is the inflationary period. Density fluctuations that are smaller than the comoving Hubble horizon today (far right, shaded green) were causally disconnected (unshaded area) except for during the very early universe (far left, shaded green). This early phase in which the relevant scales were causally connected is made possible by inflation.

Hence, this causal horizon grows monotonically with time as the universe expands. In turn, this implies that patches of the universe moving into causal contact now were causally disconnected in the past. Hence, the observed homogeneity of the Cosmic Microwave Background (CMB) that is at the foundation of the ΛCDM model poses a puzzle, since this encompasses scales that were causally independent at the time when the CMB was formed.

The second problem discussed here concerns itself with the observed lack of curvature and is hence known as the *flatness problem*. Recall that measurements are compatible with a curvature density parameter $\Omega_k \simeq 0$. However, this quantity is not time-independent; from eq. (4.14) it is clear that it grows in time if $k \neq 0$. Hence, observing $\Omega_k \simeq 0$ today requires extreme fine-tuning of the inital conditions of the universe. One can calculate that, in the Planck era, one must have [12]

$$|\Omega_k(a_{pl})| \leq 10^{-61} \,. \tag{4.33}$$

Both of these issues may be solved simultaneously by a period of accelerated expansion in the early universe, known as *inflation*. The crucial ingredient to this phase is a decrease of the Hubble radius $(aH)^{-1}$. This solves the flatness problem almost trivially: since $\Omega_k \propto (aH)^{-2}$, decreasing the Hubble radius also drives the value of Ω_k towards zero. Thus, a sufficiently pronounced period of inflation leads to $\Omega_k \simeq 0$. Secondly, the horizon problem is solved as well. Recall, the issue was that homogeneity is observed over scales that were too large to be causally connected in the past. This is solved by a phase of decreasing Hubble radius since this also implies a phase before inflation in which the comoving horizon was larger than the density fluctuations, implying a causal connection between the relevant regions. This mechanism is illustrated in figure 4.1.

There exist many different methods of implementing such an inflationary phase. Most of these rely on the existence of a scalar *inflaton* field φ with a certain potential $V(\varphi)$, minimally coupled to standard Einstein gravity. These different models can be tested by their predictions

for cosmological observables related to cosmic perturbations. In the following, we will briefly discuss the origin of these predictions before making the connection to observations. For a more detailed overview, see [12].

In order to obtain predictions beyond homogeneity and isotropy, one may perturb the metric and the stress-energy tensor. The decomposition of the metric perturbations is given by

$$\mathrm{d}s^2 = -(1+2\Phi)\mathrm{d}t^2 + 2aB_i\mathrm{d}x^i\mathrm{d}t + a^2\big((1-2\Psi)\delta_{ij} + E_{ij}\big)\mathrm{d}x^i\mathrm{d}x^j\,, \tag{4.34}$$

where a is the familiar scale factor. Furthermore, the symmetric traceless 3-tensor E_{ij} is given by

$$E_{ij} = 2(\partial_i\partial_j - \frac{1}{3}\delta_{ij}\partial^2)E + \partial_i F_j + \partial_j F_i + h_{ij}\,. \tag{4.35}$$

The only parameters of importance in eqs. (4.34) and (4.35) are the tensor fluctuation h_{ij} and the scalar curvature perturbation Ψ. One combines the scalar perturbation Ψ with a momentum density perturbation δq to form the gauge-invariant *comoving curvature perturbation* $\mathcal{R}$. The next step towards observables involves calculating the (rescaled) power spectra of the scalar and tensor perturbations, $\Delta^2_{\mathcal{R}}(k)$ and $\Delta^2_h(k)$, respectively.[4] The scale-dependence of these quantities is captured in the scalar index n_s and the tensor-to-scalar ratio r by

$$n_s - 1 \equiv \frac{\mathrm{d}\ln\Delta^2_{\mathcal{R}}(k)}{\mathrm{d}\ln k}\,, \tag{4.36}$$

$$r \equiv \frac{\Delta^2_h}{\Delta^2_{\mathcal{R}}}\,. \tag{4.37}$$

These observable quantities are often quoted in the context of observations. Since the predicted values of these observables depends on the specific inflationary model, one can use observations to test the plausibility of a certain model. The current values for these quantities are compatible with [52]

$$n_s = 0.9677 \pm 0.0060\,, \tag{4.38a}$$

$$r < 0.11\,. \tag{4.38b}$$

Matching these with the predictions from different inflationary models, one finds that the *Starobinsky model* is the current best fit to the data [52]. It is described by the action

$$S[g] = \frac{1}{16\pi G}\int \mathrm{d}^4x\sqrt{-g}(R - BR^2)\,. \tag{4.39}$$

Hence, Starobinsky inflation adds a higher-order curvature term to the action, instead of a scalar field. The R^2-term gives rise to inflation through the classical equations of motion [53–55]. To illustrate how one concludes that this specific model is the best fit to the data, we discuss this model in the context of the *slow-roll approximation* below.

[4] The scale k here signals the comoving wave number of a perturbation and has no relation to the renormalization scale.

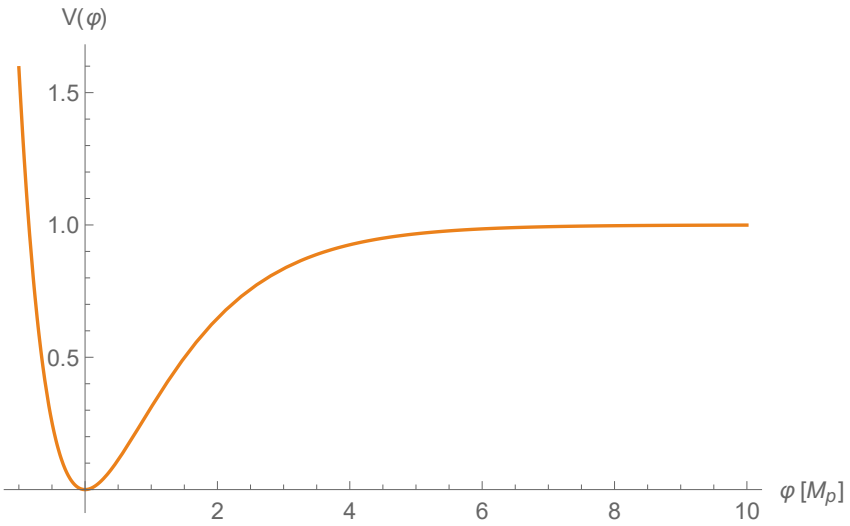

Figure 4.2: The scalar field potential (4.40) with the prefactor $-M_P^2/(8B)$ set to unity for convenience. The scalar field φ is given in Planck units.

Even though the action (4.39) does not contain a scalar field, one can show that it is in fact equivalent to the theory of a scalar field minimally coupled to gravity, with a scalar field potential. This equivalence is shown in appendix B. The explicit form of the scalar field potential is found to be

$$V(\varphi) = -\frac{M_P^2}{8B}\left(1 - \mathrm{e}^{-\sqrt{2/3}\varphi/M_P}\right)^2 \tag{4.40}$$

where M_P is the reduced Planck mass defined as

$$M_P = (8\pi G)^{-1/2}\,. \tag{4.41}$$

The shape of the potential (4.40) is illustrated in figure 4.2.

Dynamics of inflation is regularly investigated in the slow-roll approximation. To introduce this, we start with the equations of motion (EOM) of the system. The EOM for the scalar field on a FLRW geometry are given by

$$H^2 = \frac{1}{3M_P^2}\left(\frac{1}{2}\dot{\varphi}^2 + V(\varphi)\right)\,, \tag{4.42}$$

$$\ddot{\varphi} + 3H\dot{\varphi} + \frac{\mathrm{d}V}{\mathrm{d}\varphi} = 0\,, \tag{4.43}$$

where dots denote time derivatives. For inflation to be sustained for a sufficiently long period of time, these derivatives of φ must be small. This requirement is implemented via the slow-roll conditions

$$\dot{\varphi}^2 \ll V\,, \tag{4.44a}$$

$$|\ddot{\varphi}| \ll |3H\dot{\varphi}|, \left|\frac{\mathrm{d}V}{\mathrm{d}\varphi}\right|\,. \tag{4.44b}$$

Satisfying these conditions requires the smallness of dimensionless slow-roll parameters which

capture the features of the potential. These slow-roll parameters are defined as

$$\epsilon_V \equiv \frac{M_P^2}{2}\left(\frac{V'}{V}\right)^2 , \tag{4.45a}$$

$$\eta_V \equiv M_P^2 \frac{V''}{V} , \tag{4.45b}$$

where primes on the potential V denote derivatives w.r.t. the argument φ. Slow-roll inflation then requires $\epsilon_V, |\eta_V| \ll 1$ and it ends when either of these parameters equals one. The number of e-foldings that occur before the end of inflation is calculated by

$$N(\varphi) \equiv \ln\left(\frac{a(t_{\text{end}})}{a}\right) \simeq \frac{1}{M_p}\int_{\varphi_{\text{end}}}^{\varphi} \frac{\mathrm{d}\varphi'}{\sqrt{2\epsilon_V(\varphi')}} . \tag{4.46}$$

The value of N necessary to solve the horizon and flatness problems depends on the energy scale of inflation and details regarding the reheating phase after inflation ends. One commonly uses the value $N_{\text{tot}} \simeq 60$ [12].

Getting back to observables, one can show that the slow-roll parameters are related to the scalar index n_s and the tensor-to-scalar ratio r by

$$n_s = 1 + 2\eta_V^* - 6\epsilon_V^* , \tag{4.47}$$

$$r = 16\epsilon_V^* , \tag{4.48}$$

where the superscript '*' indicates that the quantities are evaluated at the time when the perturbations cross the Hubble radius.

In order to illustrate why Starobinsky inflation is a good fit to the listed values (4.38), we now discuss the slow-roll analysis of this inflationary model. Using the potential (4.40), one obtains

$$\epsilon_V = \frac{4}{3}\left(1 - \mathrm{e}^{\sqrt{2/3}\varphi/M_P}\right)^{-2} , \tag{4.49}$$

$$\eta_V = \frac{4}{3}\frac{2 - \mathrm{e}^{\sqrt{2/3}\varphi/M_P}}{\left(1 - \mathrm{e}^{\sqrt{2/3}\varphi/M_P}\right)^2} , \tag{4.50}$$

$$N(\varphi) = \sqrt{\frac{3}{8}}\frac{1}{M_P}\int_{\varphi_{\text{end}}}^{\varphi} \left|1 - \mathrm{e}^{\sqrt{2/3}\varphi'/M_P}\right| . \tag{4.51}$$

The aim is to use these expressions to obtain predictions for n_s and r. This requires inverting eq. (4.51) to obtain $\varphi(N)$ and subsequently inserting this into equations (4.49) and (4.50). This calculation is too involved for the purposes of this thesis; instead, we note that inflation occurs for large values of the field φ. Hence, we expand the expressions (4.49) - (4.51) up to first order in $\exp(-\sqrt{2/3}\varphi/M_P)$. Doing so, one easily obtains the relations

$$\epsilon_V = \frac{3}{4N^2} , \tag{4.52a}$$

$$\eta_V = -\frac{1}{N} . \tag{4.52b}$$

Combining with the relations (4.47) and (4.48), one obtains

$$n_s = 1 - \frac{2}{N} - \frac{9}{2N^2}\,, \tag{4.53a}$$

$$r = \frac{12}{N^2}\,. \tag{4.53b}$$

These expressions are compatible with those quoted in the literature [52]. If we plug in $N \simeq 60$, the predicted values are

$$n_s \simeq 0.9654\,, \tag{4.54a}$$

$$r \simeq 0.0033\,, \tag{4.54b}$$

which are both compatible with the observational bounds (4.38).

4.2 Capturing observed phenomena with one ansatz

As was mentioned in the previous section, there is compelling evidence suggesting that the universe is currently undergoing a phase of accelerated expansion and also went through a period of inflation at early times. In the remainder of this thesis, we explore the possibility that physics at trans-Planckian energies may set the seed for this observed dynamics of gravity below the Planck scale.

Our starting point is power-law $f(R)$ gravity, truncated at the second order in the Ricci scalar R,

$$S[g] = \frac{1}{16\pi G}\int \mathrm{d}^4x\sqrt{-g}(2\Lambda - R + BR^2)\,. \tag{4.55}$$

At early times, this action gives rise to inflation realised as a purely gravitational effect, where the inflaton field is simply the additional degree of freedom described by the $f(R)$ action. Moreover, the cosmological constant drives the late time accelerated expansion. Hence, the system described by eq. (4.55) takes both cosmological phenomena of the previous section into account. It is parametrized by three couplings, the cosmological constant Λ, Newton's coupling G and the R^2-coupling B. Cosmological observations impose restrictions on these parameters. Each of them is measured over a different distance scale, as explained in detail in section 4.3 and summarized in table 4.1. The purpose of the rest of this thesis is to investigate whether the measured values of the parameters are consistent with the asymptotic safety scenario of quantum gravity.

Cosmological implications of Asymptotic Safety have received considerable attention [56–74], of which an overview is given in [75]. These works incorporate the leading quantum gravity effects by a so-called *renormalization group improvement* procedure which identifies the energy scale k with a physical quantity. In contrast, we pioneer a different path: instead of generating effective dynamics via such a renormalization group improvement, we construct the effective average action of the theory valid at the corresponding energy scale by solving the underlying renormalization group equations. Contact to the constraints listed in table 4.1 is then made by following the RG flow emanating from the NGFP to lower energies.

Energy scale (eV)	Constraint
$k_{\rm infl} = 10^{22}$	$B = -6.7 \times 10^{-39}$ eV^{-2}
$k_{\rm lab} = 10^{-5}$	$G = 6.7 \times 10^{-57}$ eV^{-2}
$k_{\rm Hub} = 10^{-33}$	$\Lambda = 4 \times 10^{-66}$ eV^{2}

Table 4.1: Observational constraints on the parameters of the action (4.55). For each parameter we indicate the energy scale corresponding to the distance over which the measurement is performed. These are the scale of inflation $k_{\rm infl}$, the laboratory scale $k_{\rm lab}$, and the Hubble scale $k_{\rm Hub}$.

Energy scale (eV)	RG constraint
$k \gg M_P = 2.4 \times 10^{27}$	NGFP
$k \simeq k_{\rm infl} = 10^{22}$	$B_k \simeq B_{\rm infl} = -6.7 \times 10^{-39}$ eV^{-2}
$k \simeq k_{\rm lab} = 10^{-5}$	$G_k \simeq G = 6.7 \times 10^{-57}$ eV^{-2}
$k \simeq k_{\rm Hub} = 10^{-33}$	$\Lambda_k \simeq \Lambda = 4 \times 10^{-66}$ eV^{2}

Table 4.2: Constraints on the $f(R)$ action parameters in the RG framework at various scales. The observational constraints are the same as in table 4.1. Moreover, we require that beyond the (reduced) Planck scale $M_P \equiv (8\pi G)^{-1/2}$, the RG flows towards a non-Gaussian fixed point (NGFP).

To this end, we employ the following (Euclidean) action[5]

$$S_k[g] = \frac{1}{16\pi G_k} \int \mathrm{d}^4x \sqrt{g} (2\Lambda_k - R + B_k R^2) \,. \tag{4.56}$$

Within this setting, an asymptotically safe RG trajectory should satisfy the requirements summarized in table 4.2. The rest of this work is organized as follows. In section 4.3 we derive the observational constraints on the parameters in the action (4.56). This is followed by a discussion of the structural properties of the RG phase diagram of the R^2-model in section 4.4. In section 4.5 we impose the observational constraints on the RG flow, and show the existence of a RG trajectory satisfying all of them. We end this chapter with a discussion of the implications of these results in section 4.6.

4.3 Observational constraints on gravity

The main goal of this investigation is the construction of a RG trajectory passing through all points listed in table 4.2. Here, we derive the values of the couplings at the corresponding energy scales based on cosmological observations made over different distance scales.

At this point, a remark is in order. Table 4.2 may suggest that only one parameter is constrained at each given energy scale. The derivation of these values, however, assumes that

[5]The relation between gravitational RG flows calculated in a Lorentzian and Euclidean setting has been studied in [76]. It was shown that the two settings lead to qualitatively equivalent phase diagrams. Hence, we assume that this result also holds at the level of the R^2-type actions (4.55) and (4.56).

the other parameters take "reasonable values" at the specified scale (the meaning of this will be made precise below when discussing the individual constraints). In particular, it is assumed that Newton's coupling G_k does not run significantly between inflationary scales and the laboratory scales where it is currently measured. Denoting the laboratory value of Newton's constant by G, we introduce the reduced Planck mass M_P by the standard relation

$$M_P = (8\pi G)^{-1/2} = 2.4 \times 10^{27} \text{ eV}\,. \tag{4.57}$$

At this stage we adopt these properties as a working hypothesis. Once a viable RG trajectory is found, we can check a posteriori that these working assumptions are met.

4.3.1 Primordial cosmology

Assuming that the inflationary phase in the early universe originates from the R^2-term (Starobinsky inflation), the parameter B can be constrained by early time cosmological observations. In the context of primordial cosmology, it is generally assumed that the energy density of matter and of the cosmological constant are negligible, meaning that these components do not influence the background dynamics significantly. We take as a working assumption that the RG flow of the cosmological constant is such that it does not spoil this approximation and the contribution of $\Lambda_{k_{\text{infl}}}$ to the early universe dynamics can be considered as subdominant. Then, once a viable RG trajectory is selected, we can check a posteriori that this approximation is indeed met.

Neglecting the contribution of Λ, the action (4.55) reduces to the so-called Starobinsky model for inflation. Inflationary models can be constrained using observations of the cosmic microwave background, as done most recently by the Planck collaboration [52]. Because these constraints rely on the inferred properties of primordial perturbations when they left the Hubble horizon, we take the Hubble parameter at that time as the relevant energy scale:[6]

$$k_{\text{infl}} = H_{\text{infl}} \simeq 10^{22}\,\text{eV}. \tag{4.58}$$

Constraints on inflationary models usually refer to parameters of the inflaton field potential $V(\varphi)$ [46, 52]. We can apply these results to the R^2-model we are interested in, since at the classical level $f(R)$-gravity can be rewritten using the equations of motion into an action for gravity coupled to a scalar field φ, with a potential $V(\varphi)$. This equivalence is discussed in appendix B. Thus, this system is similar to the tensor-scalar model discussed in chapter 3. The main difference is the form of the potential $V(\varphi)$, which will be evident below.

Following the derivation of appendix B, the action (4.55) with $\Lambda = 0$ leads to a scalar potential

$$V(\varphi) = \frac{M_P^2}{8B}\left[1 - e^{-\sqrt{2/3}\varphi/M_P}\right]^2, \tag{4.59}$$

which characterizes the Higgs inflation model [77, 78]. Recent constraints on this model are

[6] What observations actually provide is an upper bound on the value of the Hubble parameter, $H_{\text{infl}} < 3.6 \times 10^{-5} M_P$. The fact that this is an upper bound rather than an estimate is because $H_{\text{infl}} \propto \sqrt{\frac{r}{0.1}}$, and we only have upper bounds on the tensor-to-scalar ratio r [52]. The order of magnitude estimate that we give in eq. (4.58) is based on the general expectation that r should not be much smaller than its current upper bound.

reported in [46]:[7]

$$M \simeq 4 \times 10^{-5} M_P \,, \tag{4.60}$$

where $M^4 = -\frac{{M_P}^2}{8B}$. When written in terms of the parameters (4.56) this constraint implies

$$M_P^2 \, B_k \simeq -4 \times 10^{16} \,, \tag{4.61}$$

with k taken at horizon crossing, $k = k_{\text{infl}}$.

Before we continue, a remark is in order. The constraint listed above should be seen as an *order-of-magnitude* bound due to experimental uncertainties. However, since there is no clear quantitative idea of the accuracy of the RG truncation, these experimental uncertainties are not important for our analysis.

4.3.2 Late time cosmology

Previously, we showed that early time cosmology provides a constraint on the R^2 coupling at high energy scales, k_{infl}. In contrast, late time cosmology is sensitive to the value of the cosmological constant at very low energy scales corresponding roughly to the current value of the Hubble parameter. Thus, measurements of the cosmological constant are made at an energy scale

$$k_{\text{Hub}} = 10^{-33} \text{ eV}. \tag{4.62}$$

While the constraint on B derived in the previous section relies on the assumption that the R^2 term dominates dynamics at early times, here we make the complementary assumption that late-time dynamics is only sensitive to the standard Einstein-Hilbert term R and the cosmological constant Λ (i.e. we rely on the standard ΛCDM cosmological model). Because the curvature is very small, the R^2 term can be considered negligible, as long as the RG flow does not drive the coupling B to extremely large values.

Current late time cosmological observations are fully compatible with a universe dynamics governed at late times by a $R - 2\Lambda$ action [51]. Specifically, the cosmological constant density parameter takes the value

$$\Omega_\Lambda \simeq 0.7 \,. \tag{4.63}$$

Together with the current value of the Hubble parameter [79],

$$H_0 \simeq 70 \, \text{km} \, \text{s}^{-1} \, \text{Mpc}^{-1} \,, \tag{4.64}$$

this allows to estimate the cosmological constant using eq. (4.13):[8]

$$\Omega_\Lambda \equiv \frac{\rho_\Lambda}{\rho_c} = \frac{\Lambda}{8\pi G} \frac{8\pi G}{3H_0^2} \tag{4.65}$$

$$\Rightarrow \Lambda = \Omega_\Lambda \cdot 3H_0^2 \simeq 4 \times 10^{-66} \text{ eV}^2 \,. \tag{4.66}$$

[7] As explained in appendix B, we are using an action with opposite overall sign with respect to the one conventionally used in cosmology.

[8] Note that the main uncertainty on the value of the cosmological constant comes from the tension in competing estimates of the Hubble constant, from the CMB [51] and from astrophysical observations (e.g. [80]). However, this uncertainty is not significant for the purposes of our analysis.

4.3.3 Newton's gravitational constant

Current estimates of Newton's gravitational constant are based on laboratory experiments, made on scales of about $10^{-2} - 10^{0}$ m [79], corresponding to energies of $10^{-4} - 10^{-6}$ eV. We use as reference scale the intermediate value:

$$k_{\text{lab}} \simeq 10^{-5} \text{ eV}. \tag{4.67}$$

The most up-to-date value of Newton's coupling is provided in [79]:

$$G = 6.7 \times 10^{-57} \text{ eV}^{-2}\,. \tag{4.68}$$

Since this value is obtained from a local measurement where the laws of gravity are captured by Newtonian gravity, the result (4.68) is not sensitive to the value of the cosmological constant or to the R^2 coupling.

4.4 RG structure

The next ingredient of our analysis is the gravitational RG flow resulting from an effective average action of the type (4.56). In order to keep this part of the thesis less technically involved than chapter 3, we base our analysis on the flow equation derived in [81] which is reviewed in appendix C.[9] Our results extend the earlier work [84].

The scale-dependence of the couplings G_k, Λ_k and B_k is most conveniently analyzed in terms of their dimensionless counterparts

$$\lambda_k \coloneqq \Lambda_k\, k^{-2}\,, \quad g_k \coloneqq G_k\, k^2\,, \quad b_k \coloneqq B_k\, k^2\,. \tag{4.69}$$

The k-dependence of these couplings is governed by their β-functions

$$\partial_t g_k = \beta_g(g,\lambda,b)\,, \qquad \partial_t \lambda_k = \beta_\lambda(g,\lambda,b)\,, \qquad \partial_t b_k = \beta_b(g,\lambda,b)\,, \tag{4.70}$$

where $t = \log(k/k_0)$ denotes the logarithmic RG time and k_0 is an arbitrary reference scale. The functions $\beta_i(g,\lambda,b)$ are obtained by solving the system (C.14). In order to get an idea about the RG trajectory realized by Nature we first investigate the fixed point and singularity structure of the β-functions in section 4.4.1 before constructing sample trajectories in section 4.4.2. The main result of this section is given in figure 4.3.

4.4.1 Fixed points, singularities and separation lines

Investigating the system (C.14), one finds the existence of two fixed points relevant for the present analysis. The GFP is located at

$$\lambda_* = 0\,, \quad g_* = 0\,, \quad b_* = 0\,. \tag{4.71}$$

[9] A different flow equation, based on a physical gauge fixing condition and derived in [82], was originally the subject of our investigation. However, that system exhibits a singular hypersurface that separates the NGFP from the classical region, see [83] for further analysis.

In addition, the system exhibits a NGFP situated at

$$\lambda_* = 0.133\,, \quad g_* = 1.59\,, \quad b_* = 0.119\,. \tag{4.72}$$

Evaluating the stability matrix for the GFP yields the critical exponents

$$\text{GFP:} \qquad \theta_1 = +2\,, \quad \theta_2 = -2\,, \quad \theta_3 = -2\,. \tag{4.73}$$

Combining this information with the associated eigenvectors shows that the GFP is UV-attractive in the $g = 0$ plane and UV-repulsive in the other two eigendirections. The analogous analysis for the NGFP yields

$$\text{NGFP:} \qquad \theta_{1,2} = 1.26 \pm 2.45i\,, \quad \theta_3 = 27.0\,, \tag{4.74}$$

indicating that the NGFP acts as an UV-attractor for RG trajectories entering its vicinity. The large positive eigenvalue θ_3 is typical for the R^2 system (see e.g. [24]). Its value reduces significantly once higher-order curvature terms are included [81,85,86]. These results also show that the critical exponents associated with curvature terms of order R^3 and higher come with a negative real part, so that the present approximation most likely includes all the free parameters occurring in asymptotically safe gravity.

Besides their fixed points, the singular loci of the β-functions play an essential role in constructing the phase diagram. The region containing the GFP and the NGFP is bounded by two planes where $\beta_i(g, \lambda, b)$ is infinite. These planes are shown in the left panel of figure 4.3 and labeled by the letters "A" and "B", respectively. The surface A is parabola-shaped and extends approximately parallel to the b-axes. This surface constitutes a possible termination point for RG-trajectories flowing to positive values of λ at small values k. The surface B bounds the region containing the GFP and NGFP towards positive values b. Typically RG trajectories do not terminate in this surface since they are repelled once they come close to it.

Finally, one finds that the β-function for the Newton coupling, $\beta_g(g, \lambda, b)$, vanishes as $g = 0$. As a consequence RG trajectories can not cross the $g = 0$ plane. Since the observed value of the Newton coupling is positive at laboratory scales, this feature limits the physically interesting sector of the phase diagram to positive values g_k.

4.4.2 Construction of sample trajectories

Following up on determining the relevant fixed point and singularity structures linked to the RG flow of the R^2-action (4.56) we proceed by constructing explicit sample solutions by integrating the flow equations (4.70) numerically. Our primary focus is on RG trajectories which emanate from the NGFP (4.72) at large values of t and undergo a crossover to the GFP as t is lowered. Typical examples exhibiting this behavior are shown in the right panel of figure 4.3. Following the discussion [23,84,87] it is this type of solutions which give rise to a classical regime resembling general relativity at low energy.

Following the classification in [23] for the Einstein-Hilbert truncation, a useful discriminator for the solutions is the IR value of the cosmological constant. Similarly to the Einstein-Hilbert

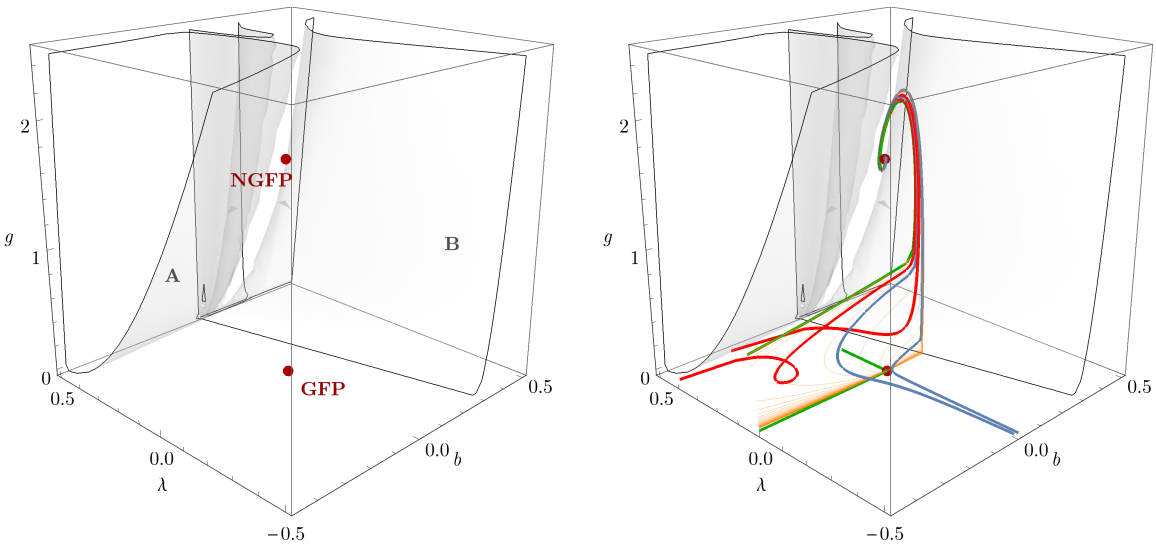

Figure 4.3: Overview of the flow diagram. 4.3a: the Gaussian fixed point (4.71) and non-Gaussian fixed point (4.72) are marked by the red dots. The singular planes stretch out in negative-b direction (A) and in negative-λ direction (B). 4.3b: selected RG trajectories. The red curves lead to a positive IR value of the cosmological constant and are denoted as trajectories of Type IIIa. These trajectories eventually terminate in the singular plane (A). The blue curves denote trajectories of Type Ia and possess a negative IR value of the cosmological constant. These curves avoid any singularities. The surface spanned by the orange curves marks the trajectories of Type IIa. Their IR limit is given by the GFP. These solutions separate the trajectories of Type Ia and IIIa. Finally, the green curve marks the trajectory that meets the observational constraints. It flows out of this diagram at $b = -0.5$ to large negative values of b, before turning around and flowing back into the diagram.

classifications one encounters trajectories which flow towards negative (Type Ia, blue curves) and positive Λ (Type IIIa, red curves) as t is lowered. The former are typically well-defined for all values of t while the latter terminate in the singular locus A. Finally, there are solutions (orange lines) which start at the NGFP and end at the GFP as $t \to -\infty$. These trajectories give rise to a vanishing IR value of the cosmological constant. They span a two-dimensional plane which separates the solutions of Type Ia and Type IIIa.

It is also instructive to discuss the flow of the R^2-coupling b_k along these trajectories. In all cases, b flows to zero in the IR. Let us first consider the trajectories that flow towards $b \to 0$ from positive b. Starting in the IR ($g_k \ll 1$) and following the flow into the UV, one finds that after approaching the GFP, these trajectories make a sharp turn towards positive b. As the trajectories approach the singular plane B, they are eventually repelled in the direction of the NGFP. This fixed point then provides the UV completion of the trajectory as $t \to \infty$.

Trajectories that approach $b_k \to 0$ from negative b show a different behavior. Tracing the flow from IR to the UV, they first flow towards the GFP before making a turn towards negative b. After obtaining a minimum value of b, they take a sharp turn and flow back into the direction of the GFP before entering the NGFP regime. In contrast to the trajectories with positive b, the flow of this type of trajectories may be bounded by the singular plane A. This ceiling may prevent the solutions from reaching the basin of attraction of the NGFP so that they terminate

at a finite value t once they leave the $g \ll 1$ region.

4.5 A complete cosmic history from Asymptotic Safety

Based on the phase space analysis of the previous section, we are ready to check if there is an RG trajectory satisfying all the conditions listed in table 4.2. The values of the couplings listed in this table refer to different energy scales which turns the search of the corresponding RG trajectory into a rather complicated boundary value problem. In order to simplify the analysis we first convert this setup into an initial value problem in section 4.5.1 before constructing the corresponding RG trajectory numerically in section 4.5.2. The main result of this section is the trajectory displayed in figure 4.4 which meets all cosmological requirements.

4.5.1 Initial values for the RG trajectory realized by Nature

Our first task is to determine the value of b_k and λ_k at the scale $k_0 \equiv k_{\rm lab}$ which will be used to set up the initial value problem. Since inflation and the measurement of the cosmological constant occur well below the Planck scale, $g_k \ll 1$ in this regime. Thus an expansion of the β-functions in powers of g_k which retains the leading quantum corrections is sufficient to capture all relevant features of the RG flow in this regime.[10] From a practical viewpoint, it is convenient to rewrite the β-functions (4.70) in terms of the new couplings

$$g_k\,, \quad u^1_k \equiv g_k\lambda_k\,, \quad u^2_k \equiv \frac{b_k}{16\pi g_k}\,, \tag{4.75}$$

since this allows to find analytic expressions relating the values of the couplings at different scales k.

We start with the expansion of the $\beta_g(g, u^1, u^2)$. This gives up to second order in g

$$\beta_g(g, u^1, u^2) = 2g_k - \frac{23}{24\pi}g_k^2 + \mathcal{O}(g_k^3), \tag{4.76}$$

which is independent of u^1 and u^2. The flow of g_k can then be integrated analytically, yielding

$$g_k = \frac{48\pi k^2 g_{k_0}}{48\pi k_0^2 + 23 g_{k_0}(k^2 - k_0^2)}\,. \tag{4.77}$$

We see that indeed, if $k \simeq k_0$, the dimensionful Newton's coupling is constant, up to corrections of order in $(k^2 - k_0^2)$. Thus it is convenient to identify $k_0 = k_{\rm lab}$ since this corresponds to the scale where G_k is measured. Converting the measured value of the dimensionful Newton's constant into dimensionless quantities gives

$$g_{k_0} = 6.71 \times 10^{-67}. \tag{4.78}$$

[10] Essentially, this setup corresponds to describing the RG flow by a one-loop approximation of the β-functions. The results displayed in table 4.3 confirm that this is indeed a valid approximation in the regime of interest.

The expansion of $\beta_{u^1}(g, u^1, u^2)$ yields

$$\beta_{u^1}(g, u^1, u^2) = -\frac{23}{12\pi} u_k^1 \, g_k - \frac{5}{12\pi} g_k^2 + \mathcal{O}(g_k^3). \tag{4.79}$$

Substituting the explicit solution for g_k, eq. (4.77), one finds that the scale-dependence of u_k^1 is given by

$$u_k^1 = \frac{48\pi \left(5 g_{k_0}^2 (1 - k^4/k_0^4) + 48\pi u_{k_0}^1\right)}{\left(48\pi + 23 g_{k_0} (k^2/k_0^2 - 1)\right)^2}. \tag{4.80}$$

Combining the solutions of g_k and u_k^1 allows to map the value of the cosmological constant measured at the Hubble scale k_{Hub} to the value of u_k^1 at the laboratory scale

$$u_{k_0}^1 = 2.68 \times 10^{-122}. \tag{4.81}$$

Finally, the expansion of $\beta_{u^2}(g, u^1, u^2)$ yields

$$\beta_{u^2}(g, u^1, u^2) = \frac{109}{2160\pi^2} + \mathcal{O}(g_k). \tag{4.82}$$

The solution of this equation gives the typical logarithmic running of a marginal coupling at one-loop level

$$u_k^2 = \frac{109}{2160\pi^2} \log\left(\frac{k}{k_0}\right) + u_{k_0}^2. \tag{4.83}$$

Inserting the measured values at k_{infl} gives the initial value

$$u_{k_0}^2 = -2.00 \times 10^{16}. \tag{4.84}$$

Combining the results (4.78), (4.81), and (4.84) with the definition (4.75) one readily arrives at the initial values for g_k, λ_k, and b_k

$$g_{k_0} = 6.71 \times 10^{-67}, \quad \lambda_{k_0} = 3.99 \times 10^{-56}, \quad b_{k_0} = -6.75 \times 10^{-49}. \tag{4.85}$$

These values serve as the starting point for integrating the flow equation numerically.

4.5.2 The RG trajectory realized by Nature

In order to obtain the RG trajectory resulting from the initial conditions (4.85), we now integrate the full β-functions numerically. For this, we use the NDSolve routine in Mathematica. Since the initial starting point is very close to zero, we increase the working precision to 124 digits. When the integration reaches a regime where the parameters take larger values, we decrease the precision to 25 digits. This allows us to track the RG flow from the classical regime up to the NGFP regime.

The resulting RG trajectory is depicted by the green curve in figure 4.3b. The scale-dependence of the corresponding dimensionful couplings Λ_k, G_k, and B_k is summarized in figure 4.4. In table 4.3, we summarize the values of the couplings at different relevant energy scales. The existence of this RG trajectory constitutes the main result of this work.

The solution shown in figure 4.4 exhibits several remarkable features. First of all, we see

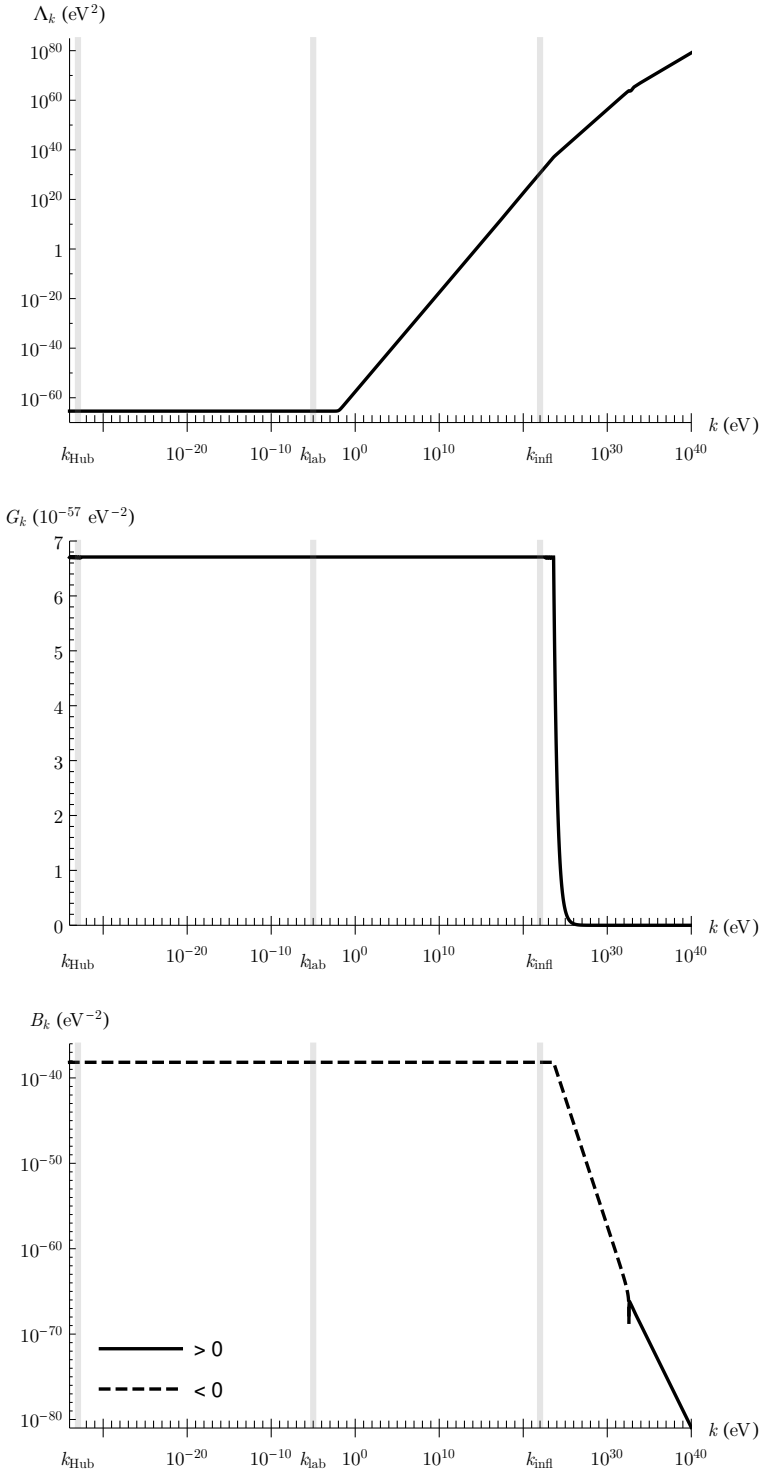

Figure 4.4: RG trajectory passing through all points identified in table 4.2. Top panel: cosmological constant Λ_k. Middle panel: Newton's coupling G_k. Bottom panel: R^2 coupling B_k. The gray bars indicate the energy scales at which constraints are imposed.

Energy scale	Λ	G	B
(eV)	(eV^2)	(10^{-57} eV^{-2})	(10^{-39} eV^{-2})
$k_{\rm Hub} \simeq 10^{-33}$	$\mathbf{4 \times 10^{-66}}$	6.71	-6.7
$k_{\rm lab} \simeq 10^{-5}$	4×10^{-66}	**6.71**	-6.7
$k_{\rm infl} \simeq 10^{22}$	4×10^{30}	6.71	**-6.7**

Table 4.3: Selected values of the RG flow satisfying the observational constraints. Within experimental uncertainty, the parameters are constant, except for the cosmological constant Λ. The bold values are constrained by observations, whereas the other values are results from the RG calculation.

that the RG flow meets all observational constraints. This means that the expansion in small g is valid, and that quantum effects only play a role at energy scales beyond inflation. In fact, both Newton's coupling and the R^2 coupling start to run at 10^{24} eV, which is beyond the upper bound on the inflation scale, 10^{22} eV. Interestingly, the Newton's coupling reaches a very small value at the Planck scale 10^{27} eV. [11]

Secondly, we observe that Λ_k starts to run at 10^{-2} eV, corresponding to a length scale of 10^{-4} m. At lower energy scales, Λ_k is constant and equal to the value quoted in table 4.1, thus not spoiling the agreement with current measurements that take place over cosmological scales.

We close our discussion by verifying that our RG trajectory meets all the working assumptions made in section 4.3. At the inflation scale, one has to check that $\Lambda_{k_{\rm infl}} = 10^{30}\,{\rm eV}^2$ does not affect the dynamics in this regime so that the constraint obtained on B is valid. Specifically, we assumed that at the scale $k_{\rm infl}$ the R^2 term dominates the background universe evolution. This amounts to the condition $\Lambda_k/(B_k R^2) \ll 1$ and $B_k R \gg 1$, both evaluated at $k = k_{\rm infl}$. Using that in an approximately de Sitter background the curvature R is related to the Hubble parameter as $R \simeq 12H^2$ and the relation that $H = k_{\rm infl}$, we find

$$B_k R \simeq 10^7 \gg 1\,, \qquad \Lambda_k/(B_k R^2) \simeq 10^{-22} \ll 1. \tag{4.86}$$

Thus our working assumptions are valid in this regime.

The analysis of the late time cosmological evolution assumed that the R^2 term does not significantly affect the background universe evolution at $k_{\rm Hub}$. Again making use of the fact that at late times we are in a quasi-de Sitter background so that $R \simeq 12(k_{\rm Hub})^2$, we find

$$B_k R^2 \simeq 10^{-168}\ {\rm eV}^2\,, \qquad \Lambda_k \simeq 10^{-66}\ {\rm eV}^2\,, \qquad R \simeq 10^{-65}\ {\rm eV}^2. \tag{4.87}$$

Together with the result (4.86) this establishes that our RG trajectory indeed fulfills all the working assumptions made when deriving table 4.2.

[11] Cosmological consequences of a Planck-scale-vanishing Newton's coupling were discussed from a different perspective in [88, 89]. We defer to a future work to investigate the relation between the two approaches.

4.6 Conclusion

In this chapter we have investigated the compatibility of the asymptotic safety mechanism with the laws of gravity observed at sub-Planckian scales. The main focus has been on obtaining a viable cosmological evolution. This question has already been subject to a significant amount of work. Starting from the seminal works [56,57], the cosmological evolution and its signatures have been studied using a modified dynamics resulting from scale-dependent couplings [58, 60–67], dilaton-gravity [59,70], Higgs-inflation inspired models [68,69], non-Gaussian fixed point driven inflation [71–73], and anisotropic models [74]. All these investigations rely on a renormalization group improvement which relates the RG scale k to a physical quantity like the Hubble scale or the Ricci scalar R in order to capture "the leading quantum gravity effects" of the system. These studies have raised the expectation that the very early universe undergoes a phase of power-law inflation and an almost flat scalar power spectrum [75].

In this work, we performed the first cosmological analysis within asymptotically safe gravity based on a "first principles" analysis. The gravitational dynamics is obtained by solving the flow equation for the effective average action at the R^2-level, giving the explicit energy dependence of the three gravitational couplings contained in (4.56). Thus the gravitational dynamics is obtained *without invoking a scale-identification procedure*. Analyzing the space of solutions compatible with Asymptotic Safety gave rise to two striking insights. First, there are solutions which are compatible with the values of Newton's coupling and the cosmological constant observed, respectively, at laboratory and cosmological scales. Moreover, these constraints from late time cosmology are compatible with an R^2-term which gives rise to a phenomenologically viable phase of inflation, without spoiling the late time cosmological evolution. The seeds for this salient physics below the Planck scale are laid by the NGFP governing the gravitational dynamics at trans-Planckian scales: mapping out the surface of asymptotically safe RG trajectories establishes that there are solutions which besides being compatible with observed low-energy physics also realize an inflationary phase based on the resulting gravitational dynamics. Thus Asymptotic Safety may naturally give rise to Starobinsky inflation and there is no need to introduce an ad hoc inflaton field. In this sense, the construction is very economic in attributing highly desirable features in the early and late-time dynamics of the universe to quantum gravity effects.[12]

As a by-product our analysis constructed the realistic RG trajectory displayed in figure 4.4.[13] An intriguing feature of this solution is that the cosmological constant Λ_k acquires an energy dependence already at 10^{-2} eV. This scale is well below the Planck scale where the energy dependence of the Newton coupling and the R^2-coupling sets in and already occurs in the vicinity of the Gaussian fixed point, i.e., way below the energy scale where the Newton coupling and the R^2-coupling exhibit an appreciable scale-dependence. As a consequence, one expects that fluctuations with a length scale of 10^{-4} m (or smaller) feel a different value of Λ_k. Assuming that a fluctuation of this size is generated at the same time as the cosmic microwave background, the subsequent cosmological evolution would expand such a structure to a size of approximately 1 m, a scale that is well below the resolution of current large-scale structure surveys. On the

[12] For a similar discussion at the level of effective field theory see [90, 91].

[13] For an earlier analysis including the observed values for G and Λ, see [87].

other hand, currently observed scales in the cosmic microwave background power spectrum would have a wavelength of 10^{-4} m during the inflationary phase, after horizon exit. It would be interesting to investigate if this effect leaves an imprint on the structure formation in the early universe.

We close our discussion with the following remark. It is clear that (free) matter fields give rise to additional contributions in the β-functions (C.13) [92–94]. Naturally, the properties of the non-Gaussian gravity-matter fixed points, including its position and stability coefficients, differ from the ones encountered in pure gravity. At least for the class of gravity-dominated gravity-matter fixed points these properties are, by definition, qualitatively similar to the ones of the pure gravity fixed point underlying this work. We thus expect that the scenario developed in this work essentially carries over to these cases as well.

Chapter 5

Summary and outlook

The framework of Asymptotic Safety provides a promising approach towards a quantum formalism for gravity. It allows to connect the trans-Planckian regime of short distances, controlled by a suitable non-Gaussian fixed point, to classical, large distance physics below the Planck scale. The emergence of this classical low-energy physics from divergence-free UV physics is linked to a crossover regime between a non-Gaussian and a Gaussian fixed point. This feature makes Asymptotic Safety an attractive mechanism for cosmological phenomenology, as it allows to study the evolution of the universe.

This thesis commenced with an overview of the important concepts of Asymptotic Safety, as well as its investigation based on the functional renormalization group. This discussion was rather abstract and not rich of concrete examples, though. Hence, a detailed derivation of the RG flow equations for a particular scalar-tensor model was given in chapter 3. This model, while being simple enough to allow for a concise illustration of typical RG calculations, was also, in principle, suited to study cosmological implications. However, it was found that due to the triviality problem, the system was unfit for a cosmological investigation. Subsequently, our analysis shifted to the investigation of a different action in chapter 4. Here, we pioneered a new path for cosmological analyses within Asymptotic Safety; while earlier research employed renormalization group improvements to capture the leading order quantum effects of the system, we solved the underlying flow equations to obtain the scale-dependence of the parameters in the action. This allowed us to obtain a complete cosmic history from Asymptotic Safety, that is, a trajectory in theory space that is not only asymptotically safe, but also satisfies the observational constraints from different cosmological eras. In particular, it was shown that the studied system allows to connect the trans-Planckian regime to a phenomenologically viable phase of inflation at early times, which in turn is linked to a phase of accelerated expansion driven by the cosmological constant during late times.

At this point, a number of remarks regarding the stability of this result are in order. A common question that arises in studies of RG flows is how the findings depend on the truncation. Of course, one desires to make conclusions that are independent of such an approximation and would therefore be stable upon extending the truncation. Regarding the system studied in chapter 4, a first extension could include higher order curvature terms in the ansatz for the effective average action. It is known, for instance from [81], that higher order curvature terms only contribute irrelevant directions. Hence, in the pure-gravity case, it is expected that the

number of free parameters is three, which are all taken into account in our present investigation. The extra parameters added by extending the truncation are fixed by the three free parameters (g, λ, b). However, the additional terms will give corrections to the scalar potential (4.59). The precise form of these corrections should be the focus of future work.

Furthermore, such an extension of the truncation also brings about technical difficulties. Since the enlargement of the truncation adds irrelevant directions, it becomes a highly non-trivial task to guarantee the Asymptotic Safety of RG trajectories. Ensuring that a trajectory lies on the UV critical hypersurface, while also satisfying observational bounds, would be an exciting but challenging task.

The work presented in this thesis may serve as a springboard for further investigations in this direction. Thus, we argue that this new approach to phenomenology within Asymptotic Safety opens up a wide range of possibilities for future research.

Acknowledgements

I would like to thank two people without whom this thesis would not have been possible. Firstly, many thanks to Chris Ripken for our numerous discussions ranging from several seconds to many hours. Secondly, I want to thank Frank Saueressig for all our meetings and, in particular, for suggesting a project that suited me exceptionally well.

Appendix A

Details of the scalar-tensor model

A.1 Functional derivatives

In this section, we derive functional derivatives needed to calculate the Hessian operator in chapter 3. Here, the variations are with respect to symmetric (0,2)-tensors v and w. The variations w.r.t. scalars that are needed to calculate the Hessian are simple enough to be calculated on the fly in appendix A.2.

The results are listed first; the proofs are given afterwards.

A.1.1 First variations

$$\delta_v g_{\mu\nu} = v_{\mu\nu} \tag{A.1}$$
$$\delta_v g^{\rho\sigma} = -g^{\sigma\nu} g^{\rho\mu} v_{\mu\nu} \tag{A.2}$$
$$\delta_v \sqrt{g} = \frac{1}{2}\sqrt{g} g^{\mu\nu} v_{\mu\nu} \tag{A.3}$$
$$\delta_v \Gamma^{\mu}{}_{\alpha\beta} = \frac{1}{2} g^{\mu\rho}(D_\alpha v_{\beta\rho} + D_\beta v_{\alpha\rho} - D_\rho v_{\alpha\beta}) \tag{A.4}$$
$$\delta_v R^{\rho}{}_{\sigma\mu\nu} = \frac{1}{2}\big(R^{\rho}{}_{\lambda\mu\nu} v^{\lambda}{}_{\sigma} - R^{\lambda}{}_{\sigma\mu\nu} v^{\rho}{}_{\lambda} + D_\mu D_\sigma v^{\rho}{}_{\nu} - D_\mu D^\rho v_{\sigma\nu} - D_\nu D_\sigma v^{\rho}{}_{\mu} + D_\nu D^\rho v_{\sigma\mu}\big) \tag{A.5}$$
$$\begin{aligned}\delta_v R_{\sigma\nu} = \frac{1}{2}\big(&R_{\lambda\nu} v^{\lambda}{}_{\sigma} + R_{\lambda\sigma} v^{\lambda}{}_{\nu} - 2R^{\lambda}{}_{\sigma\rho\nu} v^{\rho}{}_{\lambda} + D_\sigma D_\rho v^{\rho}{}_{\nu} + \Delta v_{\sigma\nu} - D_\nu D_\sigma v^{\alpha}{}_{\alpha} \\ &+ D_\nu D^\rho v_{\sigma\rho}\big)\end{aligned} \tag{A.6}$$
$$\delta_v R = \big(-R^{\rho\mu} + D^\mu D^\rho + g^{\mu\rho}\Delta\big) v_{\mu\rho} \tag{A.7}$$
$$\delta_v(\Delta\phi) = \big(v_{\mu\nu} D^\mu D^\nu + (D^\nu v_{\nu\sigma}) D^\sigma - \frac{1}{2} g^{\mu\nu}(D^\lambda v_{\mu\nu}) D_\lambda\big)\phi \tag{A.8}$$

Proofs

Inverse metric

The variation of the inverse metric is obtained from

$$0 = \delta_v \delta^{\rho}{}_{\nu} = \delta_v(g^{\rho\mu} g_{\mu\nu}) = \delta_v(g^{\rho\mu}) g_{\mu\nu} + g^{\rho\mu}\delta_v(g_{\mu\nu}) = \delta_v(g^{\rho\mu}) g_{\mu\nu} + g^{\rho\mu} v_{\mu\nu}\,, \tag{A.9}$$

from which we obtain

$$\delta_v(g^{\rho\mu})g_{\mu\nu} = -g^{\rho\mu}v_{\mu\nu}\,. \tag{A.10}$$

Multiplying with $g^{\nu\sigma}$ gives

$$\delta_v g^{\rho\sigma} = -g^{\sigma\nu}g^{\rho\mu}v_{\mu\nu}\,. \tag{A.11}$$

Metric determinant

From Jacobi's formula, one has the relation

$$\delta_v g = g g^{\mu\nu}v_{\mu\nu}\,, \tag{A.12}$$

where $g \equiv \det g$. Hence, one finds

$$\delta_v\sqrt{g} = \frac{1}{2}\sqrt{g}g^{\mu\nu}v_{\mu\nu}\,. \tag{A.13}$$

Christoffel symbol

The variation of the Christoffel symbol is found from

$$\begin{aligned}
\delta_v\Gamma^{\mu}{}_{\alpha\beta} &= \frac{1}{2}\delta_v\Big(g^{\mu\nu}(\partial_\alpha g_{\nu\beta} + \partial_\beta g_{\nu\alpha} - \partial_\nu g_{\alpha\beta})\Big) \\
&= \frac{1}{2}\Big(-g^{\mu\rho}g^{\nu\sigma}v_{\rho\sigma}(\partial_\alpha g_{\nu\beta} + \partial_\beta g_{\nu\alpha} - \partial_\nu g_{\alpha\beta}) + g^{\mu\nu}(\partial_\alpha v_{\nu\beta} + \partial_\beta v_{\nu\alpha} - \partial_\nu v_{\alpha\beta})\Big) \\
&= -g^{\mu\rho}\Gamma^{\sigma}{}_{\alpha\beta}v_{\rho\sigma} + \frac{1}{2}g^{\mu\nu}(\partial_\alpha v_{\nu\beta} + \partial_\beta v_{\nu\alpha} - \partial_\nu v_{\alpha\beta}) \\
&= \frac{1}{2}g^{\mu\nu}(\partial_\alpha v_{\nu\beta} + \partial_\beta v_{\nu\alpha} - \partial_\nu v_{\alpha\beta}) \\
&+ \frac{1}{2}g^{\mu\rho}(-\Gamma^{\sigma}{}_{\alpha\beta}v_{\sigma\rho} - \Gamma^{\sigma}{}_{\alpha\rho}v_{\beta\sigma} - \Gamma^{\sigma}{}_{\beta\alpha}v_{\sigma\rho} - \Gamma^{\sigma}{}_{\beta\rho}v_{\alpha\sigma} + \Gamma^{\sigma}{}_{\rho\alpha}v_{\sigma\beta} + \Gamma^{\sigma}{}_{\rho\beta}v_{\alpha\sigma}) \\
&= \frac{1}{2}g^{\mu\rho}(D_\alpha v_{\beta\rho} + D_\beta v_{\alpha\rho} - D_\rho v_{\alpha\beta})\,.
\end{aligned} \tag{A.14}$$

Riemann tensor

The Riemann tensor is defined as

$$R^{\rho}{}_{\sigma\mu\nu} = \partial_\mu\Gamma^{\rho}{}_{\nu\sigma} - \partial_\nu\Gamma^{\rho}{}_{\mu\sigma} + \Gamma^{\rho}{}_{\mu\lambda}\Gamma^{\lambda}{}_{\nu\sigma} - \Gamma^{\rho}{}_{\nu\lambda}\Gamma^{\lambda}{}_{\mu\sigma}\,. \tag{A.15}$$

Since the variation of a Christoffel symbol is the difference of two such symbols, it is a tensor and we can calculate its covariant derivative,

$$D_\mu(\delta_v\Gamma^{\rho}{}_{\nu\sigma}) = \partial_\mu(\delta_v\Gamma^{\rho}{}_{\nu\sigma}) + \Gamma^{\rho}{}_{\mu\lambda}\delta_v\Gamma^{\lambda}{}_{\nu\sigma} - \Gamma^{\lambda}{}_{\mu\nu}\delta_v\Gamma^{\rho}{}_{\lambda\sigma} - \Gamma^{\lambda}{}_{\mu\sigma}\delta_v\Gamma^{\rho}{}_{\nu\lambda}\,. \tag{A.16}$$

We then observe that the variation of the Riemann tensor equals the difference of two such terms,

$$\delta_v R^{\rho}{}_{\sigma\mu\nu} = D_\mu(\delta_v\Gamma^{\rho}{}_{\nu\sigma}) - D_\nu(\delta_v\Gamma^{\rho}{}_{\mu\sigma})\,. \tag{A.17}$$

Upon using eq. (A.14), one finds

$$\begin{aligned}\delta_v R^{\rho}{}_{\sigma\mu\nu} &= D_\mu\big(\frac{1}{2}g^{\rho\lambda}(D_\sigma v_{\nu\lambda} + D_\nu v_{\sigma\lambda} - D_\lambda v_{\sigma\nu})\big) - D_\nu\big(\frac{1}{2}g^{\rho\lambda}(D_\sigma v_{\mu\lambda} + D_\mu v_{\sigma\lambda} - D_\lambda v_{\sigma\mu})\big)\\ &= \frac{1}{2}\big(D_\mu D_\sigma v^{\rho}{}_{\nu} + D_\mu D_\nu v^{\rho}{}_{\sigma} - D_\mu D^\rho v_{\sigma\nu} - D_\nu D_\sigma v^{\rho}{}_{\mu} - D_\nu D_\mu v^{\rho}{}_{\sigma} + D_\nu D^\rho v_{\sigma\mu}\big)\\ &= \frac{1}{2}\big(R^{\rho}{}_{\lambda\mu\nu}v^{\lambda}{}_{\sigma} - R^{\lambda}{}_{\sigma\mu\nu}v^{\rho}{}_{\lambda} + D_\mu D_\sigma v^{\rho}{}_{\nu} - D_\mu D^\rho v_{\sigma\nu} - D_\nu D_\sigma v^{\rho}{}_{\mu} + D_\nu D^\rho v_{\sigma\mu}\big)\,, \end{aligned} \tag{A.18}$$

where in the last step we wrote $[D_\mu, D_\nu]v^{\rho}{}_{\sigma}$ in terms of two Riemann tensors.

Ricci tensor

The variation of the Ricci tensor is found by contracting suitable indices of eq. (A.18),

$$\begin{aligned}\delta_v R_{\sigma\nu} &= \delta_v R^{\rho}{}_{\sigma\rho\nu}\\ &= \frac{1}{2}\big(R_{\lambda\nu}v^{\lambda}{}_{\sigma} - R^{\lambda}{}_{\sigma\rho\nu}v^{\rho}{}_{\lambda} + D_\rho D_\sigma v^{\rho}{}_{\nu} + \Delta v_{\sigma\nu} - D_\nu D_\sigma v^{\alpha}{}_{\alpha} + D_\nu D^\rho v_{\sigma\rho}\big)\\ &= \frac{1}{2}\big(R_{\lambda\nu}v^{\lambda}{}_{\sigma} + R_{\lambda\sigma}v^{\lambda}{}_{\nu} - 2R^{\lambda}{}_{\sigma\rho\nu}v^{\rho}{}_{\lambda} + D_\sigma D_\rho v^{\rho}{}_{\nu} + \Delta v_{\sigma\nu} - D_\nu D_\sigma v^{\alpha}{}_{\alpha}\\ &\quad + D_\nu D^\rho v_{\sigma\rho}\big)\,, \end{aligned} \tag{A.19}$$

where in the last step we replaced $D_\rho D_\sigma v^{\rho}{}_{\nu}$ by $D_\sigma D_\rho v^{\rho}{}_{\nu}$ and two Riemann tensors.

Ricci scalar

The variation of the Ricci scalar follows from the previous result. One finds

$$\begin{aligned}\delta_v R &= \delta_v R^{\sigma}{}_{\sigma}\\ &= \delta_v(g^{\sigma\nu}R_{\sigma\nu})\\ &= R_{\sigma\nu}\delta_v g^{\sigma\nu} + g^{\sigma\nu}\delta_v R_{\sigma\nu}\\ &= \big(-R^{\rho\mu} + D^\mu D^\rho + g^{\mu\rho}\Delta\big)v_{\mu\rho}\,. \end{aligned} \tag{A.20}$$

Laplacian

The variation of the Laplacian acting on a scalar field ϕ is

$$\begin{aligned}\delta_v(\Delta\phi) &= \delta_v(-g^{\mu\nu}D_\mu D_\nu\phi)\\ &= \delta_v(-g^{\mu\nu})D_\mu D_\nu\phi - g^{\mu\nu}\delta_v(D_\mu D_\nu\phi)\\ &= v_{\mu\nu}D^\mu D^\nu\phi - g^{\mu\nu}\delta_v(\partial_\mu\partial_\nu\phi - \Gamma^{\lambda}{}_{\mu\nu}\partial_\lambda\phi)\\ &= v_{\mu\nu}D^\mu D^\nu\phi + g^{\mu\nu}\delta_v\Gamma^{\lambda}{}_{\mu\nu}\partial_\lambda\phi\\ &= v_{\mu\nu}D^\mu D^\nu\phi + g^{\mu\nu}\frac{1}{2}g^{\lambda\sigma}(D_\mu v_{\nu\sigma} + D_\nu v_{\mu\sigma} - D_\sigma v_{\mu\nu})\partial_\lambda\phi\\ &= \big(v_{\mu\nu}D^\mu D^\nu + (D^\nu v_{\nu\sigma})D^\sigma - \frac{1}{2}g^{\mu\nu}(D^\lambda v_{\mu\nu})D_\lambda\big)\phi\,. \end{aligned} \tag{A.21}$$

A.1.2 Second variations

$$\delta_v\delta_w\sqrt{g} = \sqrt{g}v_{\alpha\beta}\left(\frac{1}{4}g^{\mu\nu}g^{\alpha\beta} - \frac{1}{2}g^{\mu\alpha}g^{\nu\beta}\right)w_{\mu\nu} \tag{A.22}$$

$$\begin{aligned}\delta_v\delta_w(\Delta\phi) = &-v_{\rho\sigma}g^{\rho\mu}w_{\mu\nu}D^\sigma D^\nu\phi - v_{\rho\sigma}g^{\rho\nu}w_{\mu\nu}D^\mu D^\sigma\phi - w_{\mu\nu}g^{\nu\beta}(D^\mu v_{\beta\sigma})D^\sigma\phi\\ &- v_{\rho\gamma}g^{\nu\rho}(D^\gamma w_{\nu\sigma})D^\sigma\phi - g^{\lambda\rho}(D^\nu v_{\nu\rho})w_{\lambda\sigma}D^\sigma\phi\\ &+ \frac{1}{2}g^{\nu\alpha}(D^\lambda v_{\alpha\nu})w_{\lambda\sigma}D^\sigma\phi + \frac{1}{2}v_{\rho\sigma}g^{\mu\rho}g^{\nu\sigma}(D^\lambda w_{\mu\nu})D_\lambda\phi\\ &+ \frac{1}{2}g^{\mu\nu}v_{\rho\sigma}(D^\sigma w_{\mu\nu})D^\rho\phi + \frac{1}{2}w_{\rho\nu}g^{\mu\nu}g^{\rho\sigma}(D^\lambda v_{\mu\sigma})D_\lambda\phi\\ &- g^{\lambda\rho}v_{\lambda\sigma}(D^\nu w_{\nu\rho})D^\sigma\phi\end{aligned} \tag{A.23}$$

$$\delta_v\delta_w R = w_{\mu\nu}\left(-\frac{1}{2}g^{\mu\nu}g^{\rho\sigma}\Delta + g^{\rho\mu}R^{\nu\sigma} - R^{\rho\mu\nu\sigma} - g^{\mu\sigma}D^\nu D^\rho - \frac{1}{2}g^{\nu\sigma}D^\mu D^\rho\right)v_{\rho\sigma} \tag{A.24}$$

Proofs

Metric determinant

$$\delta_v\delta_w\sqrt{g} = \sqrt{g}v_{\alpha\beta}\left(\frac{1}{4}g^{\mu\nu}g^{\alpha\beta} - \frac{1}{2}g^{\mu\alpha}g^{\nu\beta}\right)w_{\mu\nu}\,. \tag{A.25}$$

Ricci scalar

For the second variation of the Ricci scalar, one finds

$$\delta_v\delta_w R = \delta_v(-w_{\mu\nu}R^{\mu\nu} + D^\mu D^\nu w_{\mu\nu} + g^{\mu\nu}\Delta w_{\mu\nu})\,. \tag{A.26}$$

The first of these three terms yields

$$\delta_v(w_{\mu\nu}R^{\mu\nu}) = w_{\mu\nu}\left(-g^{\mu\rho}R^{\nu\sigma} + R^{\sigma\mu\nu\rho} + g^{\mu\rho}D^\nu D^\sigma + \frac{1}{2}g^{\mu\rho}g^{\nu\sigma}\Delta - \frac{1}{2}g^{\rho\sigma}D^\mu D^\nu\right)v_{\rho\sigma}\,. \tag{A.27}$$

For the second term, $\delta_v D_\alpha D_\beta w^{\alpha\beta}$, we first define $C^\alpha \equiv D_\beta w^{\alpha\beta}$ and calculate

$$\begin{aligned}\delta_v D_\alpha C^\beta &= \delta_v\partial_\alpha C^\beta + \delta_v(\Gamma^\beta{}_{\alpha\lambda}C^\lambda)\\ &= \partial_\alpha\delta_v C^\beta + \Gamma^\beta{}_{\alpha\lambda}\delta_v C^\lambda + C^\lambda\delta_v\Gamma^\beta{}_{\alpha\lambda}\\ &= D_\alpha(\delta_v C^\beta) + C^\lambda\delta_v\Gamma^\beta{}_{\alpha\lambda}\\ &= D_\alpha(\delta_v C^\beta) + \frac{1}{2}C^\lambda g^{\beta\sigma}(D_\alpha v_{\sigma\lambda} + D_\lambda v_{\sigma\alpha} - D_\sigma v_{\alpha\lambda})\end{aligned} \tag{A.28}$$

Via the same method, one also obtains

$$\begin{aligned}\delta_v C^\beta &= \delta_v D_\alpha w^{\alpha\beta}\\ &= D_\alpha(\delta_v w^{\alpha\beta}) + \frac{1}{2}w^{\lambda\beta}g^{\alpha\sigma}(D_\alpha v_{\lambda\sigma} + D_\lambda w_{\alpha\sigma} - D_\sigma w_{\alpha\lambda})\\ &\quad + \frac{1}{2}w^{\lambda\alpha}g^{\beta\sigma}(D_\alpha v_{\lambda\sigma} + D_\lambda v_{\alpha\sigma} - D_\sigma w_{\alpha\lambda})\,.\end{aligned} \tag{A.29}$$

Applying these results, collecting all terms and throwing away total derivatives, one can reduce this term to the simple expression

$$\delta_v D_\mu D_\nu w^{\mu\nu} = w_{\mu\nu}\left(-\frac{1}{2}g^{\rho\sigma}D^\mu D^\nu\right)v_{\rho\sigma}\,. \tag{A.30}$$

Using the same method, one finds for the third term of eq. (A.26)

$$\delta_v(g^{\mu\nu}\Delta w_{\mu\nu}) = w_{\mu\nu}\left(-\frac{1}{2}g^{\mu\nu}g^{\rho\sigma}\Delta\right)v_{\rho\sigma}\,. \tag{A.31}$$

Hence, we may write for the second variation of the Ricci scalar

$$\delta_v\delta_w R = w_{\mu\nu}\big(-\frac{1}{2}g^{\mu\nu}g^{\rho\sigma}\Delta + g^{\rho\mu}R^{\nu\sigma} - R^{\rho\mu\nu\sigma} - g^{\mu\sigma}D^\nu D^\rho - \frac{1}{2}g^{\nu\sigma}D^\mu D^\rho\big)v_{\rho\sigma}\,, \tag{A.32}$$

where we have discarded all total derivatives.

Laplacian

To obtain the second variation of the Laplacian, $\delta_v\delta_w(\Delta\phi)$, we tackle the three terms in the first variation one by one. Firstly,

$$\begin{aligned}\delta_v(w_{\mu\nu}D^\mu D^\nu\phi) = &-v_{\rho\sigma}g^{\rho\mu}w_{\mu\nu}D^\sigma D^\nu\phi - v_{\rho\sigma}g^{\rho\nu}w_{\mu\nu}D^\mu D^\sigma\phi - w_{\mu\nu}g^{\nu\rho}(D^\mu v_{\rho\sigma})D^\sigma\phi\\ &+\frac{1}{2}w_{\mu\nu}g^{\mu\rho}g^{\nu\sigma}(D^\lambda v_{\rho\sigma})D_\lambda\phi\,.\end{aligned} \tag{A.33}$$

Secondly,

$$\begin{aligned}\delta_v\Big((D^\nu w_{\nu\sigma})D^\sigma\phi\Big) = &-v_{\rho\lambda}g^{\nu\rho}(D^\lambda w_{\nu\sigma})D^\sigma\phi - g^{\lambda\rho}(D^\nu v_{\nu\rho})w_{\lambda\sigma}D^\sigma\phi\\ &+\frac{1}{2}g^{\nu\rho}(D^\lambda v_{\rho\nu})w_{\lambda\sigma}D^\sigma\phi - \frac{1}{2}g^{\nu\mu}g^{\lambda\rho}(D_\sigma v_{\mu\rho})w_{\nu\lambda}D^\sigma\phi\\ &-g^{\mu\rho}v_{\mu\sigma}(D^\nu w_{\nu\rho})D^\sigma\phi\,.\end{aligned} \tag{A.34}$$

Thirdly,

$$\begin{aligned}\delta_v\Big(g^{\mu\nu}(D^\lambda w_{\mu\nu})D_\lambda\phi\Big) = &-v_{\rho\sigma}g^{\mu\rho}g^{\nu\sigma}(D^\lambda w_{\mu\nu})D_\lambda\phi - g^{\mu\nu}v_{\rho\sigma}(D^\sigma w_{\mu\nu})D^\rho\phi\\ &-w_{\rho\nu}g^{\mu\nu}g^{\rho\sigma}(D^\lambda v_{\mu\sigma})D_\lambda\phi\,.\end{aligned} \tag{A.35}$$

Combining these, we obtain

$$\begin{aligned}\delta_v\delta_w(\Delta\phi) = &-v_{\rho\sigma}g^{\rho\mu}w_{\mu\nu}D^\sigma D^\nu\phi - v_{\rho\sigma}g^{\rho\nu}w_{\mu\nu}D^\mu D^\sigma\phi - w_{\mu\nu}g^{\nu\beta}(D^\mu v_{\beta\sigma})D^\sigma\phi\\ &-v_{\rho\gamma}g^{\nu\rho}(D^\gamma w_{\nu\sigma})D^\sigma\phi - g^{\lambda\rho}(D^\nu v_{\nu\rho})w_{\lambda\sigma}D^\sigma\phi\\ &+\frac{1}{2}g^{\nu\alpha}(D^\lambda v_{\alpha\nu})w_{\lambda\sigma}D^\sigma\phi + \frac{1}{2}v_{\rho\sigma}g^{\mu\rho}g^{\nu\sigma}(D^\lambda w_{\mu\nu})D_\lambda\phi\\ &+\frac{1}{2}g^{\mu\nu}v_{\rho\sigma}(D^\sigma w_{\mu\nu})D^\rho\phi + \frac{1}{2}w_{\rho\nu}g^{\mu\nu}g^{\rho\sigma}(D^\lambda v_{\mu\sigma})D_\lambda\phi\\ &-g^{\lambda\rho}v_{\lambda\sigma}(D^\nu w_{\nu\rho})D^\sigma\phi\,.\end{aligned} \tag{A.36}$$

A.2 Hessian calculations

Since the space of fields consists of both tensors and scalars, the Hessian contains four components; a tensor-tensor component, a scalar-scalar component and two off-diagonal components. We will discuss each of these separately.

A.2.1 Tensor-tensor component

The tensor-tensor component of the Hessian, $\Gamma^{(2)}_{k,hh}$ is obtained by calculating the second variation of Γ_k with respect to symmetric (0,2)-tensors v and w. Specifically, we define

$$\delta_v\delta_w\Gamma_k \equiv \langle v, \Gamma^{(2)}_{k,hh} w\rangle \equiv \int \mathrm{d}^d x\sqrt{g} v_{\mu\nu}\mathcal{G}^{\mu\nu\rho\sigma}\left(\Gamma^{(2)}_{k,hh}w\right)_{\rho\sigma} \tag{A.37}$$

where the inner product on the space of $(0,2)$-tensors is defined via a supermetric $\mathcal{G}$ given by

$$\mathcal{G}^{\mu\nu\rho\sigma} = \mathbb{1}^{\mu\nu\rho\sigma} - \varpi g^{\mu\nu}g^{\rho\sigma} \tag{A.38}$$

and the unit operator is $\mathbb{1}^{\mu\nu\rho\sigma} = \frac{1}{2}(g^{\mu\rho}g^{\nu\sigma} + g^{\mu\sigma}g^{\nu\rho})$. The inverse of $\mathcal{G}$ is then found to be

$$\tilde{\mathcal{G}}_{\mu\nu\rho\sigma} = \mathbb{1}_{\mu\nu\rho\sigma} + \tilde{\varpi} g_{\mu\nu}g_{\rho\sigma}\,, \tag{A.39}$$

where $\tilde{\varpi} = \frac{\varpi}{1-\varpi d}$.

Gravitational sector

We start with the contribution of the gravitational EAA. One has

$$\begin{aligned}
\delta_v\delta_w\Gamma^{\mathrm{grav}}_k &= -\frac{1}{16\pi G_k}\delta_V\delta_w\int \mathrm{d}^d x\sqrt{g}R \\
&= -\frac{1}{16\pi G_k}\int \mathrm{d}^d x\big((\delta_v\delta_w\sqrt{g})R + (\delta_v\sqrt{g})\delta_w R + (\delta_w\sqrt{g})\delta_v R + \sqrt{g}\delta_v\delta_w R\big) \\
&\equiv \int \mathrm{d}^d x\sqrt{g}v_{\mu\nu}\mathcal{G}^{\mu\nu\rho\sigma}\Big(\left[\Gamma^{\mathrm{grav},(2)}_{k,hh,1}w\right]_{\rho\sigma} + \left[\Gamma^{\mathrm{grav},(2)}_{k,hh,2}w\right]_{\rho\sigma} \\
&\quad + \left[\Gamma^{\mathrm{grav},(2)}_{k,hh,3}w\right]_{\rho\sigma} + \left[\Gamma^{\mathrm{grav},(2)}_{k,hh,4}w\right]_{\rho\sigma}\Big)\,.
\end{aligned} \tag{A.40}$$

In the last line, we defined some new notation to calculate the four terms appearing separately. One finds

$$\left[\Gamma^{\mathrm{grav},(2)}_{k,hh,1}\right]_{\mu\nu}{}^{\rho\sigma} = \frac{1}{32\pi G_k}\left(-\frac{1}{2}g_{\mu\nu}g^{\rho\sigma}\big[1+\tilde{\varpi}(d-2)\big]R + \delta^\rho{}_\mu\delta^\sigma{}_\nu R\right)\,, \tag{A.41}$$

$$\left[\Gamma^{\mathrm{grav},(2)}_{k,hh,2}\right]_{\mu\nu}{}^{\rho\sigma} = \frac{1}{32\pi G_k}\left(-g_{\mu\nu}(1+d\tilde{\varpi})[-R^{\rho\sigma} + g^{\alpha\rho}g^{\beta\sigma}D_\alpha D_\beta + g^{\rho\sigma}\Delta]\right)\,, \tag{A.42}$$

$$\left[\Gamma^{\mathrm{grav},(2)}_{k,hh,3}\right]_{\mu\nu}{}^{\rho\sigma} = \frac{1}{32\pi G_k}\left(-g^{\rho\sigma}\big[-R_{\mu\nu} + D_\mu D_\nu - (\tilde{\varpi}(1-d)-1)g_{\mu\nu}\Delta - \tilde{\varpi}g_{\mu\nu}R\big]\right)\,, \tag{A.43}$$

$$\begin{aligned}
\left[\Gamma^{\mathrm{grav},(2)}_{k,hh,4}\right]_{\mu\nu}{}^{\rho\sigma} &= \frac{1}{32\pi G_k}\Big(\big(1+\tilde{\varpi}(d+1)\big)g_{\mu\nu}g^{\rho\sigma}\Delta - 2\delta^\rho{}_\mu R^\sigma{}_\nu + 2R^\rho{}_{\mu\nu}{}^\sigma + 2\delta^\sigma{}_\mu D_\nu D^\rho \\
&\quad + \delta^\rho{}_\mu\delta^\sigma{}_\nu\Delta - 4\tilde{\varpi}g_{\mu\nu}R^{\rho\sigma} + 2\tilde{\varpi}g_{\mu\nu}D^\sigma D^\rho\Big)\,.
\end{aligned} \tag{A.44}$$

The occurence of the factors of $\tilde{\varpi}$ is due to the introduction of the supermetric $\mathcal{G}$, which is achieved by inserting $\mathbb{1}^{\rho\sigma}{}_{\mu\nu} = \mathcal{G}^{\rho\sigma\alpha\beta}\tilde{\mathcal{G}}_{\alpha\beta\mu\nu}$. Using the form of the inverse supermetric (A.39) then allows us to find the expressions (A.41) - (A.44).

Gauge-fixing sector

Moreover, for the gauge-fixing action (3.6), one finds

$$\begin{aligned}\left[\Gamma^{\mathrm{gf},(2)}_{k,hh}\right]_{\mu\nu}{}^{\rho\sigma} &= -2\delta^{\rho}{}_{\mu}D_{\nu}D^{\sigma} + \big(1+\tilde{\varpi}(d-2)\big)g_{\mu\nu}D^{\sigma}D^{\rho} + g^{\rho\sigma}D_{\mu}D_{\nu} \\ &\quad + \frac{1}{2}g_{\mu\nu}g^{\rho\sigma}\big(1+\tilde{\varpi}(d-2)\big)\Delta\,. \end{aligned} \tag{A.45}$$

Matter sector

Finally, we require the contribution of the matter sector (3.4). Here, one obtains

$$\begin{aligned}\left[\Gamma^{\mathrm{matter},(2)}_{k,hh}\right]_{\mu\nu}{}^{\rho\sigma} &= -\frac{1}{2}\delta^{\rho}{}_{\mu}\delta^{\sigma}{}_{\nu}V_k(\phi) - \frac{1}{4}g^{\rho\sigma}(D_{\mu}\phi)(D_{\nu}\phi) + \frac{1}{2}\frac{1}{2-d}g_{\mu\nu}(D^{\rho}\phi)(D^{\sigma}\phi) \\ &\quad + \delta^{\sigma}{}_{\mu}(D^{\rho}\phi)(D_{\nu}\phi) - \frac{1}{4}\frac{1}{2-d}g_{\mu\nu}g^{\rho\sigma}(D^{\lambda}\phi)(D_{\lambda}\phi) \\ &\quad - \frac{1}{4}\delta^{\sigma}{}_{\mu}\delta^{\rho}{}_{\nu}(D^{\lambda}\phi)(D_{\lambda}\phi) \end{aligned} \tag{A.46}$$

where we have made the choice $\varpi = \frac{1}{2}$. Combining the previously obtained results, this choice allows us to write

$$\begin{aligned}\left[\Gamma^{(2)}_{k,hh}\right]_{\mu\nu}{}^{\rho\sigma} =& \frac{1}{32\pi G_k}\Big(\delta^{\rho}{}_{\mu}\delta^{\sigma}{}_{\nu}R + \frac{1}{2-d}g_{\mu\nu}g^{\rho\sigma}R - \frac{2}{2-d}g_{\mu\nu}R^{\rho\sigma} + g^{\rho\sigma}R_{\mu\nu} - 2\delta^{\rho}{}_{\mu}R^{\sigma}{}_{\nu} \\ &+ 2R^{\rho}{}_{\mu\nu}{}^{\sigma} + \delta^{\rho}{}_{\mu}\delta^{\sigma}{}_{\nu}\Delta\Big) - \frac{1}{2}\delta^{\rho}{}_{\mu}\delta^{\sigma}{}_{\nu}V_k(\phi) - \frac{1}{4}g^{\rho\sigma}(D_{\mu}\phi)(D_{\nu}\phi) \\ &+ \frac{1}{2}\frac{1}{2-d}g_{\mu\nu}(D^{\rho}\phi)(D^{\sigma}\phi) + \delta^{\sigma}{}_{\mu}(D^{\rho}\phi)(D_{\nu}\phi) - \frac{1}{4}\frac{1}{2-d}g_{\mu\nu}g^{\rho\sigma}(D^{\lambda}\phi)(D_{\lambda}\phi) \\ &- \frac{1}{4}\delta^{\sigma}{}_{\mu}\delta^{\rho}{}_{\nu}(D^{\lambda}\phi)(D_{\lambda}\phi)\,. \end{aligned} \tag{A.47}$$

for the entire tensor-tensor component of the Hessian.

A.2.2 Scalar-scalar component

The scalar-scalar component of the Hessian is found by taking the second variation of Γ_k w.r.t. scalar fluctuations χ and ξ. In particular, we have

$$\delta_{\chi}\delta_{\xi}\Gamma_k \equiv \langle \chi, \Gamma^{(2)}_{k,\phi\phi}\xi\rangle \equiv \int \mathrm{d}^d x\sqrt{g}\chi\Gamma^{(2)}_{k,\phi\phi}\xi\,. \tag{A.48}$$

Due to the lack of tensor structure, the calculation of this component is much less involved than the tensor-tensor component. Since only the matter sector contains scalar field contributions, the variations of the other sectors vanish. Hence, we have

$$\begin{aligned}\delta_{\chi}\delta_{\xi}\Gamma_k^{\mathrm{matter}} &= \delta_{\chi}\delta_{\xi}\int \mathrm{d}^d x\sqrt{g}\left(\frac{1}{2}\phi\Delta\phi + V_k(\phi)\right) \\ &= \int \mathrm{d}^d x\sqrt{g}\chi\left(\Delta + V_k''(\phi)\right)\xi\,, \end{aligned} \tag{A.49}$$

from which we read off

$$\Gamma^{(2)}_{k,\phi\phi} = \Delta + V_k''(\phi)\,. \tag{A.50}$$

A.2.3 Tensor-scalar component

To obtain the tensor-scalar off-diagonal component, we calculate the variation w.r.t. a tensor fluctuation v and a scalar fluctuation ξ. Specifically, we have

$$\delta_v\delta_\xi\Gamma_k \equiv \langle v, \Gamma^{(2)}_{k,h\phi}\xi\rangle \equiv \int \mathrm{d}^d x\sqrt{g} v_{\mu\nu}\mathcal{G}^{\mu\nu\rho\sigma}\left[\Gamma^{(2)}_{k,h\phi}\right]_{\rho\sigma}\xi\,. \tag{A.51}$$

Since the first variation is w.r.t. ξ, we again only need to consider $\Gamma_k^{\mathrm{matter}}$. One finds

$$\begin{aligned}
\delta_v\delta_\xi\Gamma_k &= \delta_v\left[\int \mathrm{d}^d x\sqrt{g}\left(\phi\Delta\xi + \xi V_k'(\phi)\right)\right] \\
&= \int \mathrm{d}^d x\sqrt{g}\left[\frac{1}{2}v_{\mu\nu}g^{\mu\nu}\left(\phi\Delta\xi + V_k'(\phi)\xi\right) + \phi\delta_v(\Delta\xi)\right] \\
&= \int \mathrm{d}^d x\sqrt{g} v_{\mu\nu}\left[\frac{1}{2}g^{\mu\nu}\left(\phi\Delta + V_k'(\phi)\right) - (D^\mu\phi)D^\nu + \frac{1}{2}g^{\mu\nu}(D^\lambda\phi)D_\lambda - \frac{1}{2}g^{\mu\nu}\phi\Delta\right]\xi\,.
\end{aligned} \tag{A.52}$$

Inserting the unit operator in the form of $\mathbb{1} = \mathcal{G}\tilde{\mathcal{G}}$ and setting $\varpi = \frac{1}{2}$, one is able to read off the tensor-scalar component of the Hessian,

$$\left[\Gamma^{(2)}_{k,h\phi}\right]_{\rho\sigma} = \frac{1}{2-d}g_{\rho\sigma}V_k'(\phi) - (D_\rho\phi)D_\sigma\,. \tag{A.53}$$

A.2.4 Scalar-tensor component

To calculate the scalar-tensor component we perform the variations w.r.t. a tensor fluctuation v and a scalar ξ and calculate this component of the Hessian as

$$\delta_\xi\delta_v\Gamma_k = \langle\xi, \Gamma^{(2)}_{k,\phi h}v\rangle = \int \mathrm{d}^d x\sqrt{g}\xi\left[\Gamma^{(2)}_{k,\phi h}\right]^{\mu\nu} v_{\mu\nu}\,. \tag{A.54}$$

Again, we only need the matter sector of Γ_k. One obtains

$$\begin{aligned}
\delta_\xi\delta_v\Gamma_k^{\text{matter}} &= \delta_\xi\delta_v \int \mathrm{d}^d x\sqrt{g}\left(\frac{1}{2}\phi\Delta\phi + V_k(\phi)\right)\\
&= \delta_\xi \int \mathrm{d}^d x\sqrt{g}\Big[\frac{1}{2}g^{\mu\nu}v_{\mu\nu}\left(\frac{1}{2}\phi\Delta\phi + V_k(\phi)\right) + \frac{1}{2}\phi v_{\mu\nu}(D^\mu D^\nu\phi)\\
&\quad + \frac{1}{2}\phi(D^\nu\phi)(D^\mu v_{\mu\nu}) - \frac{1}{4}\phi g^{\mu\nu}(D^\lambda\phi)(D_\lambda v_{\mu\nu})\Big]\\
&= \int \mathrm{d}^d x\sqrt{g}\Big(\frac{1}{2}g^{\mu\nu}\left(\frac{1}{2}\phi\Delta\xi + \frac{1}{2}\xi\Delta\phi + V_k'(\phi)\xi\right)v_{\mu\nu} + \frac{1}{2}(D^\mu D^\nu\phi)\xi v_{\mu\nu}\\
&\quad + \frac{1}{2}\phi(D^\mu D^\nu\xi)v_{\mu\nu} + \frac{1}{2}\phi(D^\nu\xi)(D^\mu v_{\mu\nu}) + \frac{1}{2}\xi(D^\nu\phi)(D^\mu v_{\mu\nu})\\
&\quad - \frac{1}{4}\phi g^{\mu\nu}(D^\lambda\xi)(D_\lambda v_{\mu\nu}) - \frac{1}{4}\xi g^{\mu\nu}(D^\lambda\phi)(D_\lambda v_{\mu\nu})\Big)\\
&= \int \mathrm{d}^d x\sqrt{g}\xi\Big(\frac{1}{2}g^{\mu\nu}(\Delta\phi) + \frac{1}{2}g^{\mu\nu}V_k'(\phi) + (D^\mu D^\nu\phi) + (D^\mu\phi)D^\nu\\
&\quad - \frac{1}{2}g^{\mu\nu}(D^\lambda\phi)D_\lambda\Big)v_{\mu\nu}
\end{aligned} \tag{A.55}$$

from which we read off

$$\left[\Gamma_{k,\phi h}^{(2)}\right]^{\mu\nu} = \frac{1}{2}g^{\mu\nu}(\Delta\phi) + \frac{1}{2}g^{\mu\nu}V_k'(\phi) - \frac{1}{2}g^{\mu\nu}(D^\lambda\phi)D_\lambda + (D^\mu D^\nu\phi) + (D^\mu\phi)D^\nu\,, \tag{A.56}$$

concluding the calculation of the Hessian.

A.3 Trace evaluation

In order to evaluate the traces that occur on the right-hand-side of the FRGE we employ heat kernel techniques. For a detailed exposition, see [95] and references therein. Here, we follow the exposition of [96] which focuses on the details important to us. The heat kernel expansion is given by

$$\mathrm{Tr}\left[\exp\left(is\Delta\right)\right] = \left(\frac{i}{4\pi s}\right)^{\frac{d}{2}}\mathrm{tr}(\mathbb{1})\int \mathrm{d}^d x\sqrt{g}\Big(1 - \frac{1}{6}isR + \mathcal{O}(R^2)\Big)\,. \tag{A.57}$$

Here $\mathbb{1}$ represents the unit operator of the space on which Δ acts. For example, for scalars, $\mathrm{tr}_S(\mathbb{1}) = 1$ and for vectors $\mathrm{tr}_V(\mathbb{1}) = d$.

The traces in the FRGE are of the generic form $\mathrm{Tr}[W(\Delta)]$. This is related to the expansion (A.57) by a Fourier transform,

$$\mathrm{Tr}[W(\Delta)] = \int_{-\infty}^{\infty} ds\tilde{W}(s)\mathrm{Tr}[\exp(is\Delta)]\,. \tag{A.58}$$

Combining equations (A.57) and (A.58), one finds

$$\mathrm{Tr}[W(\Delta)] = (4\pi)^{-\frac{d}{2}}\mathrm{tr}(\mathbb{1})\Big(Q_{\frac{d}{2}}[W]\int \mathrm{d}^d x\sqrt{g} + \frac{1}{6}Q_{\frac{d}{2}-1}[W]\int \mathrm{d}^d x\sqrt{g}R + \mathcal{O}(R^2)\Big) \tag{A.59}$$

where one introduces the *Q-functionals*

$$Q_n[W] = \int_{-\infty}^{\infty} ds(-is)\tilde{W}(s)\,. \tag{A.60}$$

Expressing these in terms of the function $W(z)$ one obtains

$$Q_o[W] = W(0)\,, \tag{A.61a}$$

$$Q_n[W] = \frac{1}{\Gamma(n)}\int_n^{\infty} dz z^{n-1}W(z) \qquad \text{for } n>0\,, \tag{A.61b}$$

$$Q_n[W] = \left(-\frac{d}{dz}\right)^{|n|} W(z)\Big|_{z=0} \qquad \text{for } n<0\,. \tag{A.61c}$$

We are now in position to combine equations (A.59) and (A.61) to evaluate the traces.

A.3.1 Gravitational sector

The equation of interest is (3.36), which we repeat here for convenience:

$$\begin{aligned}\mathcal{S}_k(R) = {}& \mathrm{Tr}_T[\mathcal{N}\mathcal{A}^{-1}] + \mathrm{Tr}_S[\mathcal{N}\mathcal{A}^{-1}] + \mathrm{Tr}_S[\mathcal{N}_0\,(\mathcal{A}_0+2u_{k,2})^{-1}] - 2\mathrm{Tr}_V[\mathcal{N}_0\mathcal{A}_0^{-1}] \\ & - R\big(C_T\mathrm{Tr}_T[\mathcal{N}\mathcal{A}^{-2}] + C_S\mathrm{Tr}_S[\mathcal{N}\mathcal{A}^{-2}] - 2C_V\mathrm{Tr}_V[\mathcal{N}_0\mathcal{A}_0^{-2}]\big) + \mathcal{O}(R^2)\,.\end{aligned} \tag{A.62}$$

Hence, the first trace to be evaluated is

$$\begin{aligned}\mathrm{Tr}_T[\mathcal{N}\mathcal{A}^{-1}] = (4\pi)^{-\frac{d}{2}}\frac{1}{2}(d-1)(d+2)\Big(& Q_{\frac{d}{2}}[\mathcal{N}\mathcal{A}^{-1}]\int \mathrm{d}^d x\sqrt{g} \\ & + \frac{1}{6}Q_{\frac{d}{2}-1}[\mathcal{N}\mathcal{A}^{-1}]\int \mathrm{d}^d x\sqrt{g}R\Big)\,.\end{aligned} \tag{A.63}$$

Here, we used that $\mathrm{tr}_T(\mathbb{1}) = \frac{1}{2}(d-1)(d+2)$ for symmetric, traceless $(0,2)$-tensors.

We start with

$$\begin{aligned}Q_{\frac{d}{2}}[\mathcal{N}\mathcal{A}^{-1}] &= \frac{1}{\Gamma(\frac{d}{2})}\int_0^{\infty} dz z^{\frac{d}{2}-1}\frac{R^{(0)}(z/k^2) - \frac{z}{k^2}R^{(0)\prime}(z/k^2)}{\frac{z}{k^2}+R^{(0)}(z/k^2) - 2\frac{\Lambda_k}{k^2}} \\ &\quad - \frac{1}{2}\eta_N(k)\frac{1}{\Gamma(\frac{d}{2})}\int_0^{\infty} dz z^{\frac{d}{2}-1}\frac{R^{(0)}(z/k^2)}{\frac{z}{k^2}+R^{(0)}(z/k^2) - 2\frac{\Lambda_k}{k^2}} \\ &= k^d\frac{1}{\Gamma(\frac{d}{2})}\int_0^{\infty} dz z^{\frac{d}{2}-1}\frac{R^{(0)}(z) - zR^{(0)\prime}(z)}{z+R^{(0)}(z) - 2\frac{\Lambda_k}{k^2}} \\ &\quad - k^d\frac{1}{2}\eta_N(k)\frac{1}{\Gamma(\frac{d}{2})}\int_0^{\infty} dz z^{\frac{d}{2}-1}\frac{R^{(0)}(z)}{z+R^{(0)}(z) - 2\frac{\Lambda_k}{k^2}} \\ &= k^d\Phi^1_{\frac{d}{2}}\left(-2\frac{\Lambda_k}{k^2}\right) - \frac{1}{2}k^d\eta_N(k)\tilde{\Phi}^1_{\frac{d}{2}}\left(-2\frac{\Lambda_k}{k^2}\right)\,,\end{aligned} \tag{A.64}$$

where in the final step we used the definition of the threshold functions, (3.37).

Similarly, one finds

$$Q_{\frac{d}{2}-1}[\mathcal{N}\mathcal{A}^{-1}] = k^{d-2}\Phi^1_{\frac{d}{2}-1}\left(-2\frac{\Lambda_k}{k^2}\right) - \frac{1}{2}k^{d-2}\eta_N(k)\tilde{\Phi}^1_{\frac{d}{2}-1}\left(-2\frac{\Lambda_k}{k^2}\right)\,. \tag{A.65}$$

This completes the calculation of the first term in (A.62). The second term in (A.62) is almost the same, except for the different prefactor from $\mathrm{tr}_S(\mathbb{1}) = 1$.

For the next term, we calculate

$$Q_{\frac{d}{2}}[\mathcal{N}_0 (\mathcal{A}_0 + 2u_{k,2})^{-1}] = k^d \Phi^1_{\frac{d}{2}}\left(2\frac{u_{k,2}}{k^2}\right), \tag{A.66}$$

$$Q_{\frac{d}{2}-1}[\mathcal{N}_0 (\mathcal{A}_0 + 2u_{k,2})^{-1}] = k^{d-2} \Phi^1_{\frac{d}{2}-1}\left(2\frac{u_{k,2}}{k^2}\right). \tag{A.67}$$

For the final trace at $\mathcal{O}(1)$ we have

$$Q_{\frac{d}{2}}[\mathcal{N}_0 \mathcal{A}_0^{-1}] = k^d \Phi^1_{\frac{d}{2}}(0), \tag{A.68}$$

$$Q_{\frac{d}{2}-1}[\mathcal{N}_0 \mathcal{A}_0^{-1}] = k^{d-2} \Phi^1_{\frac{d}{2}-1}(0). \tag{A.69}$$

Next, at $\mathcal{O}(R)$, we find

$$Q_{\frac{d}{2}}[\mathcal{N}\mathcal{A}^{-2}] = k^{d-2}\Phi^2_{\frac{d}{2}}\left(-2\frac{\Lambda_k}{k^2}\right) - \frac{1}{2}\eta_N(k) k^{d-2}\tilde{\Phi}^2_{\frac{d}{2}}\left(-2\frac{\Lambda_k}{k^2}\right), \tag{A.70}$$

$$Q_{\frac{d}{2}}[\mathcal{N}_0\mathcal{A}_0^{-2}] = k^{d-2}\Phi^2_{\frac{d}{2}}(0). \tag{A.71}$$

Note that we do not need $Q_{\frac{d}{2}-1}[\mathcal{N}\mathcal{A}^{-2}]$ and $Q_{\frac{d}{2}-1}[\mathcal{N}_0\mathcal{A}_0^{-2}]$ as these only play a role at $\mathcal{O}(R^2)$.

Combining these results, one obtains the flow equations (3.38) and (3.39).

A.3.2 Matter sector

In this section, we evaluate the traces appearing in the calculations of the flow equations of the matter sector. The expressions under investigation are given by (3.51). To evaluate these, we again employ the heat kernel expansion. As we are dealing with flat space, this now reduces to

$$\mathrm{Tr}[W(\Delta)] = (4\pi)^{-\frac{d}{2}}\mathrm{tr}(\mathbb{1}) Q_{\frac{d}{2}}[W] \int \mathrm{d}^d x\,. \tag{A.72}$$

Hence, S_1 contains $Q_{\frac{d}{2}}[\mathcal{N}\mathcal{B}^{-1}]$ which is calculated to be

$$Q_{\frac{d}{2}}[\mathcal{N}\mathcal{B}^{-1}] = k^d \Phi^1_{\frac{d}{2}}\left(-16\pi k^{-2} G_k V_k(\bar{\phi})\right) - \frac{1}{2}\eta_N k^d \tilde{\Phi}^1_{\frac{d}{2}}\left(-16\pi k^{-2} G_k V_k(\bar{\phi})\right). \tag{A.73}$$

However, the traces S_2 and S_3 cannot be expressed in terms of these threshold functions. To this end, we use the definition of the *generalized threshold functionals* (3.52). In terms of these, one finds

$$\begin{aligned} &Q_{\frac{d}{2}}\left[\mathcal{B}^{-1}\left(\mathcal{E} - \frac{1}{2}\frac{1}{2-d}\mathcal{B}^{-1}\right)^{-1}\mathcal{B}^{-1}\mathcal{N}\right] = \\ &32\pi k^{d-4} G_k V_k'(\bar{\phi})^2 \left[\Phi^{(2,1)}_{\frac{d}{2}}\left[-16\pi k^{-2} G_k V_k(\bar{\phi}), \rho\right] - \frac{1}{2}\eta_N \tilde{\Phi}^{(2,1)}_{\frac{d}{2}}\left[-16\pi k^{-2} G_k V_k(\bar{\phi}), \rho\right]\right] \end{aligned} \tag{A.74}$$

with the function ρ defined in eq. (3.54). Furthermore, one calculates

$$Q_{\frac{d}{2}}\left[\left(\mathcal{D}-16\pi G_k\frac{d}{2-d}V_k'(\bar{\phi})^2\mathcal{B}^{-1}\right)^{-1}2\mathcal{N}_0\right]=2k^d\Phi^{(0,1)}_{\frac{d}{2}}[0,\rho]\,. \tag{A.75}$$

Combining these results, one finds the expressions for the traces S_1, S_2 and S_3 as given in (3.53).

Appendix B

$f(R)$-gravity in the Jordan and Einstein frame

When analyzing the dynamical consequences of an $f(R)$-type gravity model, it is convenient to recast the theory into the Einstein frame. The resulting action then consists of an Einstein-Hilbert term supplemented by an additional scalar degree of freedom.[1] In this appendix we demonstrate the relation between these two formulations, following [98].

We start from a generic (Lorentzian) $f(R)$-theory supplemented by a generic action for matter fields $S_m[g_{\mu\nu}]$

$$S = \frac{M_P^2}{2}\int d^4x\sqrt{-g}f(R) + S_m[g_{\mu\nu}]\,. \tag{B.1}$$

We keep track of the matter action, even though this part does not influence the dynamics during inflation and becomes relevant at later stages of the cosmological evolution. Subsequently, we introduce an auxiliary field ϕ and rewrite the action (B.1) according to

$$S = \frac{M_P^2}{2}\int d^4x\sqrt{-g}\,\left[f(\phi) + f'(\phi)(R-\phi)\right] + S_m[g_{\mu\nu}]\,, \tag{B.2}$$

where the prime denotes a derivative with respect to the argument. Presupposing that $f''(\phi) \neq 0$, the field equations derived from (B.2) include $\phi = R$, entailing that eqs. (B.1) and (B.2) are dynamically equivalent on-shell. If $f'(\phi) > 0$, the conformal transformation $f'(\phi)g_{\mu\nu} \equiv \tilde{g}_{\mu\nu}$ brings the gravitational part of the action into Einstein-Hilbert form

$$\begin{aligned} S \;=\; & \tfrac{M_P^2}{2}\int d^4x\sqrt{-\tilde{g}}\left[\tilde{R} - \frac{3}{2f'(\phi)^2}\tilde{g}^{\mu\nu}\tilde{D}_\mu f'(\phi)\tilde{D}_\nu f'(\phi) - \frac{1}{f'(\phi)^2}\left(\phi f'(\phi) - f(\phi)\right)\right] \\ & + S_m[\tilde{g}_{\mu\nu}/f'(\phi)]\,. \end{aligned} \tag{B.3}$$

The kinetic term for the scalar field ϕ can be brought into canonical form by introducing the new field φ according to

$$f'(\phi) \equiv \mathrm{e}^{\sqrt{2/3}\varphi/M_P}\,. \tag{B.4}$$

If $f'(\phi)$ is monotonic, this relation implicitly defines a map $\phi(\varphi)$. Substituting this map into

[1] At the one-loop level the on-shell equivalence of the two formulations has recently been demonstrated in [97].

the action (B.3) yields

$$S = \int d^4x\sqrt{-\tilde{g}}\left[\frac{M_P^2}{2}\tilde{R} - \frac{1}{2}(\tilde{D}\varphi)^2 - V(\varphi)\right] + S_m[\tilde{g}_{\mu\nu}/F'], \tag{B.5}$$

with the scalar potential given by

$$V(\varphi) = \frac{M_P^2}{2f'(\phi(\varphi))^2}\Big(\phi(\varphi)f'(\phi(\varphi)) - f(\phi(\varphi))\Big). \tag{B.6}$$

For the $f(R)$-type action (4.55), the transformation from Jordan to Einstein frame can be carried out explicitly. For this specific case,[2]

$$f(R) = -2\Lambda + R - BR^2. \tag{B.7}$$

For $B = 0$ the theory already is in the Einstein frame, so we assume that $B \neq 0$. Evaluating (B.4) for $f(\phi)$ which is quadratic in ϕ leads to the following relation between the scalar fields:

$$1 - 2B\phi = e^{\sqrt{2/3}\varphi/M_p} \quad \Rightarrow \quad \phi = \frac{1 - e^{\sqrt{2/3}\varphi/M_p}}{2B}. \tag{B.8}$$

Finally, the scalar potential resulting from (B.7) is

$$V(\varphi) \;=\; \frac{M_P^2}{2}\left[-\frac{1}{4B} + \frac{1}{2B}e^{-\sqrt{2/3}\varphi/M_P} + \left(-\frac{1}{4B} + 2\Lambda\right)e^{-2\sqrt{2/3}\varphi/M_P}\right]. \tag{B.9}$$

This potential provides the starting point for analyzing the cosmological dynamics in section 4.3.

[2]Note that we are working with an action that differs from (4.55) by an overall minus sign. To make up for this, in the main text in (4.59) we write the potential $V(\varphi)$ with opposite sign with respect to the one we get here.

Appendix C

RG machinery of $f(R)$-gravity

The investigation of chapter 4 builds on the flow equation derived in [81]. The main features and results of this construction are reviewed in this appendix.

The full ansatz of the EAA is taken to be

$$\Gamma_k[g;\bar{g}] = \bar{\Gamma}_k[g] + S_{\rm gf}[g-\bar{g};\bar{g}] + S_{\rm gh} + S_{\rm aux}\,, \tag{C.1}$$

with

$$\bar{\Gamma}_k[g] = \frac{1}{16\pi G_k}\int \mathrm{d}^4x\sqrt{g}f_k(R)\,. \tag{C.2}$$

This term is supplemented by a scale-independent gauge-fixing term implementing geometrical gauge in the Landau limit. The anstaz for Γ_k is then completed by the corresponding ghost action and auxiliary fields exponentiating Jacobians arising from field redefinitions. Details on these terms can be found in the original article [81].

Substituting the ansatz (C.1) into the FRGE and projecting on functions of the scalar curvature yields a partial differential equation governing the scale-dependence of $f_k(R)$. This equation is most conveniently written in terms of the dimensionless quantities

$$r \coloneqq k^{-2}R \quad \text{and} \quad \mathcal{F}_k(r) \coloneqq \frac{1}{16\pi G_k}k^{-4}f_k(rk^2)\,. \tag{C.3}$$

The partial differential equation satisfied by $\mathcal{F}_k$ then reads

$$384\pi^2\left(\partial_t\mathcal{F}_k + 4\mathcal{F}_k - 2r\mathcal{F}_k'\right) = \sum_{i=1}^{6} c_i \tag{C.4}$$

with the c_i given by

$$c_1 = \left[5r^2\theta\left(1-\tfrac{r}{3}\right) - (12+4r-\tfrac{61}{90})r^2\right]\left[1-\tfrac{r}{3}\right]^{-1}, \tag{C.5}$$

$$c_2 = 10r^2\theta\left(1-\tfrac{r}{3}\right), \tag{C.6}$$

$$c_3 = \left[10r^2\theta\left(1-\tfrac{r}{4}\right) - r^2\theta\left(1+\tfrac{r}{4}\right) - (36+6r-\tfrac{67}{60}r^2)\right]\left[1-\tfrac{r}{4}\right]^{-1}, \tag{C.7}$$

$$c_4 = \left[\eta_f\left(10-5r-\tfrac{271}{36}r^2+\tfrac{7249}{4536}r^3\right) + (60-20r-\tfrac{271}{18}r^2)\right]\left[1+\tfrac{\mathcal{F}_k}{\mathcal{F}_k'}-\tfrac{r}{3}\right]^{-1}, \tag{C.8}$$

$$\begin{aligned} c_5 = {} & \tfrac{5r^2}{2}\Big[\eta_f\left(\left(1+\tfrac{r}{3}\right)\theta\left(1+\tfrac{r}{3}\right) + \left(2+\tfrac{r}{3}\right)\theta\left(1+\tfrac{r}{6}\right)\right) + 2\theta\left(1+\tfrac{r}{3}\right) + 4\theta\left(1+\tfrac{r}{6}\right)\Big]\times \\ & \times\left[1+\tfrac{\mathcal{F}_k}{\mathcal{F}_k'}-\tfrac{r}{3}\right]^{-1}, \end{aligned} \tag{C.9}$$

$$\begin{aligned} c_6 = {} & \Big[\mathcal{F}_k'\,\eta_f\,\left(6+3r+\tfrac{29}{60}r^2+\tfrac{37}{1512}r^3\right) + \left(\partial_t\mathcal{F}_k''-2r\mathcal{F}_k'''\right)\left(27-\tfrac{91}{20}r^2-\tfrac{29}{30}r^3-\tfrac{181}{3360}r^4\right) \\ & + \mathcal{F}_k''\left(216-\tfrac{91}{5}r^2-\tfrac{29}{15}r^3\right) + \mathcal{F}_k'\left(36+12r+\tfrac{29}{30}r^2\right)\Big]\times \\ & \times\left[2\mathcal{F}_k + 3\mathcal{F}_k'\left(1-\tfrac{2}{3}r\right) + 9\mathcal{F}_k''\left(1-\tfrac{r}{3}\right)^2\right]^{-1}. \end{aligned} \tag{C.10}$$

Here, a prime denotes a derivative w.r.t. the dimensionless curvature r and η_f is the anomalous dimension of $f_k'(r)$,

$$\eta_f = \frac{1}{\mathcal{F}_k'}(\partial_t\mathcal{F}_k' + 2\mathcal{F}_k' - 2r\mathcal{F}_k''). \tag{C.11}$$

Using the dimensionless variables introduced in eq. (4.69), the dimensionless function $\mathcal{F}_k(r)$ corresponding to the action (4.56) is

$$\mathcal{F}_k(r) = \frac{1}{16\pi g_k}(2\lambda_k - r + b_k r^2). \tag{C.12}$$

Substituting this expression into (C.4) and subsequently expanding the result in a power series around $r=0$ allows for the β-functions for the couplings λ_k, g_k and b_k to be read off from the three lowest order terms in this expansion. Concretely,

$$\partial_t g_k = \beta_g(g,\lambda,b), \qquad \partial_t\lambda_k = \beta_\lambda(g,\lambda,b), \qquad \partial_t b_k = \beta_b(g,\lambda,b), \tag{C.13}$$

where the β_i are obtained as the solution of the following linear system of equations

$$\begin{aligned} & -\frac{6\left(9g_k\beta_b - 9b_k\beta_g + 72b_kg_k + \beta_g - 8g_k\right)}{g_k(18b_k+4\lambda_k-3)} \\ & \qquad + \frac{48\left(-\pi\lambda_k\beta_g + \pi g_k\beta_\lambda + 4\pi g_k\lambda_k\right)}{g_k^2} - \frac{80-\frac{10\beta_g}{g_k}}{1-2\lambda_k} + 48 = 0\,, \end{aligned} \tag{C.14a}$$

$$
\begin{aligned}
&- \frac{-20\beta_b + 40b_k + \frac{5\beta_g}{g_k} - 30}{1-2\lambda_k} - \frac{3\left(4g_k\beta_b - 4b_k\beta_g + 24b_k g_k + \beta_g - 6g_k\right)}{g_k(18b_k + 4\lambda_k - 3)} \\
&\quad - \frac{36b_k\left(9g_k\beta_b - 9b_k\beta_g + 72b_k g_k + \beta_g - 8g_k\right)}{g_k(18b_k + 4\lambda_k - 3)^2} - \frac{2(6b_k\lambda_k - 1)\left(80 - \frac{10\beta_g}{g_k}\right)}{3(2\lambda_k - 1)^2} \\
&\quad - \frac{24\pi\left(2g_k - \beta_g\right)}{g_k^2} + 23 = 0 \ , \qquad \text{(C.14b)}
\end{aligned}
$$

$$
\begin{aligned}
&- \frac{216b_k^2\left(9g_k\beta_b - 9b_k\beta_g + 72b_k g_k + \beta_g - 8g_k\right)}{g_k(18b_k + 4\lambda_k - 3)^3} \\
&\quad - \frac{18b_k\left(4g_k\beta_b - 4b_k\beta_g + 24b_k g_k + \beta_g - 6g_k\right)}{g_k(18b_k + 4\lambda_k - 3)^2} \\
&\quad - \frac{2(6b_k\lambda_k - 1)\left(-20\beta_b + 40b_k + \frac{5\beta_g}{g_k} - 30\right)}{3(2\lambda_k - 1)^2} \\
&\quad - \frac{-186g_k\beta_b + 186b_k\beta_g - 744b_k g_k + 29\beta_g - 116g_k}{60g_k(18b_k + 4\lambda_k - 3)} \\
&\quad - \frac{-40b_k\beta_b + 10\beta_b + 80b_k^2 - 20b_k + \frac{271\beta_g}{36g_k} - \frac{271}{9}}{1-2\lambda_k} + \frac{24\pi\left(g_k\beta_b - b_k\beta_g\right)}{g_k^2} \\
&\quad - \frac{\left(-72b_k^2\lambda_k + 30b_k\lambda_k + 9b_k - 4\right)\left(80 - \frac{10\beta_g}{g_k}\right)}{9(2\lambda_k - 1)^3} + \frac{15\left(4g_k - \beta_g\right)}{2g_k(2\lambda_k - 1)} - \frac{872}{45} = 0 \ , \qquad \text{(C.14c)}
\end{aligned}
$$

The β-functions (C.14) are the main result of this appendix and underlie the analysis of the gravitational RG flow performed in section 4.4.

Bibliography

[1] R. Oerter. *The Theory of Almost Everything: The Standard Model, the Unsung Triumph of Modern Physics*. Plume, 2006.

[2] M. H. Goroff and A. Sagnotti. Quantum gravity at two loops. *Physics Letters B*, 160:81, 1985.

[3] G. 't Hooft and M. J. G. Veltman. One loop divergencies in the theory of gravitation. *Ann. Inst. H. Poincare Phys. Theor.*, A20:69–94, 1974.

[4] J. Ambjorn, A. Görlich, J. Jurkiewicz, and R. Loll. Causal dynamical triangulations and the search for a theory of quantum gravity. *International Journal of Modern Physics D*, 22(09):1330019, 2013.

[5] S. Weinberg. Ultraviolet divergences in quantum theories of gravitation. In S. W. Hawking and W. Israel, editors, *General Relativity: An Einstein centenary survey*, pages 790–831, 1979.

[6] L. P. Kadanoff. *Statistical Physics: Statics, Dynamics and Renormalization*. World Scientific, 2000.

[7] K. G. Wilson and J. Kogut. The renormalization group and the ϵ expansion. *Physics Reports*, 12(2):75 – 199, 1974.

[8] K. G. Wilson. The Renormalization Group: Critical Phenomena and the Kondo Problem. *Rev. Mod. Phys.*, 47:773, 1975.

[9] A. H. Guth. Inflationary universe: A possible solution to the horizon and flatness problems. *Phys. Rev. D*, 23:347–356, Jan 1981.

[10] A. D. Linde. A new inflationary universe scenario: A possible solution of the horizon, flatness, homogeneity, isotropy and primordial monopole problems. *Physics Letters B*, 108(6):389 – 393, 1982.

[11] A. Albrecht and P. J. Steinhardt. Cosmology for grand unified theories with radiatively induced symmetry breaking. *Phys. Rev. Lett.*, 48:1220–1223, Apr 1982.

[12] D. Baumann. Inflation. In *Physics of the large and the small, TASI 09, proceedings of the Theoretical Advanced Study Institute in Elementary Particle Physics, Boulder, Colorado, USA, 1-26 June 2009*, pages 523–686, 2011.

[13] M. Reuter and F. Saueressig. *Quantum Gravity and the Functional Renormalization Group: The Road towards Asymptotic Safety.* Cambridge University Press, to be published in October 2018.

[14] A. Nink, M. Reuter, and F. Saueressig. Asymptotic Safety in quantum gravity. *Scholarpedia*, 8(7):31015, 2013. revision #135541.

[15] C. Wetterich. Exact evolution equation for the effective potential. *Phys. Lett.*, B301:90–94, 1993.

[16] A. Wipf. *Statistical Approach to Quantum Field Theory.* Springer, 2013.

[17] M. Reuter and C. Wetterich. Quantum Liouville field theory as solution of a flow equation. *Nucl. Phys.*, B506:483–520, 1997.

[18] F. J. Wegner. Some invariance properties of the renormalization group. *Journal of Physics C: Solid State Physics*, 7(12):2098, 1974.

[19] C. Rovelli. *Quantum Gravity.* Cambridge University Press, 2004.

[20] L.D. Faddeev and V.N. Popov. Feynman diagrams for the yang-mills field. *Physics Letters B*, 25(1):29 – 30, 1967.

[21] B. S. DeWit. *Dynamical Theory of Groups and Fields.* Gordon and Breach, 1965.

[22] B. S. DeWitt. *The Global Approach to Quantum Field Theory.* Clarendon Press, 2003.

[23] M. Reuter and F. Saueressig. Renormalization group flow of quantum gravity in the Einstein-Hilbert truncation. *Phys. Rev.*, D65:065016, 2002.

[24] O. Lauscher and M. Reuter. Flow equation of quantum Einstein gravity in a higher derivative truncation. *Phys. Rev.*, D66:025026, 2002.

[25] A. Codello, R. Percacci, and C. Rahmede. Investigating the Ultraviolet Properties of Gravity with a Wilsonian Renormalization Group Equation. *Annals Phys.*, 324:414–469, 2009.

[26] M. Niedermaier and M. Reuter. The asymptotic safety scenario in quantum gravity. *Living Reviews in Relativity*, 9(1):5, Dec 2006.

[27] D. F. Litim. Renormalisation group and the Planck scale. *Phil. Trans. Roy. Soc. Lond.*, A369:2759–2778, 2011.

[28] M. Reuter and F. Saueressig. Quantum Einstein Gravity. *New J. Phys.*, 14:055022, 2012.

[29] S. Nagy. Lectures on renormalization and asymptotic safety. *Annals Phys.*, 350:310–346, 2014.

[30] A. Eichhorn. Status of the asymptotic safety paradigm for quantum gravity and matter. In *Black Holes, Gravitational Waves and Spacetime Singularities Rome, Italy, May 9-12, 2017*, 2017.

[31] R. Percacci. *An Introduction to Covariant Quantum Gravity and Asymptotic Safety.* World Scientific, 2017.

[32] H. Gies, B. Knorr, S. Lippoldt, and F. Saueressig. Gravitational Two-Loop Counterterm Is Asymptotically Safe. *Phys. Rev. Lett.*, 116(21):211302, 2016.

[33] D. Becker and M. Reuter. En route to Background Independence: Broken split-symmetry, and how to restore it with bi-metric average actions. *Annals Phys.*, 350:225–301, 2014.

[34] D. Becker and M. Reuter. Propagating gravitons vs. 'dark matter' in asymptotically safe quantum gravity. *JHEP*, 12:025, 2014.

[35] D. Becker and M. Reuter. Towards a C-function in 4D quantum gravity. *JHEP*, 03:065, 2015.

[36] A. Codello, G. D'Odorico, and C. Pagani. Consistent closure of renormalization group flow equations in quantum gravity. *Phys. Rev.*, D89(8):081701, 2014.

[37] E. Manrique, M. Reuter, and F. Saueressig. Bimetric Renormalization Group Flows in Quantum Einstein Gravity. *Annals Phys.*, 326:463–485, 2011.

[38] K. G. Wilson and M. E. Fisher. Critical exponents in 3.99 dimensions. *Phys. Rev. Lett.*, 28:240–243, Jan 1972.

[39] G. Narain and R. Percacci. Renormalization Group Flow in Scalar-Tensor Theories. I. *Class. Quant. Grav.*, 27:075001, 2010.

[40] A. Eichhorn and H. Gies. Ghost anomalous dimension in asymptotically safe quantum gravity. *Phys. Rev.*, D81:104010, 2010.

[41] K. Groh and F. Saueressig. Ghost wave-function renormalization in Asymptotically Safe Quantum Gravity. *J. Phys.*, A43:365403, 2010.

[42] S. Weinberg. *Gravitation and Cosmology: Principles and Applications of the General Theory of Relativity.* John Wiley and Sons, 1972.

[43] D. F. Litim. Optimization of the exact renormalization group. *Phys. Lett.*, B486:92–99, 2000.

[44] A. Vereijken. Functional renormalization group for scalar field theories. Bachelor's thesis, Radboud University Nijmegen, 2017.

[45] J. Berges, N. Tetradis, and C. Wetterich. Nonperturbative renormalization flow in quantum field theory and statistical physics. *Phys. Rept.*, 363:223–386, 2002.

[46] J. Martin, C. Ringeval, and V. Vennin. Encyclopædia Inflationaris. *Phys. Dark Univ.*, 5-6:75–235, 2014.

[47] G. Gubitosi, R. Ooijer, C. Ripken, and F. Saueressig. Consistent early and late time cosmology from the RG flow of gravity. 2018.

[48] A. G. Riess et al. Observational evidence from supernovae for an accelerating universe and a cosmological constant. *Astron. J.*, 116:1009–1038, 1998.

[49] S. Perlmutter et al. Measurements of Omega and Lambda from 42 high redshift supernovae. *Astrophys. J.*, 517:565–586, 1999.

[50] S. Carroll. *Spacetime and Geometry: An Introduction to General Relativity*. Pearson, 2014.

[51] P. A. R. Ade et al. Planck 2015 results. XIII. Cosmological parameters. *Astron. Astrophys.*, 594:A13, 2016.

[52] P. A. R. Ade et al. Planck 2015 results. XX. Constraints on inflation. *Astron. Astrophys.*, 594:A20, 2016.

[53] A.A. Starobinsky. A new type of isotropic cosmological models without singularity. *Physics Letters B*, 91(1):99 – 102, 1980.

[54] V. F. Mukhanov and G. V. Chibisov. Quantum Fluctuations and a Nonsingular Universe. *JETP Lett.*, 33:532–535, 1981. [Pisma Zh. Eksp. Teor. Fiz.33,549(1981)].

[55] A. A. Starobinsky. The Perturbation Spectrum Evolving from a Nonsingular Initially De-Sitter Cosmology and the Microwave Background Anisotropy. *Soviet Astronomy Letters*, 9:302–304, June 1983.

[56] A. Bonanno and M. Reuter. Cosmology with selfadjusting vacuum energy density from a renormalization group fixed point. *Phys. Lett.*, B527:9–17, 2002.

[57] A. Bonanno and M. Reuter. Cosmology of the Planck era from a renormalization group for quantum gravity. *Phys. Rev.*, D65:043508, 2002.

[58] B. Guberina, R. Horvat, and H. Stefancic. Renormalization group running of the cosmological constant and the fate of the universe. *Phys. Rev.*, D67:083001, 2003.

[59] M. Reuter and H. Weyer. Renormalization group improved gravitational actions: A Brans-Dicke approach. *Phys. Rev.*, D69:104022, 2004.

[60] A. Babic, B. Guberina, R. Horvat, and H. Stefancic. Renormalization-group running cosmologies. A Scale-setting procedure. *Phys. Rev.*, D71:124041, 2005.

[61] M. Reuter and F. Saueressig. From big bang to asymptotic de Sitter: Complete cosmologies in a quantum gravity framework. *JCAP*, 0509:012, 2005.

[62] A. Bonanno, G. Esposito, C. Rubano, and P. Scudellaro. The Accelerated expansion of the Universe as a crossover phenomenon. *Class. Quant. Grav.*, 23:3103–3110, 2006.

[63] A. Bonanno and M. Reuter. Entropy signature of the running cosmological constant. *JCAP*, 0708:024, 2007.

[64] S. Weinberg. Asymptotically Safe Inflation. *Phys. Rev.*, D81:083535, 2010.

[65] A. Bonanno, A. Contillo, and R. Percacci. Inflationary solutions in asymptotically safe f(R) theories. *Class. Quant. Grav.*, 28:145026, 2011.

[66] Y.F. Cai and D. A. Easson. Asymptotically safe gravity as a scalar-tensor theory and its cosmological implications. *Phys. Rev.*, D84:103502, 2011.

[67] A. Contillo, M. Hindmarsh, and C. Rahmede. Renormalisation group improvement of scalar field inflation. *Phys. Rev.*, D85:043501, 2012.

[68] Y.F. Cai, Y.C. Chang, P. Chen, D. A. Easson, and T. Qiu. Planck constraints on Higgs modulated reheating of renormalization group improved inflation. *Phys. Rev.*, D88:083508, 2013.

[69] I. D. Saltas. Higgs inflation and quantum gravity: An exact renormalisation group approach. *JCAP*, 1602:048, 2016.

[70] A. Tronconi. Asymptotically Safe Non-Minimal Inflation. *JCAP*, 1707(07):015, 2017.

[71] A. Bonanno. An effective action for asymptotically safe gravity. *Phys. Rev.*, D85:081503, 2012.

[72] A. Bonanno and A. Platania. Asymptotically safe inflation from quadratic gravity. *Phys. Lett.*, B750:638–642, 2015.

[73] A. Bonanno, A. Platania, and F. Saueressig. Cosmological bounds on the field content of asymptotically safe gravity-matter models. 2018.

[74] G. D'Odorico and F. Saueressig. Quantum phase transitions in the Belinsky-Khalatnikov-Lifshitz universe. *Phys. Rev.*, D92(12):124068, 2015.

[75] A. Bonanno and F. Saueressig. Asymptotically safe cosmology – A status report. *Comptes Rendus Physique*, 18:254–264, 2017.

[76] E. Manrique, S. Rechenberger, and F. Saueressig. Asymptotically Safe Lorentzian Gravity. *Phys. Rev. Lett.*, 106:251302, 2011.

[77] F. L. Bezrukov and M. Shaposhnikov. The Standard Model Higgs boson as the inflaton. *Phys. Lett.*, B659:703–706, 2008.

[78] A. O. Barvinsky, A. Yu. Kamenshchik, and A. A. Starobinsky. Inflation scenario via the Standard Model Higgs boson and LHC. *JCAP*, 0811:021, 2008.

[79] C. Patrignani et al. Review of Particle Physics. *Chin. Phys.*, C40(10):100001, 2016.

[80] A. G. Riess et al. A 2.4% Determination of the Local Value of the Hubble Constant. *Astrophys. J.*, 826(1):56, 2016.

[81] P. F. Machado and F. Saueressig. On the renormalization group flow of f(R)-gravity. *Phys. Rev.*, D77:124045, 2008.

[82] N. Ohta, R. Percacci, and G. P. Vacca. Flow equation for $f(R)$ gravity and some of its exact solutions. *Phys. Rev.*, D92(6):061501, 2015.

[83] G. P. De Brito, N. Ohta, A. D. Pereira, A. A. Tomaz, and M. Yamada. Asymptotic safety and field parametrization dependence in the $f(R)$ truncation. 2018.

[84] S. Rechenberger and F. Saueressig. The R^2 phase-diagram of QEG and its spectral dimension. *Phys. Rev.*, D86:024018, 2012.

[85] A. Codello, R. Percacci, and C. Rahmede. Ultraviolet properties of f(R)-gravity. *Int. J. Mod. Phys.*, A23:143–150, 2008.

[86] K. Falls, D. F. Litim, K. Nikolakopoulos, and C. Rahmede. Further evidence for asymptotic safety of quantum gravity. *Phys. Rev.*, D93(10):104022, 2016.

[87] M. Reuter and H. Weyer. Quantum gravity at astrophysical distances? *JCAP*, 0412:001, 2004.

[88] G. Amelino-Camelia, M. Arzano, G. Gubitosi, and J. Magueijo. Gravity as the breakdown of conformal invariance. *Int. J. Mod. Phys.*, D24(12):1543002, 2015.

[89] F. Brighenti, G. Gubitosi, and J. Magueijo. Primordial perturbations in a rainbow universe with running Newton constant. *Phys. Rev.*, D95(6):063534, 2017.

[90] A. Codello and R. K. Jain. On the covariant formalism of the effective field theory of gravity and its cosmological implications. *Class. Quant. Grav.*, 34(3):035015, 2017.

[91] A. Codello and R. K. Jain. A Unified Universe. *Eur. Phys. J.*, C78(5):357, 2018.

[92] P. Donà, A. Eichhorn, and R. Percacci. Matter matters in asymptotically safe quantum gravity. *Phys. Rev.*, D89(8):084035, 2014.

[93] N. Christiansen, D. F. Litim, J. M. Pawlowski, and M. Reichert. Asymptotic safety of gravity with matter. *Phys. Rev.*, D97(10):106012, 2018.

[94] N. Alkofer and F. Saueressig. Asymptotically safe $f(R)$-gravity coupled to matter I: the polynomial case. 2018.

[95] I. G. Avramidi. *Heat Kernel and Quantum Gravity.* Springer, 2000.

[96] M. Reuter. Nonperturbative evolution equation for quantum gravity. *Phys. Rev.*, D57:971–985, 1998.

[97] M. S. Ruf and C. F. Steinwachs. Quantum equivalence of $f(R)$ gravity and scalar-tensor theories. *Phys. Rev.*, D97(4):044050, 2018.

[98] T. Chiba. 1/R gravity and scalar - tensor gravity. *Phys. Lett.*, B575:1–3, 2003.